The Assessment of the Fatigue Behaviour of Offshore Wind Farm Support Structures

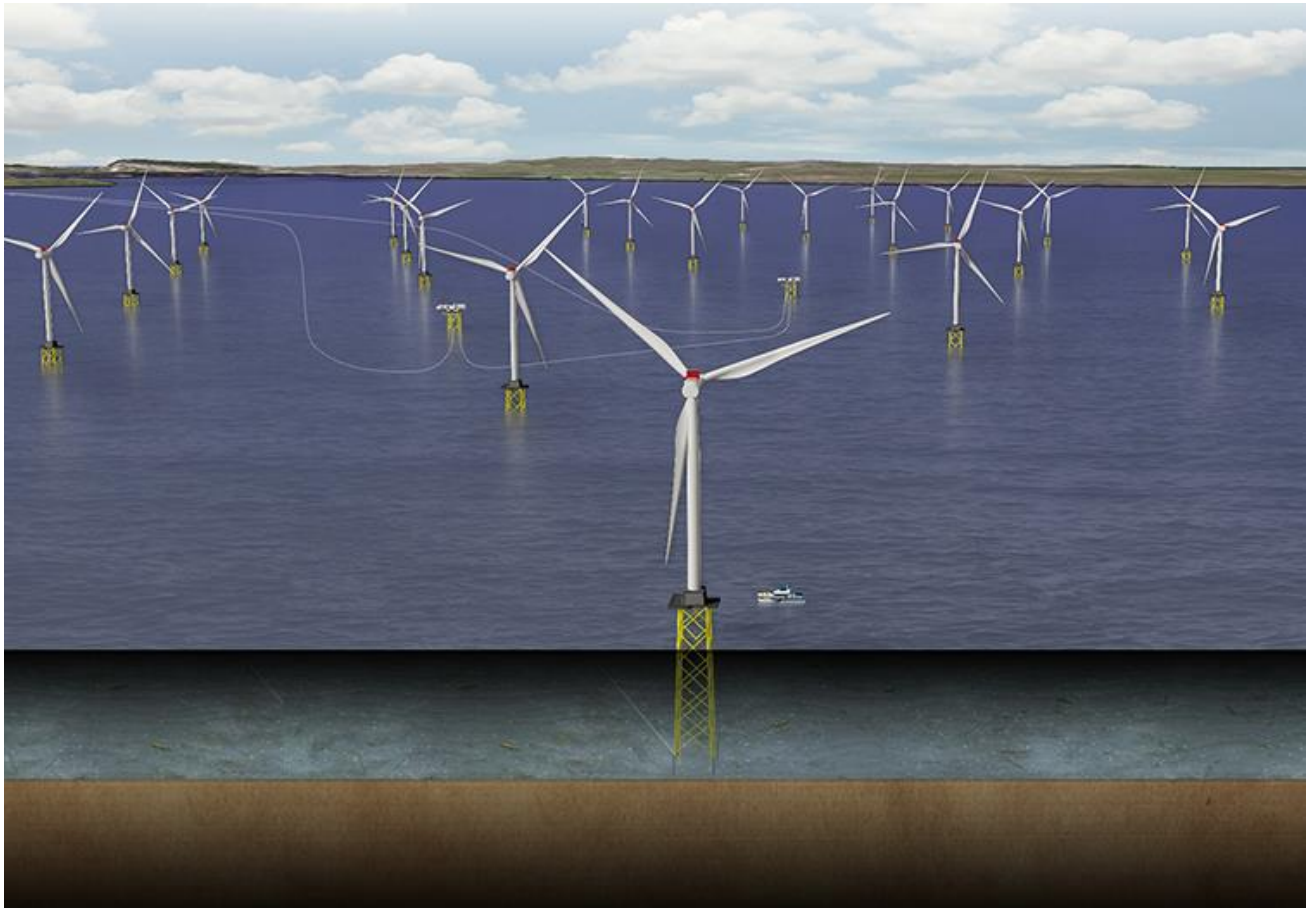

Dynamic Amplification of the Braces of Offshore Wind Farm Support Structures

By

Maxime L. Roozendaal

The Assessment of the Fatigue Behaviour of Offshore Wind Farm Support Structures

Dynamic Amplification of the Braces of Offshore Wind Farm Support Structures

By

Maxime L. Roozendaal

to obtain the degree of Master of Science
at the Delft University of Technology,
to be defended publicly on 9th of June 2017

Student number: 4076206

Thesis committee:

Prof. Dr. A.V. Metrikine	TU Delft
Ir. P.G.F. Sliggers,	TU Delft, chairman
Ir P. van der Male,	TU Delft, supervisor
Ir. M. Kwa,	Seaway Heavy Lifting, supervisor

ACKLOWLEDGEMENT

This thesis is submitted in partial fulfilment of the requirements for a Master's Degree in Offshore and Dredging Engineering at Delft University of Technology. This was performed over the course of 9 months in corporation with Seaway Heavy Lifting.

I would like to express my sincere gratitude towards my graduation committee for their guidance and feedback throughout this research. Thank you Ir. P.G.F. Sliggers for your clever criticism and thank you Ir. P. van der Male for our regular meetings, you always knew to ask the right questions which made me think in a critical way about my own research. Additionally I would like send my great appreciation to Ir. M. Kwa for his true dedication and his daily time and effort. His genuine interest in my research ensured I felt motivated throughout the process.

Furthermore my special thanks goes to Seaway Heavy Lifting for this opportunity to perform my Master research. I especially would like to thank the Naval and FEM department for their continuous support. Also my graduate goes towards the Geomechanics and CAD department for their time. Not to forget, I would like send my gratitude to David Paul for his helpful input.

Finally I would like to thank my parents, Vicenta Roozendaal and Frans Roozendaal, for guiding me throughout my studies. Without their support and the way they always believed in me I could not have done this.

ABSTRACT

Renewable energy generated by offshore wind turbines (OWT) are nowadays more frequently used in the offshore industry. The design of OWT foundations share similarities with a typical offshore oil and gas construction, however a OWT farm usually consist of multiple foundations whose installation are more cost-sensitive compared to one oil and gas platform. Furthermore the profit target of the wind farm is generated at a later stage of the project. Thereby it is preferable to design a light OWT foundation that is cheaply fabricated and easily installed.

Due to these reasons the OWTs are designed as slender constructions. When designing a structure the aim is to generate a design of which the natural frequencies do not overlap with the applied forcing frequencies. This is required to avoid resonance which results in low estimated fatigue life of the structure. A challenge regarding the slender OWT structures is that the natural frequencies are close to the forcing frequencies.

This thesis is based on a project having OWT structures with the foundation consisting of a jacket design having a framework of four bays of cross braces. During a later stage of the project it was found by the substructure designer that the structure would have a low estimated fatigue life. The cause being that the applied external forces on the structure are in the same frequency range as the natural frequency of particular cross braces in the jackets, in the range of 2 – 2.5Hz. Consequently, due to resonance large brace excitation was found in the jacket model, created by the designer, which resulted in a low expected fatigue life. To mitigate this, double sided welds and external toe grinding were implemented. However no clear explanation regarding this issue was provided and not all parties involved obtained the same results and conclusions. Therefore further investigation regarding this theoretic fatigue issue was requested.

The goal of this research is to identify and provide a clear explanation of the vibration amplification movement of the braces and thus independently assess if there is a fatigue problem with the OWT jackets. Furthermore this thesis focusses on alternative solutions to this problem, had the vibration issue been found during an earlier stage of the project.

The first part of this thesis focusses on the identification of the problem. The approach was structured in three stages;

First the identification of the forcing vibration in the critical frequency zone was performed with the use of a Fast Fourier analysis of time domain data of the applied forces on the OWT. The obtained frequency response demonstrated excitations around the critical frequency zone, which are due to the eigen-frequencies of the tower and the blades of the turbine.

This was followed by the analysis of the eigen-frequencies of the cross braces of the jacket in bay 3 and 4 for the local and global response. This was performed with the use of ANSYS modal analysis in combination with a build-up of simplified brace models. Hand calculations were performed to verify the obtained results.

Finally, a comparison was made regarding the overlapping of frequencies of the forcing frequencies and eigen-frequencies of the braces. This was done to determine if large brace amplification due to resonance would occur, resulting in a low estimated fatigue life.

The second part of this research evaluates alternative solutions to this problem. Possible concepts were elaborated with their ad- and disadvantages, followed by a multi criteria analysis. Three concepts were selected for further investigation and examined in terms of whether a successful outcome could be achieved by their implementation.

This thesis also provides a procedure with regards to identifying to the potential for resonance at an early stage of the design process. Keeping track of changes during all design phases will lead to avoiding the unexpected discovery of a short fatigue life, due to resonance, at a late design stage.

TABLE OF CONTENTS

TABLE OF FIGURES

TABLE OF TABLES

ABBREVIATIONS

Name	Explanation
ALS	Accidental Limit state
CHS	Circular Hollow Cross section
Di	inner diameter
Do	outer diameter
DOF	Degrees of freedom
EPCI	Engineering Procurement Construction Installation
FFT	Fast Fourier Transform
FLS	Fatigue limit state
FT	Fourier Transform
KC	Keulegan Carpenter
MCA	multi criteria analysis
MG	Marine Growth
NF	Natural Frequency
OWT	Offshore Wind Turbine
PSD	Power spectral density
SHL	Seaway Heavy Lifting
SLS	Serviceability limit stat
TLCD	Tuned liquid column damper
TLD	Tuned Liquid Damper
TMD	Tuned Mass Damper
TP	Transition Piece
ULS	Ultimate limit state

1. PROJECT BACKGROUND

This chapter provides some detailed information about the [redacted] Project.

1.1. OFFSHORE WIND TURBINE SUPPORT STRUCTURES

Renewable energy such as Offshore Wind Turbines (OWT's) are becoming in demand in the current offshore industry. More research and development is performed to obtain OWTs that are sustainable and profitable.

The offshore wind industry is placing new wind farms at larger water depths. This brings several challenges with that pushes the engineer to obtain bright and efficient solutions. Floating and bottom founded wind turbines could be possible design concepts to be selected. This Thesis only focusses on bottom founded OWT's, meaning the substructure is placed on the seabed.

Different types of bottom founded substructures exist, such as monopoles, gravity based and tower/jacket structures. This thesis only concentrates on tower type substructures with the wind turbine on top, since this layout is used for the [redacted] Project.

[redacted]

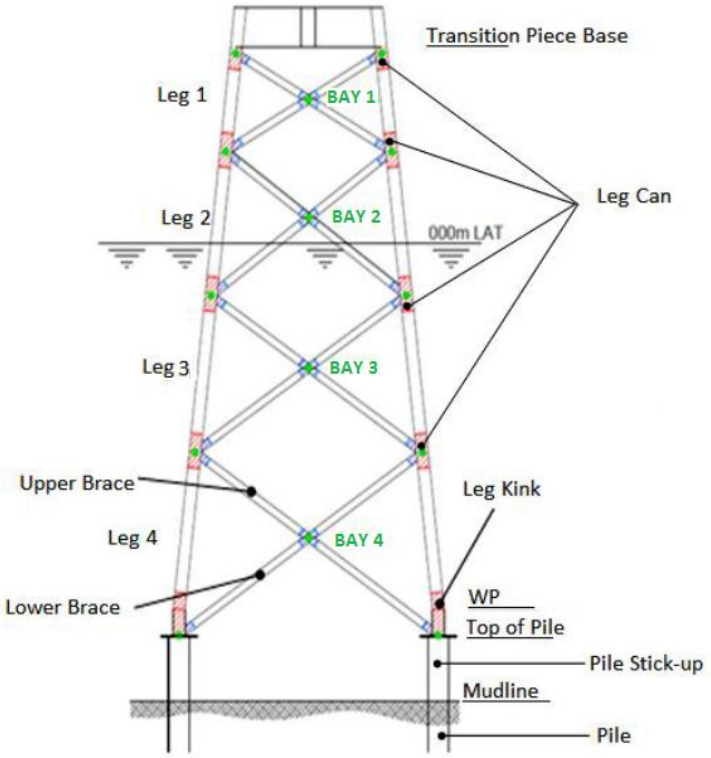

FIGURE 1-1 JACKET LEGEND [32]

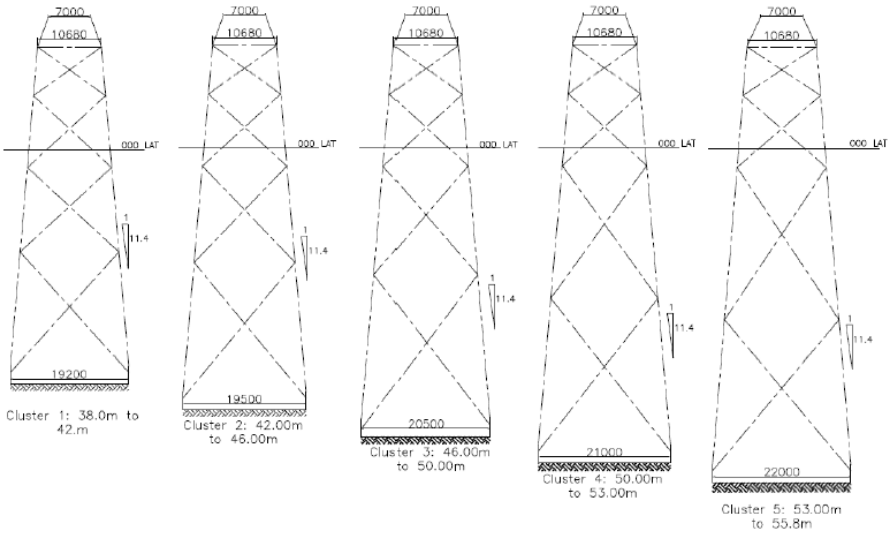

FIGURE 1-2 JACKET LAYOUT - 5 CLUSTERS [33]

2. INTRODUCTION

This chapter provides the problem description and the goal of this research followed by the current selected solution. Furthermore the approach used in this research is deliberated.

2.1. PROBLEM DISCRIPTION

It is believed by the substructure designer that a short estimated fatigue life of the jacket structure of the reference project is obtained, since the applied external forces on the structure are in the same frequency range as the natural frequency of particular cross braces within the jackets, causing it to resonate. Due to this, large brace excitation is obtained which results in this reduced fatigue life. The repeated movement of the braces due to the vibration creates stresses and strain in the weld. Since the fatigue life of the structure is defined by the number of cycles of stresses that the material can withstand before fatigue failure occurs, a low fatigue life for the OWT substructure is obtained.

Calculations performed by the substructure designer showed that the brace excitation is caused by the turbine loads. The turbine blades showed edgewise and flapwise forward and backward whirling as well as lateral tower bending movements in the critical frequency zone. It is believed that the turbine forces vibrate in the frequency range of 2.0 – 2.5 Hz, which would be the same as the eigen-frequency of the braces in bay 3 and 4 of the jacket structure. However no clear explanation regarding this issue was provided by the substructure designer and not all parties involved with this issue obtained the same results and conclusions. For safety reasons, mitigation measurements were implemented to avoid this problem. Therefore further investigation regarding this academic fatigue issue was requested by SHL.

2.2. GOAL

The goal of this research is to identify and provide a clear explanation of the amplification of the brace vibration movement and thus independently assess if there is a fatigue problem with the OWT jackets of the reference project.

This research can be separated in two main sections.

1. Identification of the overlapping of eigen-frequencies of the substructure and the forcing frequencies, resulting in the short estimated fatigue life.
2. Alternative solutions to this problem, had the vibration issue been found in an earlier stage of the project.

This thesis also provides a procedure with regards to identifying to the potential for resonance at an early stage of the design process.

2.3. CURRENT SOLUTION

The selected solution to reduce the fatigue issues in braces of the reference project is to use double sided welds and apply external toe grinding. This solution is rather expensive but was selected since it was the best solution at this stage in the project. By the time the brace fatigue issues were apparent, it was too late to implement major design changes to the jacket structure.

With regards to the selected solution; it is worth mentioning that the weld toe is an important source of the fatigue cracking due to the high stress concentrations it produces at this location. The toe of the weld is the top of the weld, shown in Figure 2-1. The weld obtains miniature crack flaws prone to fatigue propagation and due to the quick transition from the steel to the weld, fatigue failure is likely to occur. To improve the weld toe geometry by grinding, the size of these crack flaws can be reduced which increases the fatigue life. Furthermore, by adjusting the geometry a smooth transition from the steel to the weld is achieved which reduces the local stress concentration. All of this results in an increase of fatigue life of the structure. [11]

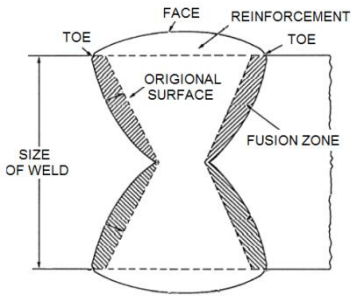

FIGURE 2-1 SCHEMATIC VIEW OF DOUBLE SIDED WELD [22]

2.4. APPROACH

In this research the following steps are taken to identify the fatigue problem and to provide alternative solutions if this problem had been revealed at an earlier stage of the project;

- First a detailed literature study was performed regarding this particular case and aspects involved. Chapter 3 explains the general challenges in designing an offshore wind turbine structure. Furthermore, a basic fatigue description is provided followed a short definition of the Fourier Transform. Additionally a comprehensive explanation regarding damping mechanism and the effect on marine growth on structures is deliberated.

- Chapter 4 provides a general design procedure with regards to avoiding the realization of the short estimated fatigue life due to resonance at a late stage of the design process.

- Chapter 5 identifies the problem. This is separated in three parts;
    - The identification of the forcing vibration due to the turbine loads in the critical frequency zone;

      For this MATLAB is used to perform a Fast Fourier analysis on time domain data of the applied forces on the OWT. The obtained frequency response is evaluated and the frequency peaks are analysed.

    - Analysis of the natural frequencies of the cross braces of the jacket in bay 3 and 4;

      Local cross brace analysis of bay 3 and 4 and a global OWT jacket analysis is done using ANSYS 17.1 modal analysis. The eigen-frequency of the local and global sections is determined in this manner. A build-up of simplified models was assessed by hand calculations and compared with ANSYS to verify the obtained results.

    - Both the forcing frequencies from section 1 and eigen-frequencies of section 2 are then compared to conclude if large amplification of the brace vibration movement due to resonance would occur, resulting in a low estimated fatigue life.

- Chapter 6 provides a concept study regarding possible solutions to this particular problem in case of earlier detection of it. These concepts focus on adjustments of the current design as well as different design lay outs which create an increase of frequency shift in natural frequency so large brace amplification is avoided. First all possible concepts are elaborated with their ad- and disadvantages. Then a multi criteria analysis is conducted and three concepts are selected for further investigation. Finally these three concepts are evaluated in terms of whether a successful outcome could be achieved by their implementation.

- In chapter 7 a conclusion is given summarizing the findings of this research.

- Finally, chapter 8 provides recommendations for further investigations on this topic.

3. LITERATURE

There are several factors that influence the fatigue life time of the structure. Previous research has been done to examine what kind of effect several factors have on the jacket structure of the OWT. This chapter provides a literature study and explains some fundamental aspects that are relevant to this Thesis.

First the general design challenges for OWT jacket structures are provided in section 3.1. It explains the effects the environmental forces such as the wind, wave and current and the vibrations of the wind turbine have on the jacket design.

Section 3.2 presents a short description about fatigue and what effects it has on structures. Rainflow counting is also deliberated in this section.

In this research the Fourier transformation is used, therefore a short explanation regarding this is given in section 3.3.

Damping is an important aspect to consider when designing a structure. Section 3.4 focusses on a variety of damping factors and elaborates on the behaviour of it.

Section 3.5 elaborates on the marine growth on the structure. After a structure is placed on the seabed, living organisms will attach it-self, called marine growth. It is an important aspect to consider since it changes the structural integrity of the members and has influence on the natural frequency of the structure. The section provides details about previous conducted research and explains the effects it has on the structure.

Section 3.6 focusses on coupled versus decoupled analysis. Since large structures are rather complex to analyse, it is common to consider coupled and decoupled models to simplify and reduce the calculations.

3.1. GENERAL DESIGN CHALLENGES FOR OWT JACKET STRUCTURES

Jacket structures are widely used in the offshore oil and gas industry. Large platforms are placed on top of stable jacket structures that are designed for the desired life time of the structure. With the upcoming offshore wind industry, jacket structures with the wind turbines placed on top would be assumed to be no different. However fatigue issues are more dominant in OWT compared to the oil and gas platforms. This is because of several factors, including the slender jacket structure compared to large offshore oil and gas structures, in combination with the vibration introduced by the rotation of the blades of the wind turbine. Overall the OWT needs to be structurally sound, low in cost and able to be installed.

The two main challenges regarding the OWT jacket structure are that (1) the structures experience overturning moments and are (2) dynamically sensitive to resonance. The latter is because the natural frequencies of these slender substructures are close to the forcing frequencies. The forcing frequencies are caused by the environmental forces such as the wind, wave/current and current and vibrations at the hub level due to the wind turbine; 1P / 3P. [3]

The aim is to design a structure for which the natural frequencies do not overlap with the forcing frequencies implied on the structure. A power spectral density graph with on the x-axis the frequency ranges of the forcing frequencies is a useful tool to obtain which frequencies the structure should be designed for. The forcing frequencies outlined in the graph are the wind, wave/current and 1P / 3P of the turbine, an example is illustrated in Figure 3-1.

More detailed information regarding the wind and wave/current spectra shown in the diagram is provided in section 3.1.1. The forcing frequencies due to the wind turbine is elaborated in section 3.1.2 and the possible design ranges for the substructure; 'soft-soft', 'soft-stiff' and 'stiff-stiff', are described in section 3.1.3. Finally in section 3.1.4 the company's involvement and interaction is deliberated.

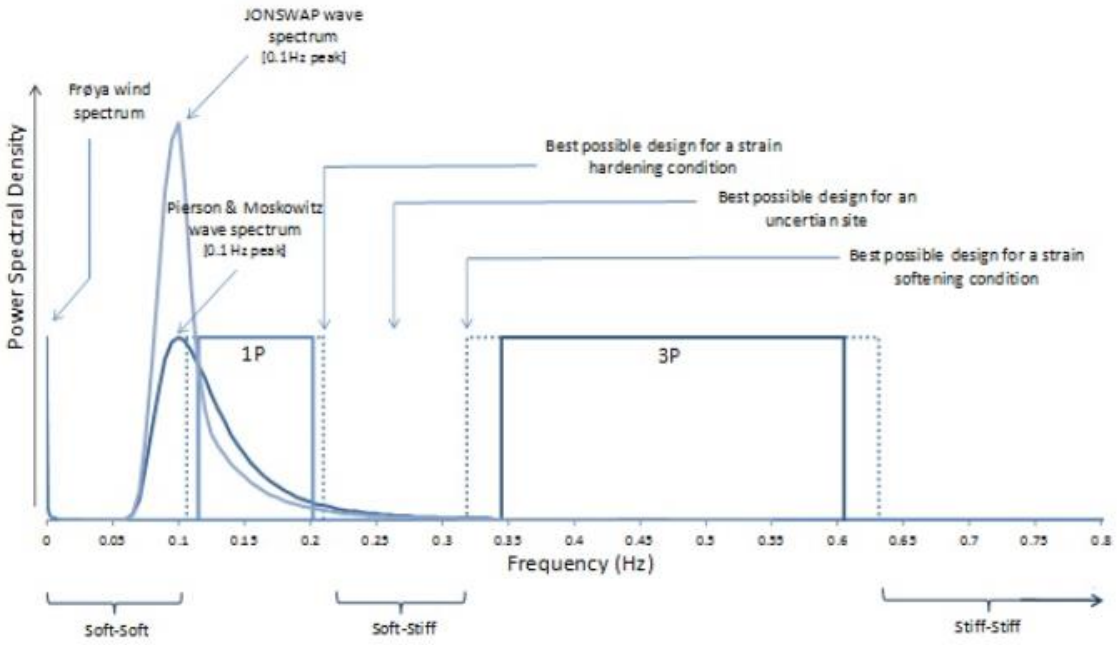

FIGURE 3-1 POWER SPECTRAL DENSITY GRAPH [3]

3.1.1. WIND / WAVE / CURRENT SPECTRUM

The wind and wave frequency ranges are identified in Figure 3-1. A suitable shape to define the wave forces on the power spectral density graph could be the 'Pierson Moskowitz' (PM) or the 'JONSWAP' curve. These spectrums are defined with the equations (1) and (2) respectively, specified in DNV code. [6] The JONSWAP equation is applicable to young sea states and the PM equation for fully developed states in deep water.

$$S_{PM}(\omega) = \frac{5}{16} H_s^2 \, \omega_p^4 \, \omega^{-5} exp\left(-\frac{5}{4}\left(\frac{\omega}{\omega_p}\right)^{-4}\right) \tag{1}$$

$$S_J(\omega) = A_\gamma S_{PM}(\omega) \gamma^{exp\left(-0.5\left(\frac{\omega-\omega_p}{\sigma\omega_p}\right)^2\right)} \tag{2}$$

Where,

H_s	= wave height	[m]
ω	= angular frequency	[rad/s]
ω_p	= angular peak frequency $2\pi/T_p$	[rad/s]

σ = spectral width parameter [-]
$\sigma = \sigma_a$ for $\omega < \omega_p$
$\sigma = \sigma_b$ for $\omega < \omega_p$

usual JONSWAP values
$\sigma_a = 0.07$
$\sigma_b = 0.09$

Aγ = peak shape parameter [-]
$1 - 0.287\ln(\gamma)$

γ = non-dimensional peak shape parameter [-]

Since the PM spectrum represents the fully developed conditions in deep water, the peak frequency only depends on the wind speed. The spectra perceived for the JONSWAP has a sharper peak compared to the PM spectrum. This is why the JONSWAP shape is defined by the PM spectrum.

Waves could be caused by wind forces; the wind applies a pressure at the water surface. In fact a maximum pressure is applied at the windward side of the wind crest and a minimum at the leeward side. This effectively means that the wind pushes the wave down where it is moving down and pulls the water surface up where is its motion is going up. This positive feedback mechanism is described by Miles and explains that due to this out of phase coupling, energy from the wind is transferred into the waves. [23] The design sea state which is used to initially analyse the fatigue damage, is shown as a frequency range of 0.05Hz – 0.3Hz on the power spectral density graph.

The overturning moment experienced by the complete structure is caused by the hydrodynamic forces acting on the substructure and the wind and thrust forces located on the tower and turbine blades. It is worth noting that the aerodynamic forces on offshore structures are in most cases smaller than the hydrodynamic forces. However due to the larger lever arm the wind acts on, a larger overturning moment is obtained by the aerodynamic forces compared to the hydrodynamic forces. Small variations in wind speed are observed compared to the wave forces. Constant aerodynamic forces on the turbine result in a constant bending moment acting on the foundation of the structure. A schematic view of this is demonstrated in Figure 3-2. [5]

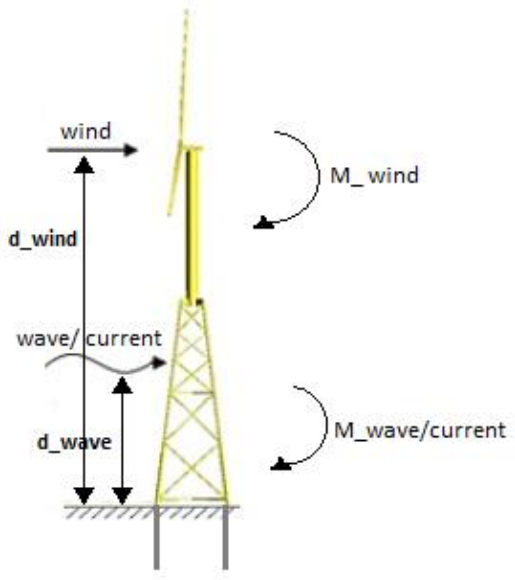

FIGURE 3-2 OVERTURNING MOMENT JACKET

3.1.2. TURBINE SPECTRUM

Forcing vibrations that must be considered when designing the OWT jacket, include the cyclic moment from the turbine. As mentioned before 1P and 3P are vibrations that occur at the hub level of the tower. 1P refers to the rotor frequency, due to the mass and the aerodynamic imbalances of the rotor. This is not one peak frequency but a frequency band caused by the lowest and highest rpm. The 3P frequency is referring to a 3 bladed turbine, in case of a turbine with 2 blades this is denoted at 2P. This phenomenon is also known as 'Tower or Bladed shadow'. The wind passes the rotor blades, at a certain point in time the blade is right in front of the tower and the lift changes, this occurs 3 times in one turn for a 3 bladed tower. When this occurs a lower level of output power is achieved which is creating movements of the turbine. Thus, even for a constant wind speed at a specific height, a turbine blade would encounter variable wind as it rotates. When designing a wind turbine a safety margin of 10% on the lower and upper bound of the frequency ranges is recommended. [4]

The turbine and the blades self, have their own natural frequencies that need to be considered when creating the complete offshore wind turbine design. The blades of the turbine can move in flapwise, edgewise and torsional direction and the turbine can deform in lateral and longitudinal bending. These vibration movements are schematically illustrated in Figure 3-3 and Figure 3-4

A flapwise vibration can be described as classical flutter. This occurs when the first torsional blade mode couples to a flapwise bending mode in a flutter mode through the aerodynamic forces. Due to the torsion of the blades, the force angle of attach changes which creates lift in an undesirable phase including the flapwise bending. This flapping movement occurs at a certain frequency. [45]

Edgewise vibrations, also known as lead-lag movement are mainly caused by lower order turbine modes caused by the torsion between the rotor hub and the generator. This torsional mode is related to the coexisting edgewise bending of the blades and is influenced by the generator control. It is worth mentioning that academically this could occur to all types of rotor blades, however this problem is more dominant when the blade size and wind strength increases. Due to the larger area of the blade, it can catch more wind and more torsion is observed. [47]

Tower bending at the base is most dominant when the wind attacks from the front and creates a maximum drag loading on the blades. The maximum top tower bending moment is produced when the wind blows in sideway direction which is causing maximum lift on the blades pointing vertically upwards, as well as rear wind loading on the rotor in combination with one blade shielded by the tower. [48]

It is found that the eigen-frequencies of the tower and the blades cause the amplification of the brace vibration movement for the OWT jackets of the reference project.

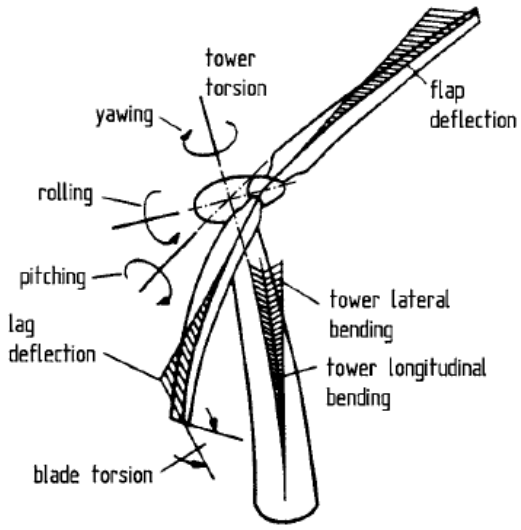

FIGURE 3-3 TOWER MOVEMENTS[46]

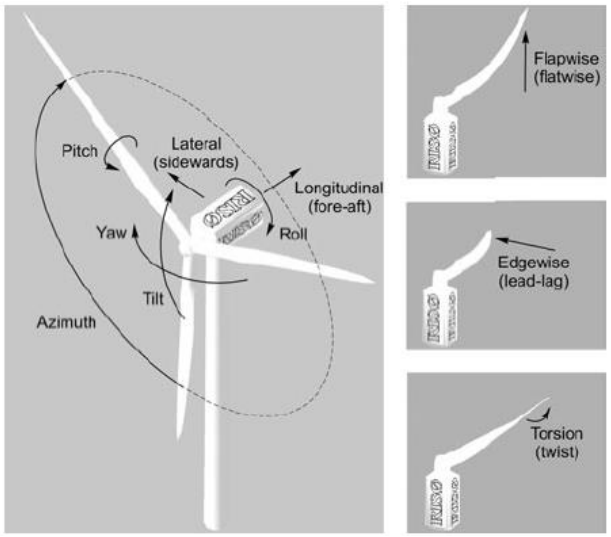

FIGURE 3-4 BLADE MOVEMENTS [45]

3.1.3. DESIGN RANGES

It can be seen that there are three ranges of frequency the structure can be designed for to avoid resonance, demonstrated in Figure 3-1. The first range is called the 'soft-soft' range; this is a very flexible structure and is roughly in the range of 0 – 0.1Hz. The second frequency range, between the 1P and 3P frequencies is named the 'soft-stiff' range. This is a relative small scope to design the structure for, but also the most desired range with the given uncertain conditions. The last range, the 'stiff-stiff' range, is the frequency above the 3P upper limit. [24]

The fatigue issues in the affected braces of the OWT jackets are mainly caused due to the fact that the natural frequency of the braces lay in the range of the forcing frequencies applied on the structure. To avoid this, a frequency shift out of the forcing frequency range is required. It is preferred to increase the frequency rather than decrease it, since low frequencies generally obtain more energy which is undesirable.

The natural frequency of a classical beam element varies according to equation (3), with respect to the dynamics of a beam. This suggests that the natural frequency can be influenced by the stiffness (k), mass (m) and length (L) of the member.

$$\omega_n = \frac{c}{2\pi}\sqrt{\frac{k}{m}} = \frac{c}{2\pi}\sqrt{\frac{E\,I}{\rho\,A\,L^4}} \tag{3}$$

Where;

ω_n	= natural frequency	[rad/s]
c	= boundary coefficient	[-]
k	= stiffness	[N/m]
m	= mass	[kg]
L	= length	[m]
E	= Young's Modulus	[kg.m/s^2]
I	= moment inertia	[m^4]
ρ	= density	[kg/m^3]

A = area [m^2]

When analysing the formula the following challenges come up when obtaining an increase in frequency;

Increasing the stiffness could be a solution to increase the frequency of the member. However, increasing the stiffness of the member is mainly achieved by increasing the diameter or wall thickness of the member, which also increases the mass. Evaluating the formula this would be an ineffective solution if both the stiffness and mass is increased, no sufficient overall rise of natural frequency is obtained.

Another possible solution to achieve an increase of natural frequency, but also involves complications, is by reducing the structural mass of the members. Nevertheless, this is rather ineffective since decreasing the mass also reduces the stiffness. Factors that could have an positive effect on the mass of the structure are anodes and marine growth. In most cases anodes are attached on the members to avoid corrosion. These possibly could be placed on another location on the structure, reducing the weight on the members that are affected. Furthermore marine growth on the members could potentially be removed to decrease the mass during the life time of the structure. This would involve cleaning measurements which may be expensive.

Something that does have a considerable effect on increasing the natural frequency of the member is the length of the member, L. Especially since it is denoted in the formula with a power to the four it will have a positive effect to reduce the length. This could be achieved by adding a span or braces to the structure.

3.1.4. COMPANY EXPERTISE

Several companies are usually involved in large projects with all having their own expertise. All those companies focus on their main speciality within the project. To attain the final complete design good team work between the different companies is essential.

The advantage of having multiple companies primarily concentrating on their speciality is that in-depth knowledge is applied for all aspects of the project. On the other hand, a disadvantage is that the different companies are lacking full understanding of each other's expertise. So is the designer company skilled in focussing on the details of the total design, however having minimal experience with T&I and the entire life time of such structures, while the T&I company has inadequate knowledge regarding the design.

It is worth noting that for the OWT coupled analysis is required between the jacket structure and the turbine. This implies that various iterations are required to ensure both turbine and jacket design are sound. Furthermore, it is rather challenging to achieve a design that satisfies not only the design aspects but also the complete life time of the structure including T&I and decommissioning. To obtain such a design good and open communication between all parties is necessary, which is in real life a challenge to achieve.

3.2. FATIGUE

Fatigue failure can be described as a material fracture caused by localised progressive brittle cracking due to repeated cycling loading. The fatigue life of a structure defines the number of cycles of stresses the material can withstand before fatigue failure occurs. The maximum amount it can hold before failure is called the fatigue strength. [25]

When calculation fatigue life, the stresses are taken into account; nominal stress is a stress that can be derived by classical beam theory. Hotspot stress, also referred as geometric stresses, include normal stresses and structural discontinuities stress. It does not include the notch stresses due to the local weld geometry. Notch stress is defined as the total stress due to the geometry of the detail and includes the non-linear stress field because of the notch at the weld toe. [10] Hotspot stress is most suitable for the fatigue calculations and is obtained by equation (4).

$$\sigma_{hotspot} = SCF * \sigma_{nominal} \tag{4}$$

Where,

SCF	= stress concentration factor	[-]
$\sigma_{nominal}$	= nominal stress	[Pa]
$\sigma_{hotspot}$	= hotspot stress	[Pa]

There are multiple ways to obtain the SCF depending on the connection. To select the correct method in obtaining the SCF can be found in DNVGL-RP-C203 [25]

There are several approaches to calculate the fatigue life of the structure. On method is the S-N curve, which is done under the assumption of linear cumulative damage. The S-N graph obtains on the x-axis the number of cycles and on the y axis the amount of stress. A schematic view of the SN curve is illustrated in Figure 3-5. [26]

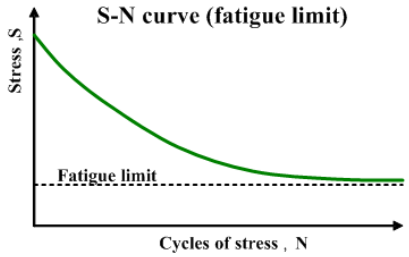

FIGURE 3-5 SCHEMATIC VIEW SN CURVE [26]

The members of the jackets will endure long term stresses during their life time due to the vibrations. These repeated stress cycles with varying amplitudes can be divided in constant stress range blocks. The fatigue damage accumulation can be calculated with formula (5), which is representing the summation of stress ranges and the number of occurrence. [25]

$$D = \sum_{i=1}^{k} \frac{n_i}{N} = \frac{1}{\overline{a}} \sum_{i=1}^{k} n_i * (\Delta\sigma_i)^m \leq \eta \tag{5}$$

Where;

D	= accumulated fatigue damage	[-]
$\overline{a}$	= intercept of the design S-N curve with the log N axis	[-]
m	= negative inverse slope S-N curve	[-]
k	= number of stress blocks	[#]
n_i	= number of stress cycles in stress block i	[#]
N_i	= number of cycles to failure at constant stress range $\Delta\sigma_i$	[#]
η	= usage factor	[-]

This is referred to as the Palmgren-Miner Rule. The rule does not include sequence effects, meaning that the sequence range of the stresses has no effect on the final result. The aim is that the estimated fatigue damage, D, is below a certain value which is stated for the project. It is worth mentioning that a fatigue factor needs to be incorporated in the design for safety reasons.

3.2.1. RAINFLOW COUNTING

Rainflow counting is a way to effectively bin equivalent stress cycles and allows the application of Miners Rule, equation (5), to determine the fatigue life. For consistent periodic loading is the application of rainflow counting is not of added value. Rainflow counting is especially useful for un-regular complex stress cycles. Each cycle obtains its own strain range and is plotted vertically, see Figure 3-6 as example. The name and method originates from the two Japanese researchers Matsuiski and Endo who described the process of rain falling from a pagoda style roof. Later this method was used as an algorithm for cycle counting and is applied to the fatigue analysis. [27]

Figure 3-6 demonstrates a schematic view of the rainflow counting method. The top of the figure illustrates the irregular stress history over a period of time. Using the peaks, indicated from A to I, the stress ranges can be determined. These stress ranges and cycles are then graphically shown in the graph below, with the stress on the y-axis and strain on the x-axis.

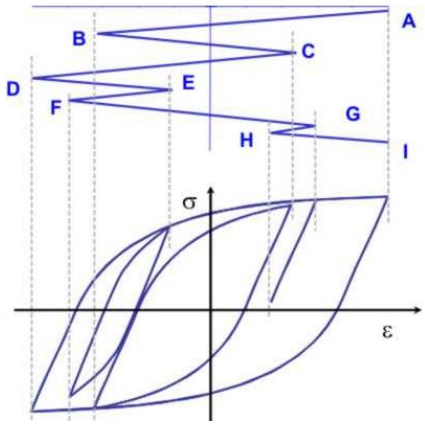

FIGURE 3-6 RAINFLOW COUNTING

3.3. FOURIER TRANSFORM

The Fourier transformation is a function that converts a time domain record into frequency domain record. When adding an infinite number of sine waves with infinite small amplitudes it is able to measure the density of frequencies. This density of these frequencies will be higher around some frequencies than others. This is eventually the frequency spectrum of a wave form. Figure 3-7 provides a schematic illustration of the connection between the time domain, demonstrated with the red f, and the frequency domain, the blue $\hat{f}$. The time domain f wave is the result of independent sinewaves added together. The frequency domain,$\hat{f}$, demonstrates the frequency peaks. [28]

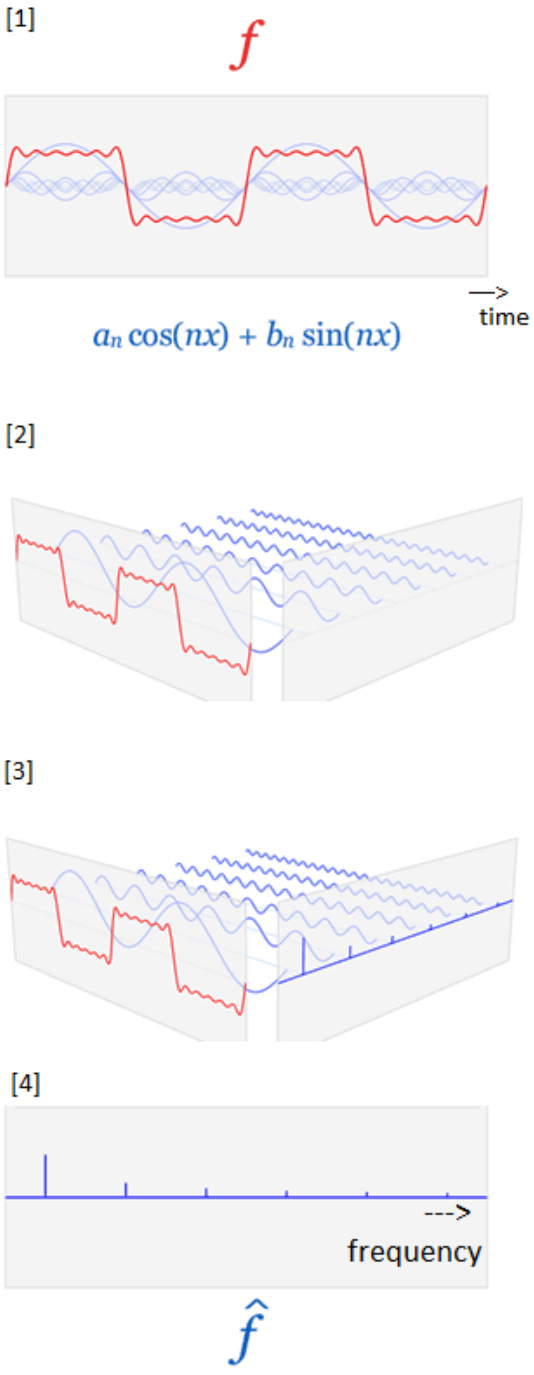

FIGURE 3-7 SCHEMATIC ILLUSTRATION FOURIER TRANSFORM

The continuous Fourier Transform (FT) is denoted in equation (6).

$$X(F) = \int_{-\infty}^{\infty} x(t) exp(-j\ 2\ \pi\ f\ t)\ dt \tag{6}$$

Where;

X(F)	= Fourier Transform	[-]
x(t)	= the function	[-]
$exp(-j\ 2\ \pi\ f\ t)$	= analysing function	[-]
f	= frequency	[Hz]
t	= time	[s]
j	= complex	

3.4. DAMPING

Since offshore wind structures are installed in deeper locations and are designed as a more flexible and lighter structure, damping is an important aspect to consider for complete dynamic analysis. Damping should be incorporated in the design model to avoid overestimation of dynamic amplifications that could result in unrealistic low estimated fatigue life. The phenomenon 'damping' is defined as the dissipation of kinetic energy for vibrating systems. The damping capacity is described as the energy dissipated in one cycle of oscillation with respect to the total energy in the structure within that cycle.

There are active and passive damping mechanisms that can be applied to the structure. The passive damping devices have no energy input into the system. It reduces the vibration problems by increasing the structural damping with regard to friction joints, viscous material or tuned mass dampers (more detail in section 3.4.3). Active damping tools control damping with a closed loop relying on sensors.

The highest loads are obtained in the structure when the wind wave and current are coming from the same direction. For the fatigue analysis it is too conservative to assume this kind of loading and wind-wave misalignment is therefore assumed. It was found that that damping should be found from the soil- , hydrodynamic- , tower oscillation-, structural material- and Rayleigh damping. Five types of damping are explained in more detail in section 3.4.1 till 3.4.5. [17] More over suggested critical damping percentages to apply to a model is provided in section 4.2.5.

3.4.1. SOIL DAMPING

When designing jacket offshore wind turbines, the pile foundation and soil damping are important aspects. To analyse these aspects standards such as DNV suggest using the Winkler Model approach. For this approach the soil is assumed as a system of closely spaced independent linear springs, with no shearing across. The pile is modelled as an elastic beam, the Winkler model is illustrated in Figure 3-8.

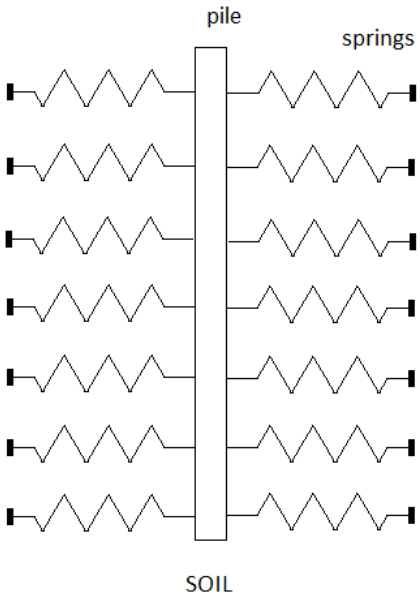

FIGURE 3-8 WINKLER MODEL

It is a method describing that the vertical resistance of a ground against external forces can be assumed to be proportional to the ground deflection. When performing a natural frequency analysis it is common to obtain a linear modal analysis where the spring stiffness is gathered from the initial spring stiffness of the

non-linear p-y curve. This p-y curve is a function of depth, soil type, pile dimension and properties. The non-linear function relates y, the deflection of the spring or in other words, the soil reaction, and p, the applied force to the spring. This method is used to determine the soil damping of the first bending mode. [13]

Previous research regarding soil damping has been performed. [12] So was the first natural bending frequency of a monopile obtained from rotor stop test to generate the corresponding damping ratio. The soil damping contribution was then determined from each individual contribution to the total system damping ratio. From this it was believed that the soil damping, as well as the implemented tower oscillation dampers, has the largest contribution to the total damping system of offshore wind turbines on a monopile foundation, when considering rotor stops.

However, limited sufficient data regarding exact amount of soil damping is available. Literature states to apply between 0.17 – 0.72% of critical soil damping for monopile structures. [64] [65]. Furthermore, for a parametric study performed by C. Latini, with a small dimeter (1:3m) hollow, flexible, steel pile in homogeneous soil layer, 2.5% of critical damping was selected. [66]

3.4.2. HYDRODYNAMIC DAMPING

Due to the applied forces the structure is vibrating in the water and experiences hydrodynamic damping. Hydrodynamic damping has a considerable effect in offshore structures. The main sources to hydrodynamic damping are radiation and drag induced effect. Drag is the dominant contributor to the hydrodynamic damping and its magnitude is depended on the drag coefficient used in the Morisons equation;

$$F = \frac{\rho}{2g} Cd\ D\ u\ |u| + \frac{\rho}{g}\ Cm\ \frac{\pi}{4} D^2 \dot{u} \tag{7}$$

Where;

F	= force	[kN]
ρ	= density water	[kg/m^3]
g	= gravity	[m/s^2]
C_d	= drag coefficient	[-]
D	= diameter	[m]
u	= flow speed	[m/s]
C_m	= inertia coefficient	[-]
$\dot{u}$	= acceleration	[m/s^2]

The damping coefficient relies on the size of the structure and the incoming wave length. This coefficient is related to Reynolds number and is affected by the shape of the structure. [17]

3.4.3. TOWER OSCIALLATION DAMPING

Wind turbine vibrations are caused by the wind interacting with the tower and rotor blades. The oscillations are initiated due to the 'tower shadowing' principle as explained in section 3.1. There are three damping control techniques for structures; the passive -, semi-active - and active feedback control method. The semi-active and active feedback control implementations have not been applied to wind turbines yet.

Conversely, several passive control systems exist that are placed in the nacelle of the turbine to damp the excitations. The 'tuned mass damper' (TMD), 'pendulum damper', 'tuned sloshing damper (TSD)' and 'tuned liquid damper (TLD)' are invented passive systems that are applied nowadays. All these dampers can be represented as a mass-spring-damping system. These passive structural control systems have no energy input into the system and consist of a constant spring and damper. It is tuned such that the energy of one of the natural frequencies is absorbed. [19]

Moreover the liquid dampers; a particular form of the TLD is the tuned liquid column damper (TLCD). This is an 'U' shaped damper filled with a liquid that uses the gravitational restoring force of the liquid as a damping mechanism, illustrated in Figure 3-9. The frequency of oscillation of the liquid is tuned for the natural frequency of the structure. The tuning ratio is the ratio of the natural frequency of the TLCD with respect to the structure. This ratio is such selected that an efficient transfer of shear forces from the TLCD to structure is created.

The TLCD have various advantages and disadvantages [20];

The advantages include being able to dissipate lower amplitude excitations compared to TMDs. Furthermore this passive damping device requires small amount of auxiliary equipment, personal and power to operate, maintain and is easy to install. Another advantage regarding the system is that it is applicable for a wide range of excitation levels. Soil properties could change over the life time of the structure. Normally a damping system is for a certain frequency specific while this system is able to dampen the shifted frequency to some degree.

Disadvantages involve the space the damper requires; the 'U' shaped damper needs some horizontal length to perform sufficiently. This is a considerable challenge when installing this in the nacelle of the wind turbine since there is not appropriate volumetric space available. That is why sometimes it is physically unable to obtain the optimal tuning conditions.

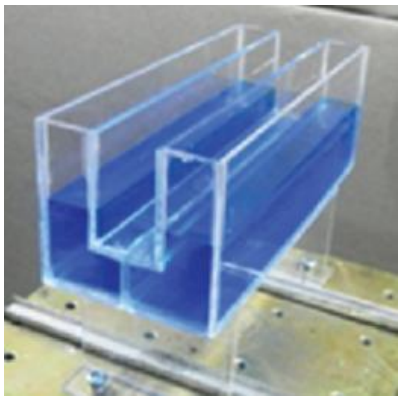

Figure 3-9 U-shaped TLCD [21]

3.4.4. STRUCTURAL MATERIAL DAMPING

Structural material damping is defined by the molecular complex interaction within the material. Therefore the material damping is related to the type of material, method of manufacturing and final finishing processes. [17] Structural damping is also known as hysteretic damping. When the structure is subjected to vibration the stress strain diagram shows a hysteresis loop, pictured in Figure 3-10.

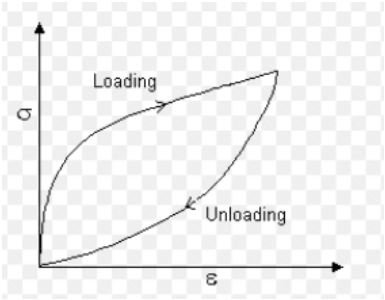

FIGURE 3-10 HYSTERESIS LOOP

The area of this loop defines the energy lost per unit volume of the structure per cycle due to damping. From experimental data is was noticed that energy loss per cycle, due to internal friction, is independent of frequency. This can be expressed in the following manner [18];

The relationship between the response 'x' and excitation force for viscous damping can be described as;

$$F(t) = (-ic\omega + k)x \tag{8}$$

Where;

F(t)	= excitation force	[kN]
i	= imaginary	[-]
c	= damping coefficient	[-]
ω	= frequency	[Hz]
k	= stiffness	[N/m]

The energy loss of one cycle is the area of the hysteresis loop and can be defined as;

$$\Delta E = \pi\omega c X^2 \tag{9}$$

Where;

ΔE	= energy dissipation	[kg.m^2/s^2]
X	= amplitude	[m]

To express the perceived behaviour, a damping coefficient is assumed to be inversely proportional to the frequency;

$$c = \frac{h}{\omega} \tag{10}$$

Where;

h	= hysteric damping coefficient	[-]

When substituting equation 10 in to equation 9 the following relationship is obtained that demonstrates that the energy dissipation is indeed independent of the frequency.

$$\Delta E = \pi h X^2 \tag{11}$$

Since the material selection is not related to the frequency, for this research the change in material has no effect on the brace amplification and is thus not considered.

3.4.5. RAYLEIGH DAMPING

Rayleigh damping is viscous damping which is a combination of the mass and stiffness term, where the stiffness is linear proportional and the mass term inversely proportional to the response frequency. The coefficient could be used in structural models. [15] When considering a general dynamic system, the Rayleigh damping coefficient is expressed as;

$$[C] = \alpha [M] + \beta [K] \tag{12}$$

Where;

α	= coefficient	[-]
β	= coefficient	[-]
[C]	= damping matrix	[-]
[M]	= mass matrix	[kg]
[K]	= stiffness matrix	[N/m]

Figure 3-11 provides a schematic example of a Rayleigh graph.

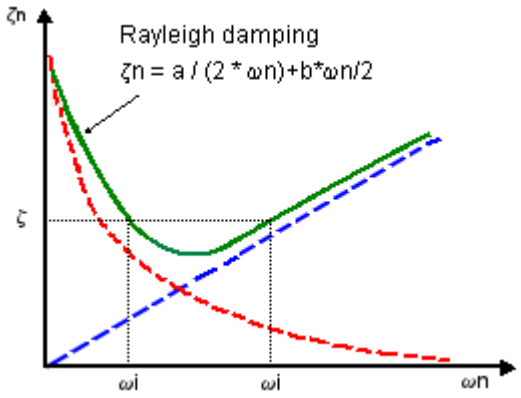

FIGURE 3-11 RAYLEIGH DAMPING [30]

Rayleigh damping has the advantage that for structures having a large number degrees of freedom (DOF) the damping matrix can be reduced using orthogonal transformation into an n-number of uncoupled equations. It is worth mentioning that the initial estimation of α and β coefficients is rather difficult, especially by increasing number of DOF. [16] The downside of Rayleigh damping is that the achieved damping ratio varies as the response frequency varies.

It can be seen in Figure 3-11 that outside the range of the two selected frequencies, the damping increases drastically, resulting in almost total cancellation of the modal response. Meaning, Rayleigh damping is effective in damping out the low and high frequency responses that are out of the frequency interest domain. It is suggested that the two chosen frequencies, which will determine the Rayleigh damping, provide acceptable damping values in all the modes that have a dominant influence on the vibration. [62]

3.5. MARINE GROWTH

Marine growth on offshore structures is the attachment of living organisms on structural components in water and the splash zone and is depth related. It is an important aspect to consider since it changes the structural integrity of the members and has influence on the natural frequency of the structure.

Previous research has been conducted regarding marine growth. [8] It was recorded at which locations certain kind of marine growth was found. Recorded species include mussels, kelp, algae, barnacles, tube worms, hydroids, bryozons, sponges, anemones, sea-squirts and alcyonium. The blue mussel needs special attention since it exist around 20 – 30 meters of water depths. The current is an important aspect to consider, even though the blue mussel mainly exists in shallow waters and shore lines, the current allows species to reach the structures. Below the mussel zone mainly tubeworms and hydroids are found.

There are two main effects that marine growth has on offshore structures that need to be deliberated;

First, the attachment of the organisms causes extra mass to the structure. Since the marine growth does not add to the structural stiffness of the structure a decrease in natural frequency is found. For large offshore platforms is the overall effect of the additional dead weight is considerably small. The added mass however, to offshore wind turbines has a more dominant influence on causing a potential shift to a lower natural frequency. This is because the offshore wind turbine structures are light weighted designs compared to offshore platform, so any additional mass is having a larger effect.

Secondly, the other effect to consider is that the hydrodynamic properties of the structure will change, when analysing the Morrison equation. Marine growth represents an increase in diameter resulting in an increase of wave and drag loading. Furthermore the drag and inertia hydrodynamic coefficients, Cd and Cm, will be affected when the surface roughness changes from smooths to rough, showing a decrease in Cm coefficient for a rough cylinder. Furthermore the vortex induced vibrations changes due to the marine growth also need to be considered.

To delay marine growth on offshore structures, control coatings could be used that provide a low-friction and smooth surface that biofouling organisms find difficult to attach to. Other new techniques are used such as the ‘wave driven marine growth preventer’; this invention consists of multiple or single rings that move up and down along the jacket members. The movement of the rings is caused by the ocean waves, swells and tidal fluctuations preventing the organisms from attaching. [7] If undesired marine growth does occur, regular cleaning measurements by deep sea divers or ROVs could be implemented.

There are uncertainties in modelling marine growth for the fatigue analysis. Several guidelines are provided for such analysis of the structure. The DNV_OS_J101 is used for the jacket structures of this particular project. This code mentions to use a uniformly distributed growth of 100mm at a depth from MSL till -40m and 50mm growth below this -40m depth, as shown in Figure 3-12. This suggests that there is a clear line in marine growth thickness differences at the 40m depth which is unrealistic. [9]

Furthermore it is unclear when to account for marine growth since in the first couple of years the structure will be clean. These assumptions will affect the fatigue analysis of the members. In this research the DNV_OS_J101 guideline with regard to marine growth is followed, but more in depth research regarding these values and assumptions is recommended.

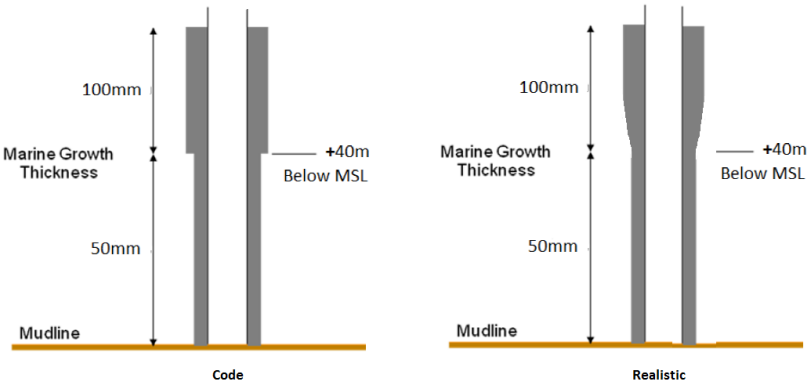

FIGURE 3-12 MARINE GROWTH

3.6. COUPLED VS DECOUPLED ANALYSIS

It is a rather complex challenge to analyse the complete offshore wind turbine and jacket substructure model. Well-thought and comprehensive models with different applied forces should be examined to ensure reliable results are obtained. It is common to consider coupled and decoupled models to simplify and reduce the calculations. Non-linear coupled models are a representation of the complete offshore wind turbine and substructure which include the soil-, hydro- and aerodynamic analysis. Decoupled models contain the substructure only with an applied dummy pile and/or point mass representing the wind turbine. For the linear decoupled model a hydro-elastic analysis is conducted with the wind loads applied by time-dependent forces and moments at the point mass.

Previous research considered two possible methods to apply the aerodynamic forces to the linear decoupled models. [14] One method is to apply the wind loads, obtained from the coupled model, as time dependent point loads in the decoupled model. The other option is that the thrust and torque from a rotor model is used as wind load on the decoupled model in combination with a linear aerodynamic damper. Several iterations between coupled and decoupled models are necessary during the designing procedure of the complete structure.

Previous research, performed by MARINTEK, compared results from both nonlinear coupled and linear decoupled models to obtain a good understanding between the differences of the two models. For this particular research a 5 MW wind turbine with a supporting jacket structure in 50m water depth was analysed. This was performed by conducting eigen-frequency analysis, decay test and dynamic simulations with wave only and wind-wave conditions. [14]

From the eigen-frequency analysis it was seen that the decoupled model provides shorter natural periods in the 1st mode compared to the coupled model. This can be explained since for the coupled model the complete turbine with flexible blades is modelled while for the decoupled model only a point mass/inertia representation is used. Due to this the non-linear coupled model acts in a ‘softer’ manner, meaning lower natural frequencies, and therefore having higher natural periods than the decoupled model.

From the dynamic simulations it could be concluded that the results for non-linear coupled and decoupled models are in good agreement. The differences obtained were due to the fact that the models have different wave load implementations and that different programs were used. The changes were not affected due the difference of using non-linear and linear models. It is preferred to do a decoupled analysis since the complexity and calculation time is reduced. Since good agreement was showed between coupled and decoupled models, this research will perform a decoupled analysis. So will the support structure be analysed with a simplified wind turbine model on top.

4. GENERAL SUBSTRUCTURE DESIGN PROCESS

This chapter provides a clear overview of the general steps involved in designing a complete offshore wind structure. It explains the flowchart shown in Appendix K and clarifies the block diagrams within. It is worth mentioning that the flowchart mainly focusses on the avoidance of resonance and where in the design process this should be considered.

In section 4.1, first the total design is explained, consisting of the wind turbine design, substructure design and pile foundation design. It shows how the different structures are connected and the global process in achieving the final complete design.

This is followed by a detailed description of the substructure design steps provided in section 4.2.

In section 4.3 the coupled analysis between the three designs is explained and the feedback mechanism that is used as optimisation of the substructure.

4.1. COMPLETE DESIGN

The flowchart is separated in three main horizontal blocks that represent the sections of the complete design;

1. Wind Turbine
2. Substructure
3. Pile foundation

1. The top block represents the wind turbine design; the wind turbine specifics are provided by the wind turbine designer when designing the substructure, hence in the flowchart the arrow pointing towards the substructure from the wind turbine design. These are input values which define the characteristics of the substructure, such as forcing frequencies generated by the wind turbine.

2. The middle block embodies the substructure design; the substructure connects the wind turbine to the seabed. It provides a load path into the pile foundation.

3. The bottom block symbolises the pile foundation design; the pile foundation and substructure have a close interaction and are therefore represented in the flow chart as a double arrow. The soil-structure interaction is evaluated at this section.

4.2. SUBSTRUCTURE DESIGN STEPS

There are several steps and iteration processes involved in designing the substructure. This section defines the ‘basis of design’, ‘concept design’, ‘preliminary design’ and ‘detailed design’ steps and also describes the looping aspects involved in the process.

4.2.1. BASIS OF DESIGN

The basis of design is provided by the client. It includes aspects such as the site location and the environmental conditions such as the wind, wave/current and possible ice conditions. The combination of the water depths and wave heights define aspects such as the height of the structure and required air gap.

Furthermore it is worth mentioning that at this stage the wind turbine design, such as information regarding the capacity, is already known and is provided by the turbine designer. This data offers as general input value regarding for instance about the required size of the substructure.

The client also specifies requirements such as the design life time of the substructure and its capabilities.

4.2.2. CONCEPT DESIGN

Once the basis of the design is known, several substructure concepts are considered that would be suitable for the particular project. This flowchart only expresses the bottom founded structures, since it is the main focus of this thesis. The substructure selection is usually obtained with the use of a MCA.

At this point in the project the overall forcing frequencies are generally known. It is essential to consider these forcing frequencies at an early stage of the project to establish at which frequency ranges the substructure should not be designed for the avoidance of resonance. At this stage once the concept lay out is selected, a rough estimate of the natural frequencies of the individual members should be gathered.

A zoom-in on the forcing frequencies is represented in the yellow block below. More details regarding this and the connection it has with the substructure detailed design is provided in section 4.2.5.

4.2.3. PRELIMINARY DESIGN

At the preliminary design stage the Front End Engineering Design, FEED, of the project is taken into account. This defines a rough estimate of the layout of the substructure. Decisions regarding the fabrication yard, transportation and installation method define the estimated weight and size of the structure. A quick check should also be performed to grasp that these member dimensions do not roughly overlap with the forcing frequencies.

During the life time of the structure maintenance is essential and needs to be incorporated at an early stage of the process as well. Finally after the structure is at the end of its life time it has to be decommissioned.

Initial assumptions are made during this step, once more detailed information regarding the substructure is known the initial assumptions should be checked. This is represented as the arrow pointing form the ‘detailed design’ to the ‘preliminary design’ named; check assumption.

4.2.4. DETAILED DESIGN

At the detailed design stage all the individual members are carefully designed. Once the member dimensions are established, various load combinations are applied to estimate the structure’s behaviour.

The members undergo several limit state design checks to ensure that the substructure including all the individual members is fit for purpose. A limit state is the condition for which a structure or a component of the structure has failed the design requirements. The limit states are mentioned in the flow chart and are described in more detail below. [56]

Ultimate Limit State (ULS)

The ultimate limit state defines the maximum load carrying resistance of the member. It describes all the possible failure modes such as;

- The loss of structural resistance due to yielding and buckling
- Failure due to brittle fracture
- Loss of equilibrium of the structure
- Ultimate deformation of members
- Collapsing of individual members or complete structure

Serviceability Limit State (SLS)

The serviceability limit state refers to the limits on acceptable performance of the structure. [57] it includes aspects such as;

- Deflections that could change the effect of the acting forces
- Deformations that possibly adjust the distribution of loads between supported rigid objects and the supporting structure
- Extreme vibrations
- Temperature-induced deformations
- Differential settlements of foundations soil causing inclination of the structure
- Motions that exceed the limitations of the equipment

Accidental Limit State (ALS)

Accidental limit state represents the limits the structure can withstand of the occurrence accidental loads. This includes;

- The structural damage
- Ultimate resistance of damaged structures
- Loss of structural integrity due to local destruction

Fatigue Limit State (FLS)

The fatigue limit state defines the limit of cumulative damage due to repeated loads that the structure can withstand.

This thesis mainly focussed on the fatigue aspects of a structure. The flowchart shows a blow up of the FLS and a detailed description of which factors to consider and the mitigation measurements to imply to avoid resonance. This is explained in more detail in section 4.2.5 and the connection between the forcing frequencies.

Design Loop

The arrow from the FLS represents a simplified design loop of the members. If any mitigation measurements are implied with regards to the natural frequencies, which results in a change of member dimensions, the other limit states should be checked again to ensure the members still comply with all the requirements.

4.2.5. FORCING FREQUENCIES VS DETAILED DESIGN

The aim is to design a structure where natural frequencies do not overlap with the forcing frequencies to avoid resonance. Once the member details are know the natural frequencies can be calculated and compared with the input forcing frequencies. The arrow between the 'forcing frequencies block' and the 'Detailed design with regard to avoiding resonance' represents this comparison.

In the sections below a comprehensive explanation regarding the two blocks 'Forcing Frequencies' and 'Detailed design with regard to avoid resonance' is provided.

As mentioned before, in the forcing frequencies are already roughly established at an early stage of the project. This is a useful tool to decide for which frequency ranges the substructure could be designed for.

There are various forcing frequencies to consider which are shown in the 'Power Spectral Density vs Frequency' graph. These frequencies are due to the environmental forces; wind, wave and current, and the wind turbine structure forcing frequencies. This is in contrast to the oil and gas jackets where the wind turbine forcing frequencies are not present.

The exact forcing frequency ranges due wind turbine structure varies for each particular turbine. This research provides the general forcing frequency ranges which are based on literature on previous installed turbines, [45] [46] [58], and the turbine of the reference project.

The forcing frequencies generated by the wind turbine of the reference project showed almost identical tower bending forcing frequencies as described for the three-bladed turbine mentioned in [45] and was therefore used as reference material. A comparison is shown in Appendix J.

When analysing the power spectral density (PSD) graph shown in the flowchart the following excitations are visible;

- *Environmental*
  The first peak shown on the graph represents the wind forcing frequencies, followed by the wave spectrum. These forcing frequency spectrums are in detailed explained in section 3.1.1
- *1P*
  This is due to the excitation of the tower movement by any rotor imbalance and turbulence excitation
- *3P*
  This is due to the blade-tower passing motion and turbulence excitation
- *6P*
  This is due to turbulence and the excitation of the forward and backward whirl by the blades passing the tower.
- *9P*
  This is due to turbulence and the excitation of the collective edgewise mode by the blade tower passing
- *Tower*
  These excitations are caused by the lateral and longitudinal tower bending movements as well as the torsion movement of the drive train.
- *Flap Forward Whirl*
  These are excitations caused by the blade movements
- *Blades*
  The edgewise and flapwise forward and backward whirl movements of the blades cause excitations in the high frequency ranges.

There are three frequency ranges indicated on the PSD graph that are suitable for substructure design;

- *Soft – soft*
  A low frequency range around the 0.1 Hz. This provides a rather flexible design.
- *Soft – stiff*
  A frequency range between the 1P and 3P excitation around the 0.3 Hz
- *Stiff – stiff*

Reaching the higher frequency ranges, starting after the 3P excitation onwards. Aiming to avoid any other tower and blade frequencies generated by the wind turbine.

DETAILED DESIGN WITH REGARDS TO AVOIDING RESONANCE

During the detailed analysis the exact dimensions of the individual members are known, which allows for calculation of the local and global eigen-frequencies of the structure. This can be performed with the ANSYS modal analysis and verified with hand calculations as described in section 5.2.1. The eigen-frequencies should be out of the range of the forcing frequencies, which are identified in the section above, to avoid resonance at all times. If resonance takes place, the estimated fatigue life of the structure decreases dramatically and will not comply with the requirements.

There are various factors that influence the natural frequency of the individual members and the way these values are obtained with the use of a model. These factors have an effect on the establishment of resonance and should be considered in the design;

Factors affecting the natural frequencies

There are multiple factors that have an effect on the natural frequencies of the members that should be considered when designing the members. These factors are summarized below;

- Mass
- Stiffness
- Hydrodynamic added mass

Aspects of the member that influence these factors are the following;

- Marine growth
- Diameter
- Shape
- Length
- Wall thickness

Factors affecting the model

A model of the structure is a simplified version of the structure that should represent the structures behaviour as close as possible. To ensure this, various aspects should be elaborated;

- *Boundary Conditions*

  The way the members within the structure are connected as well as the connection to the ground is of great importance when analysing the model. Multiple connections could provide a variety of results. The engineer should aim to select the most suitable boundary conditions with the correct assumptions
- *Mesh*

  The type and the size of the mesh express the structure's response. The goal is to obtain a mesh that provides accurate results with reasonable calculation times. A sensitivity analysis with regards to the refinement of the mesh and the results is required to obtain a good understanding which meshing is most suitable. Furthermore, the wall thickness of the elements effects the mesh selection.

- *Element selection*

  There are multiple elements that could be selected for the model, for example a beam or shell elements. These elements have their own characteristics and define the models behaviour. The engineer should be well aware of the difference between the elements to select the most appropriate one.

- *Damping*

  Damping is an important aspect that should be included in the model. Especially with regards to the fatigue, including damping is essential. To apply the correct amount of damping is rather difficult and in limited understanding regarding it is present. This research provides suggested damping percentage of the critical damping that should be added to sections of the structure. These values are based on previous research and literature on offshore wind turbine structures. These values correspond with the DOWEC study. [14][58][59][60]

Substructure	1%
Blades	0.48%
Nacelle + hub	2%
Drive train shaft	5%
Tower	1%

  Aerodynamic damping is an important aspect to take into account for slender structures such a wind turbines where the structural motion reduces the effective wind force. To determine the correct aerodynamic damping the frequency response to the wind power spectrum should be evaluated. [63]

  As mentioned before, limited sufficient data regarding soil damping is available. Literature states to apply between 0.17 – 0.72% of critical soil damping for monopile structures. [64] [65]. Furthermore, for a parametric study performed by C. Latini, with a small dimeter (1:3m) hollow, flexible, steel pile in homogeneous soil layer, 2.5% of critical damping was selected. [66]

Mitigation measures

If it turns out that the designed members show resonating behaviour in the coupled analysis, various mitigation measures can be implied to obtain a frequency shift out of the excited frequency range. The table in the flow chart demonstrates which adjustments can cause an increase or decrease in frequency.

Natural frequency for offshore structures with a free top end

The formula provided in the flowchart is the natural frequency for a single beam element. However the natural frequency for a general offshore structure with a free top end, in deep water, can be considered as a multi-mass which is supported with four spring elements.

The natural period is the defined as;

$$T_{n=} \frac{2\pi}{\omega_n} \tag{13}$$

Where;

ω_n = natural frequency [rad/s]
T_n = natural period [s]

The equation representing the fundamental natural period for the multi-mass with a free top end is the following, which is defined in chapter 9 of the 'Handbook of Bottom Founded Offshore Structures' [61]. The fundamental natural period is the highest period of a periodic wave form.

$$T_n^2 = T_{nl}^2 + T_{nr}^2 + T_{nb}^2 + T_{ns}^2 \tag{14}$$

Where;

T_n = natural period [s]
T_{nl} = natural lateral period [s]
T_{nr} = natural rotational period [s]
T_{nb} = natural bending period [s]
T_{ns} = natural shear period [s]

Since the bending period is the most dominant term in the equation, the equation becomes

$$T_n^2 = T_{nb}^2 \left[1 + \frac{T_{nl}^2}{T_{nb}^2} + \frac{T_{nr}^2}{T_{nb}^2} + \frac{T_{ns}^2}{T_{nb}^2}\right] \tag{15}$$

The natural period of any system can be generalized to;

$$T_n^2 = 2\pi \frac{m^*}{k^*} \tag{16}$$

Where;

T_n = natural period [s]
m^* = generalized mass [kg]
k^* = generalized stiffness [N/m]

The natural period for the general offshore structure with a free top end then finally becomes;

$$T_n^2 = T_{nb}^2 \left[1 + \left(\frac{m_l^*}{m_b^*} \cdot \frac{k_b^*}{k_l^*}\right) + \left(\frac{m_r^*}{m_b^*} \cdot \frac{k_b^*}{k_r^*}\right) + \left(\frac{m_s^*}{m_b^*} \cdot \frac{k_b^*}{k_s^*}\right)\right] \tag{17}$$

4.3. COUPLED ANALYSIS

Once the wind turbine, the substructure and the pile foundation designs are determined a coupled analysis is performed of the complete structure. The overall structural stability and the behaviour of the complete structure are evaluated. Furthermore the estimated fatigue life is calculated.

The modal analysis is performed during the coupled analysis with regards to the global structure and the local members. The mode shapes are obtained for various frequencies to determine the occurrence of any resonance happening.

Once the coupled analysis is performed and the global and local behaviour of the complete structure is evaluated, optimisation of the substructure is executed. For this step in the process, it loops back into the

detailed design analysis. The coupled analysis could possibly demonstrate that some members show undesired behaviour and need to be adjusted. When the members are resized the steps in the detailed analysis are repeated which involved the analysis of various load combinations and design checks.

Finally, when all sections of the complete structure; the wind turbine, substructure and pile foundation design are optimised and checked the complete design is finalised.

5. PROBLEM IDENTIFICATION

This chapter identifies the problem that was stated in the beginning of the thesis. It was found by the substructure designer that the vibration amplification of the braces are occurring since the frequencies of the applied forces are in the same frequency range as the eigen-frequency of the braces. The following steps were performed to establish this and to obtain a better understanding of the fatigue issues of the jacket.

To determine the overlapping of frequencies, both the frequencies due to the applied forces as well as the eigen-frequencies of the braces were analysed. First the applied loads were analysed with the use of Fast Fourier Transform, FFT, to analyse what frequency region is excited. A MATLAB script was created during this research to perform these analyses, moreover is found in section 5.1.

This was followed by an examination of the global and local natural frequencies of the offshore wind turbine structure, explained in section 5.2. The structure is modelled in ANSYS and a modal analysis was performed to obtain the mode shapes and natural frequencies. A modal analysis is used to determine the vibration characteristics of a system.

Section 5.3 provides a comparison of the forcing frequencies and the eigen-frequencies of the braces. Furthermore the effect of resonance is explained.

5.1. FORCING FREQUENCIES

This section explains in detail the method and results obtained of the applied forces on the offshore wind turbine structure. First the method is explained followed by the obtained results.

5.1.1. METHOD

The designer had performed a time-force analysis of the full jacket and turbine. This consisted of an analysis with a total duration of 630[s] which recorded specific information every 0.04[s] at +22m LAT of the turbine. The recordings included the forces and moments in the x, y, z, and xy direction, wind speed at the hub and deflection in x, y, z direction.

The data consisted of iteration 1.7 from cluster 1 of the jacket structures. Even though cluster 5 is analysed in this research, the data of cluster 1 is sufficient since wind-wave statistics are similar for the complete wind farm. Load case 1.2 was provided since this load case showed the brace excitation. The data included 58 cases varying in wind, wave directions and in wind speed. This research used these loads for a FFT to obtain the frequency domain of the data. This was done to examine at which frequency ranges the excitation would occur. The program MATLAB was used to import the data and with the use of a script the FFT performed. The script and the essential graphs are found in Appendix A. Nyquist sampling theorem was inserted to incorporate the aliasing effect.

5.1.2. RESULTS

The designer had found that the main excitations were caused for the moment in the y-direction, My. The y direction in this coordinate system is divined as perpendicular to the turbine blades. For different wind speeds the My, was analysed and it was observed that between 2 – 2.5 [Hz] energy is present. It was found by the substructure designer that this is the same frequency range as the eigen-frequency of the local braces in bay 3 and 4. In Figure 5-1 the power density spectra graph of a wind speed of 24 [m/s] and wind-wave direction of 75 [deg] is shown, having along the x-axis the frequency in Hz. At these conditions the most

dominant brace vibration amplification was found. Other graphs with different wind speeds and wind-wave direction can be found in Appendix B.

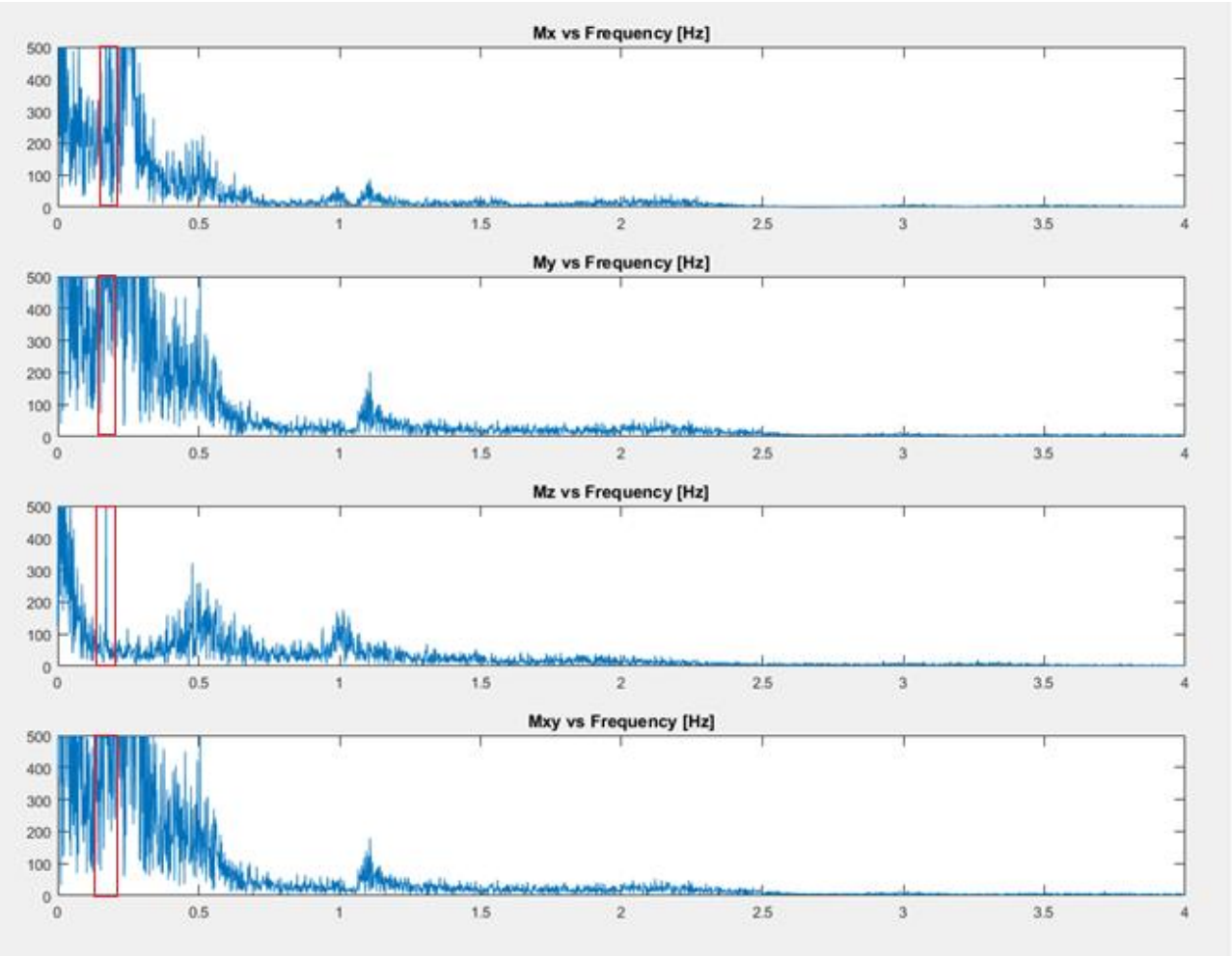

FIGURE 5-1 POWER DENSITY SPECTRA; WIND SPEED 24[M/S], WIND-WAVE DIRECTION 75[DEG]

When analysing the graph the following is observed;

- The 1P at 0.172 Hz is clearly shown. This is highlighted in red on the graph. [37]
- The Rayleigh wave distribution is clearly seen around 0.2 - 0.5 Hz
- Excitation around 2 – 2.5 Hz is visible
- 'white noise' is found from 2.5 Hz onwards

The excitations around 2 - 2.5 Hz are due to the turbine forces. The eigen-frequencies of the tower and the blades cause these vibrations. This is because of the flapwise as well as the edgewise movement of the turbine blades and the tower bending movement. Moreover this behaviour can be found in section 3.1.2.

The results demonstrate that the designer's findings are reproduced. From this graph it can be seen that designing the eigen-frequencies of the local sections of the construction above 2.5 Hz would be preferable. This is because when the forcing frequencies and the eigen-frequencies are the same resonance could occur which has negative effect on the fatigue life of the system.

5.2. STRUCTURAL EIGEN-FREQUENCIES

This section demonstrates the calculations of the structural eigen-frequencies of 1. local and 2. global members.

5.2.1. METHOD

Modal analysis within ANSYS is used to obtain the eigen-frequencies and mode shapes of the global offshore wind turbine jacket and the local braces of bay 3 and 4 of cluster 5. First the local brace modes (1) are examined followed by the global mode shapes (2). This is explained in more detail in the following sections.

1. LOCAL BRACE MODE ANALYSIS

The braces of bay 3 and 4 were modelled in ANSYS to analyse the mode shapes, illustrated in Figure 5-2. The natural frequency analysis was performed with fixed and pinned boundary conditions. The actual connection between the brace and the legs is somewhere in between, so these fixities settings provide a rough estimate. Bay 4 has an increasing diameter at the bottom of the cross brace to increase the stiffness.

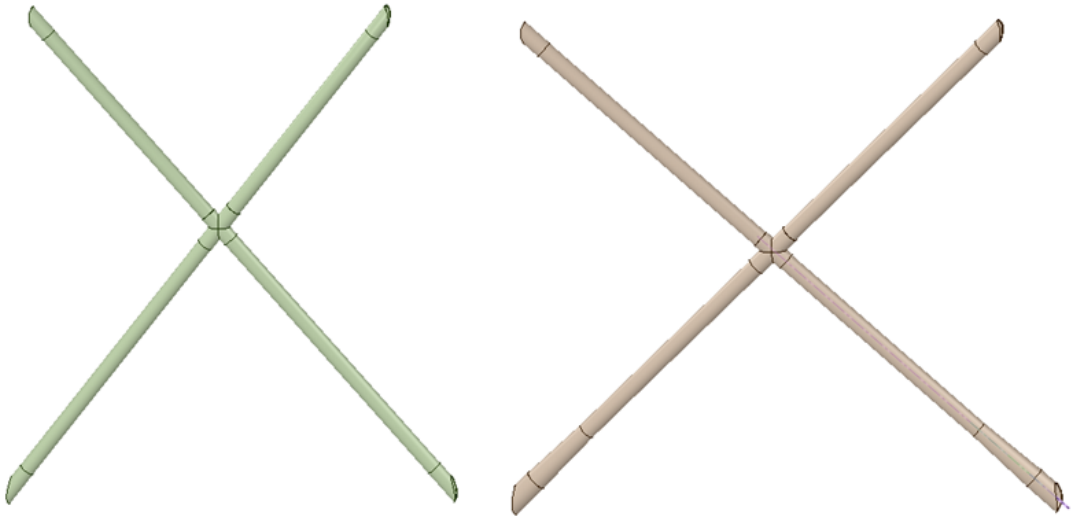

FIGURE 5-2 CROSS BRACE 3 AND 4

To verify that the obtained results of the cross braces in ANSYS are reasonable, a build-up of 3 simplistic models representing the jacket cross brace of bay 4 were analysed, shown in Figure 5-3. This was done for both fixed and pinned connection.

1. First a circular hollow cross section (CHS) with similar diameter of bay 4 is modelled in ANSYS and the natural frequency hand calculations are compared.
2. The second model has the same CHS dimensions as model 1 with a mass point at the centre. The cross brace in the jacket structure has a section with an increased diameter at the intersection to be able to create a connection between the two diagonal braces. This increased diameter is represented as a mass point in the middle of the brace.

3. The third simplistic model is a cross brace with a middle mass. Furthermore to be able to weld the cross brace to the legs of the jacket the nodes have an increase in diameter.

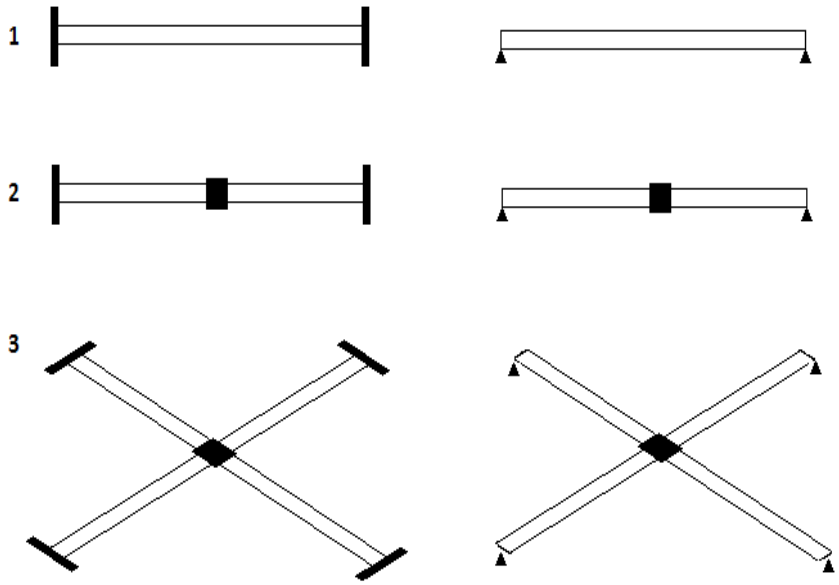

FIGURE 5-3 VERIFICATION STEPS MODEL

Sections 5.2.2.1 till 5.2.2.6 provide a detailed description regarding the analysis of the local cross braces. It is worth mentioning that the verification process was only applied to bay 4 of the jacket structure. Since bay 3 has the same lay out as bay 4 it requires the same verification steps. These steps done for bay 4 already represent that ANSYS results and the hand calculations are in good agreement.

2. GLOBAL OWT JACKET MODE ANALYSIS

The global mode shapes of the complete structure are analysed to obtain a better understanding of the structures behaviour. The jacket with a simplified transition piece and the turbine was created for the analysis in ANSYS. The turbine was modelled by creating the tapered diameters of the turbine and then transforming it to beam elements. [36] This way the mass and stiffness of the turbine is generated and are the meshing properties are simplified. The nacelle is modelled as a point mass of 431.2 ton on top of the turbine. The program controlled meshing option was selected to mesh the structure. The meshing used was carefully selected by iterations to obtain a satisfactory mesh with reasonable calculation time.

FIGURE 5-4 JACKET STRUCTURE + TP + TURBINE

To model the pile-soil reaction of the jacket piles, the piles were represented by springs of 5m long on each leg. These springs obtained coefficients that are calculated with the use of p-y, t-z and q-z curves and the soil properties, provided by the Geomechanics Department. [34] These uncoupled springs simplify the pile-soil reaction of multiple soil layers in a linear way. This is schematically illustrated in Figure 5-5 and the coefficients are provided in table. [38]

TABLE 5-1 SPRING COEFFICIENTS

Name	Symbol	Value	Unit
Rotational spring stiffness X	k_{x_rot}	5,027,284	[kNm/rad]
Rotational spring stiffness Y	k_{y_rot}	5,027,284	[kNm/rad]
Rotational spring stiffness Z	k_{z_rot}	680,490	[kNm/rad]
Translational spring stiffness X	k_{x_trans}	126,202	[kNm/m]
Translational spring stiffness Y	k_{y_trans}	126,202	[kNm/m]
Translational spring stiffness Z	k_{z_trans}	1,593,899	[kNm/m]

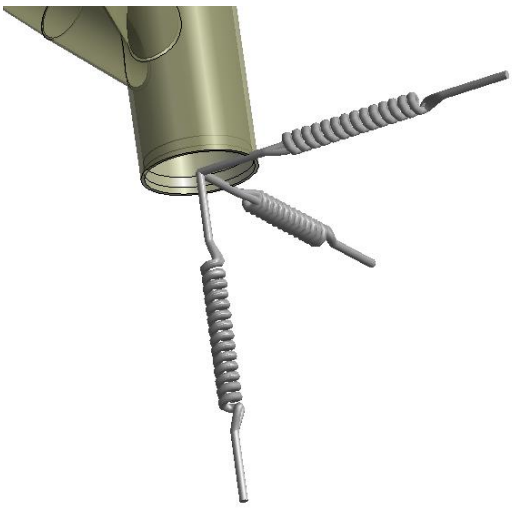

FIGURE 5-5 SPRINGS

Section 5.2.2.7 provides the obtained results of the global analysis in ANSYS and the adjustment of the frequencies to incorporate the added masses of the marine growth and the hydrodynamic forces.

5.2.2. RESULTS

This section provides the equations and the results obtained from the local and global calculations. The gathered values are discussed and validated.

5.2.2.1. CHS – FIXED-FIXED

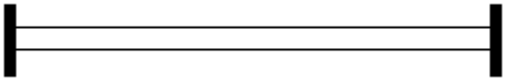

FIGURE 5-6 CHS FIXED-FIXED

To see how ANSYS calculates the natural modes within the program, a CHS with a fixed connection on both sides was analysed. The hand calculations as well as the obtained ANSYS results were compared. The dimensions selected are similar to that of the cross brace in bay 4 of the jacket structure. As mentioned, this is done to create a simplistic model that can be compared with the designed jacket cross brace. The formula used for a fixed-fixed construction is equation (19) and the values used are provided in Table 5-2. [29]

$$\omega_n = \left(n - \frac{1}{2}\right)^2 \left(\frac{\pi}{l}\right)^2 \sqrt{\frac{EI}{\rho A}} \tag{18}$$

$$\omega_n = \frac{c}{2\pi} \sqrt{\frac{EI}{\rho A L^4}} \tag{19}$$

TABLE 5-2 CHS 710X25

Name	Symbol	Value	Unit
Outer Diameter	*Do*	0.71	[m]
Inner Diameter	*Di*	0.66	[m]
Wall Thickness	*WT*	0.025	[m]
Length	*L*	30.7	[m]
Young's Modulus	*E*	2E+11	[pa]
Density	*ρ*	7850	[kg/ m^3]
Cross sectional Area; $\pi(Do^2 - Di^2)/4$	*A*	0.0538	[m^2]
Moment of Inertia; $\pi(Do^4 - Di^4)/64$	*I*	0.00316	[m^4]
Constant for the mode [29]	*c*	-	[#]
Natural Frequency	ω_n	-	[Hz]

The hand calculation, as well as the ANSYS model, results are illustrated in Table 5-3. It is clearly shown that both results are similar. As the modes increase, the difference in percentage increases. This can be explained since the hand calculations do not take into account that the roundness of the tube deforms when bent in these modes. Overall it can be said that at this point the ANSYS model approaches the natural frequency behaviour satisfactory.

TABLE 5-3 RESULTS CHS 710X25 FIXED-FIXED

Mode		Hand Calculation		ANSYS Model		Difference
n	c	ω_n	unit	ω_n	unit	[%]
1	22.4	4.63	[Hz]	4.69	[Hz]	1.16
2	61.7	12.76	[Hz]	12.79	[Hz]	0.21
3	121	25.03	[Hz]	24.74	[Hz]	-1.18
4	200	41.37	[Hz]	40.23	[Hz]	-2.84
5	298	61.64	[Hz]	58.96	[Hz]	-4.55

5.2.2.2. CHS – FIXED-FIXED WITH MIDDLE MASS

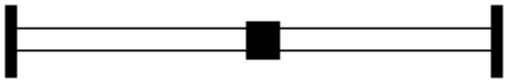

FIGURE 5-7 CHS FIXED-FIXED MIDDLE MASS

The cross brace of the jacket structure has an increased diameter at the intersection point. This is done to be able to obtain a connection between the two different diagonal braces. To be able to verify if the obtained natural frequencies of the cross braces are reasonable first a fixed-fixed CHS is modelled with a mass in the middle, representing the increase in diameter. The length of the mass is similar to the length of the connection point of the cross brace used for the jacket structure. Evaluating equation (19) and applying an extra mass in the equation due to the increased diameters provides the following equation;

$$\omega_n = \frac{c}{2\pi}\sqrt{\left(\frac{EI}{L_{rod}^3}\frac{1}{(\rho AL)_{rod} + (\rho AL)_{extra\ mass}}\right)} \tag{20}$$

TABLE 5-4 CHS 710X25 WITH MIDDLE MASS

Name	Symbol	Rod	Middle Mass	Unit
Outer Diameter	*Do*	0.71	0.76	[m]
Inner Diameter	*Di*	0.66	0.71	[m]
Wall Thickness	*WT*	0.025	0.025	[m]
Length	*L*	30.7	1.404	[m]
Young's Modulus	*E*	2.00E+11	2.00E+11	[pa]
Density	ρ	7850	7850	[kg/m^3]
Cross sectional Area; $\pi(Do^2 - Di^2)/4$	*A*	0.0538	0.0577	[m^2]
Moment of Inertia; $\pi(Do^4 - Di^4)/64$	*I*	0.00316	0.0039	[m^4]
Constant for the mode [29]	*c*	-	-	[-]
Natural Frequency	ω_n	-	-	[Hz]

Table 5-5 demonstrates the obtained values. When comparing the values obtained in Table 5-3, without and with the extra mass, it can be seen that the frequencies are lower for the model with extra mass. This makes sense because the stiffness of the complete structure is not changing while the mass is increasing. Analysing the natural frequency formula, which is defined as the square root of stiffness over the mass, it shows that an increase of mass will result in a decrease in frequency. Therefore it can be said that the obtained ANSYS values are reasonable.

TABLE 5-5 RESULTS CHS 710X25 FIXED-FIXED WITH MIDDLE MASS

Mode		Hand Calculation		ANSYS Model		Difference
n	c	ω_n	unit	ω_n	unit	[%]
1	22.4	4.52	[Hz]	4.31	[Hz]	-0.77
2	61.7	12.46	[Hz]	11.67	[Hz]	-1.00
3	121	24.44	[Hz]	22.67	[Hz]	-1.15
4	200	40.39	[Hz]	37.08	[Hz]	-1.30
5	298	60.18	[Hz]	54.82	[Hz]	-1.42

5.2.2.3. CHS – PINNED-PINNED

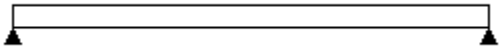

FIGURE 5-8 CHS PINNED-PINNED

To analyse the difference between fixed and pinned braces the same is done for a pinned rod. Similar dimensions and calculations are used as in Table 5-2 and equation (19). The main difference between the equations is the c constant that is used for pinned and fixed connections. The following results were obtained;

TABLE 5-6 RESULTS CHS 710X25 PINNED-PINNED

Mode		Hand Calculation		ANSYS Model		Difference
n	c	ω_n	unit	ω_n	unit	[%]
1	9.87	2.04	[Hz]	2.08	[Hz]	1.88
2	39.5	8.17	[Hz]	8.27	[Hz]	1.26
3	88.9	18.39	[Hz]	18.45	[Hz]	0.32
4	158	32.68	[Hz]	32.39	[Hz]	-0.89
5	247	51.09	[Hz]	49.84	[Hz]	-2.46

Yet again it can be concluded that both hand calculations and ANSYS results are compatible.

5.2.2.4. CHS – PINNED-PINNED WITH MIDDLE MASS

FIGURE 5-9 CHS PINNED-PINNED WITH MIDDLE MASS

The pinned-pinned model with a middle mass is investigated similar as the fixed-fixed model. The same dimensions as Table 5-4 and equation (20) were used, with varying 'c' value. The results are demonstrated in the table below.

TABLE 5-7 RESULTS CHS 710X25 PINNED-PINNED WITH MIDDLE MASS

Mode		Hand Calculation		ANSYS Model		Difference
n	c	ω_n	unit	ω_n	unit	[%]
1	9.87	1.99	[Hz]	1.97	[Hz]	-0.21
2	39.5	7.98	[Hz]	7.81	[Hz]	-0.33
3	88.9	17.95	[Hz]	17.46	[Hz]	-0.43
4	158	31.91	[Hz]	30.73	[Hz]	-0.59
5	247	49.88	[Hz]	47.43	[Hz]	-0.78

When comparing the results a good agreement is found.

5.2.2.5. SIMPLISTIC MODEL VS LOCAL BRACES

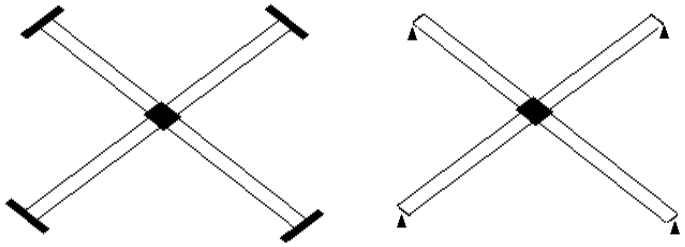

FIGURE 5-10 SIMPLISTIC X-BRACE

When analysing the simplistic cross brace the following can be said; both the stiffness as well as the mass becomes twice as much which eventually results in the same frequency when analysing equation 3. Therefor eit can be concluded that the frequencies are the same for this model as shown in Table 5-5 and Table 5-7.

Table 5-8 demonstrates the first natural mode of the actual cross brace design bay 4 and the simplistic model analysed by ANSYS for comparison. It can be seen that the natural frequency for the actual jacket cross brace is higher than compared to that of the simplistic model. This can be explained with the following;

As mentioned before, the cross brace used for the jacket has more details compared to the simplistic cross braces examined in section. So have the bottom ends of cross brace 4 a tapered increase in diameter to increase the stiffness. By increasing the stiffness of the brace the natural frequency shall increase as well.

For both bay 3 and bay 4 all the way at the end sections of the cross braces, an cans are applied with larger diameter to connect it to the jacket legs. The increase of diameter at the end sections of the cross brace results in an increase of stiffness and hence an increase of natural frequency.

Furthermore the simplistic cross brace had a length around 30m while the actual cross brace in bay 4 has a smaller length of roughly 28m, this decrease in length also results in an increase of natural frequency.

Due to these reasons therefore a higher natural frequency is expected of the actual jacket cross brace. This increase in frequency for the actual cross brace is also seen for the pinned and fixed boundary conditions.

In conclusion, since both frequencies of the actual and simplistic cross braces show the expected behaviour, it could be concluded that the actual cross brace of bay 4 modelled in ANSYS provides a demonstrative natural frequency.

TABLE 5-8 JACKET VS SIMPLISTIC X-BRACE BAY 4

Mode	**bay 4 Fixed - Fixed ω_n**		**bay 4 Pinned – Pinned ω_n**		
n	**Jacket x-brace**	**Simplistic x-brace**	**Jacket x-brace**	**Simplistic x-brace**	**Unit**
1	6.22	4.31	3.79	1.97	[Hz]

5.2.2.6. LOCAL BRACES NATURAL FREQUENCY

The natural frequency for both bay 3 and 4 of cluster 5 are shown in Table 5-9 for pinned and fixed boundary conditions. These values are obtained by ANSYS 17.1 by modelling the exact dimensions of the braces and doing a modal analysis. It is worth mentioning that these frequencies are generated with the braces are placed in air. No added mass from the water and marine growth is incorporated. When applying the additional mass of the marine growth and water, the natural frequency will decrease. [35].

TABLE 5-9 BAY 3 AND 4 NATURAL FREQUENCIES

	Bay 4 ωn [Hz]	Bay 3 ωn [Hz]
Fixed	6.22	5.49
Pinned	3.79	4.17

With use of hand calculations the eigen-frequencies obtained in ANSYS are adjusted, to include the additional mass of marine growth and water. When analysing equation (19) the following can sections can be simplified;

$$k = \frac{EI}{L^3} \tag{21}$$

$$\beta = \frac{c}{2\pi} \tag{22}$$

When substituting the simplification in the natural frequency equation it becomes;

$$\omega_{n\_air} = \beta \sqrt{\frac{k}{(m)_{steel}}} \tag{23}$$

Since the ωn is provided by the ANSYS calculations, the k of the cross brace can be calculated.

$$k = m_{steel} \left(\frac{\omega_n}{\beta}\right)^2 \tag{24}$$

It is assumed that the stiffness is not changing when incorporating the added mass of the marine growth and the water. So, the natural frequency of the braces in water is calculated by;

$$\omega_{n_{water+MG}} = \beta \sqrt{\frac{k}{(m)_{steel+water+mg}}} \tag{25}$$

More over the additional mass due to the marine growth; the total mass of 100mm marine growth to the brace is calculated. [31] This is done by sectioning the braces in different segments to easily calculate the additional volume of the marine growth. An overview of the calculation is provided in Appendix C. This volume is then times by the density of marine growth;

$$m_{MG} = volume_{MG} * \rho_{MG} \tag{26}$$

The added mass due to the water is calculated by obtaining the total volume of the brace including the marine growth and incorporating the Ca value.

$$m_{water} = volume_{structure} * \rho_{water} * Ca \tag{27}$$

Where Ca = Cm – 1. The Ca value is obtained by analysing the graph provided in Offshore Hydromechanis – TU Delft book, shown in Appendix D. [40] This is done by using the surface roughness in combination with the Keulegan Carpenter (KC) number.

The surface roughness of the braces is obtained from the DNV-RP-C205 code. For this the roughness of the marine growth is selected; 0.005 – 0.05. [31]

The KC value is generated the following;

$$KC = \frac{u_a T}{Do} \tag{28}$$

Where;

u_a	= flow speed $u_x + u_{current}$	[m/s]
T	= oscillating flow period	[s]
D_o	= outer diameter + MG	[m]

The current speed, $u_{current}$, is provided by 'ABP mer' and has a value of 0.2m/s for fatigue calculations. [39]

The flow speed, u_x, due to the waves is obtained with the following equation. [23]

$$u_x = \omega\, a\, \frac{cosh[k(d+z)]}{sinh[kd]} \tag{29}$$

Where;

ω	= angular wave speed $\frac{2\pi}{T}$	[m/s]
a	= wave amplitude $\frac{H}{2}$	[m]
k	= wave number $\frac{2\pi}{\lambda}$	[-]
λ	= wave length (deep water) $1.56T^2$	[m]
d	= total depth	[m]
z	= depth to a certain point	[m]

Different wave amplitudes and flow periods are calculated to analyse which KC value is appropriate. Detailed calculations can be found in Appendix D.

Table 5-10, demonstrates the input values used to calculate the adjusted natural frequency of the braces of bay 3 and 4. The natural frequency that takes into account the hydrodynamic added mass and the marine growth is governing for the fatigue analysis.

TABLE 5-10 MODIEFIED UNDAMPED NATURAL FREQUENCIES OF BAY 3 AND 4

	Bay 4 Fixed	Bay 4 Pinned	Bay 3 Fixed	Bay 3 Pinned	
volume steel	3.46E+09	3.46E+09	2.47E+09	2.47E+09	[mm3]
ρ steel	7.85E-06	7.85E-06	7.85E-06	7.85E-06	[kg/mm3]
mass steel	27166	27166	19386	19386	[kg]
β	3.57	2.18	3.57	2.71	[-]
ωn_air	**6.22**	**3.79**	**5.49**	**4.17**	[Hz]
k	82562	82562	45889	45889	[N/m]
volume water	3.78E+10	3.78E+10	3.81E+10	3.81E+10	[mm3]
ρ water	1.025E-06	1.025E-06	1.025E-06	1.025E-06	[kg/mm3]
Ca	0.95	0.95	0.95	0.95	[-]
mass water	36809	36809	37098	37098	[kg]
volume MG	1.45E+10	1.45E+10	1.52E+10	1.52E+10	[mm3]
ρ MG	1.40E-06	1.40E-06	1.40E-06	1.40E-06	[kg/mm3]
mass MG	20262	20262	21314	21314	[kg]
mass water + MG + steel	84238	84238	77799	77799	[kg]
ωn_water	**4.6**	**2.8**	**3.7**	**2.8**	
ωn_water+MG	**3.5**	**2.2**	**2.7**	**2.1**	[Hz]

Table 5-10 presents the obtained natural frequencies of the braces for the pinned and fixed boundary conditions. When analysing the leg-brace connection, the actual connection lies somewhere in between the pinned and fixed boundary conditions. It is useful to obtain an estimate regarding the leg-brace connection to see if the local modal analysis of bay 4 and 3 are in the critical frequency range of 2 – 2.5Hz. Therefore an analysis was performed to provide an estimation of where, between the two extreme boundary conditions, the actual leg-brace connection is.

The analysis included the following steps;

- First a part of the leg- brace connection was modelled. A force of 1000 N was applied in the direction of the breathing mode, out of plane of the bay. (breathing mode is illustrated in appendix F) Then the total deflection was calculated as 7.36E-4 m

- This was followed by a model of just the brace section, without the leg connection, with a fixed boundary connection. Again a force of 1000 N was applied in the same direction and the total deflection was generated; 5.10E-4 m.

- For both the 'leg-brace model' and the 'fixed brace only model' the deflections were compared and the percentage differences of the deflections were calculated. This was done to estimate how much the leg-brace connection acts as a fixed boundary connection. The values showed that the leg-brace connection has roughly 70% fixity.

Damping is an important aspect to consider when analysing the natural frequencies. From previous performed research literature suggests to use 1% of the critical damping with regards to structural damping of the substructure. [14][58][59][60]

The damped natural frequency is obtained with the following formula [43];

$$damped\ \omega_n = \omega_n \sqrt{1 - \zeta^2} \tag{30}$$

Where;

damped ω_n = damped natural frequency [Hz]
ω_n = undamped natural frequency [Hz]
ζ = damping factor [-]

When assuming that the pinned and fixed boundary conditions give the two extremes of the natural frequency, the natural frequency of the leg-brace connection, roughly 70% fixity can be calculated. This is demonstrated in Table 5-11 with 1% of the critical damping.

TABLE 5-11 BAY 3 AND 4 DAMPED NATURAL FREQUENCIES WITH DIFFERENT BOUNDARY CONDITIONS

damped ωn_water+MG	**Bay 4**	**Bay 3**	**[unit]**
Pinned	2.2	2.1	[Hz]
70%	2.9	2.5	[Hz]
Fixed	3.5	2.7	[Hz]

From the table it can be seen that when assuming the brace-leg connection has 70% fixity, the damped natural frequency for bay 4 is out of the critical forcing frequency range of 2 – 2.5Hz. This would suggest no resonance would occur for this particular cross brace.

The local damped natural frequency of bay 3 is determined as 2.5 Hz, meaning this could overlap with the forcing frequency and the occurrence of resonance is possible.

5.2.2.7. GLOBAL NATURAL FREQUENCY

This section focusses on the global natural frequencies of the complete OWT jacket as shown in Figure 5-4. The results obtained from ANSYS are demonstrated in Table 5-12. The values are based on the conditions in air and no marine growth is incorporated. To adjust the eigen-frequency by taking into account the added mass of water and marine growth, the same calculation steps are used as explained in section 5.2.2.6. More detailed calculations are shown in appendix E. Furthermore a damping ratio of 1% of the critical damping is incorporated. The results compare well with those obtained by the substructure designer, as demonstrated in Table 5-12.

TABLE 5-12 GLOBAL DAMPED NATURAL FREQUENCIES

n	ωn_air [Hz]	ωn_water+MG [Hz]	ωn_designer [Hz]	Mode shape
1	1.62	1.23	1.06	Global sway mode
2	1.62	1.23	1.06	Global sway mode
3	1.66	1.26	-	Jacket extend mode
4	2.61	2.00	-	Braces torsion mode
5	2.87	2.19	2.07	Breathing mode - alternating bays - bay 3 and 4 same direction
6	3.60	2.76	2.45	Braces all bays sway mode
7	3.63	2.78	2.45	Braces all bays sway mode
8	4.46	3.40	-	Breathing mode - alternating bays - bay 3 and 4 opposite direction

It can be seen that the results obtained in this thesis and by the substructure designer are quite similar. It is worth mentioning that the substructure designer predicts lower eigen-frequencies than the eigen-frequencies obtained in the thesis. Variations are due to the fact that both models are not completely identical. The main differences are;

For the thesis model it is assumed that the bottom bays 3 and 4 are under water, while in real life parts of bay 2 are also surrounded by water. It is assumed that the designer did include that bay 2 is party under water, meaning more added mass which results in lower natural frequencies.

It is also unknown with how much detail the designer modelled the transition piece. For the model used in this thesis the transition piece was simplified with only having the basics. When assuming the designer used the detailed TP more mass is added to the structure, thus lower eigen-frequencies.

Furthermore, the anodes on the braces and the legs are not included in the thesis model. Yet again, assuming the designer did include these, the mass of the structure increases and the natural frequency decreases.

When summarizing all the mentioned differences between the two models, it can be concluded that the substructure designer would find lower eigen-frequencies compared to the thesis model, which is indeed the case.

Furthermore, it can be seen that the 'breathing mode' (mode 5) overlaps with the forcing frequencies, which are the same findings of the substructure designer. In this breathing mode the braces show excitation. However the 'all braces bays sway modes' (mode 6, 7) are out of the critical frequency range of 2 – 2.5 Hz, meaning that this particular mode would not cause resonance. This is different to the substructure designer's results. Illustrations of the mode shapes are found in Appendix F.

5.3. COMPARSION BETWEEN THE FORCING FREQUENCIES AND EIGEN-FREQUENCIES

This section provides a comparison of the forcing frequencies found in section 5.1 and eigen-frequencies deliberated in section 5.2, to conclude if large amplification of the brace vibration movement due to resonance would occur, which could result in a low estimated fatigue life.

First a comparison of forcing and eigen-frequencies obtained in this research is provided in section 5.3.1., followed by some background knowledge regarding the relation between resonance and fatigue in section 5.3.2.

5.3.1. OVERLAPPING OF FORCING AND EIGEN-FREQUENCIES

For the OWT jacket of the reference project, the substructure designer found that due to resonance the amplitude of the braces vibrations would increase significantly. Therefore the stresses in the nodes of the cross brace would increase dramatically which would result in a short fatigue life.

The substructure designer was convinced that resonance would occur since the natural frequency of the braces would equal the forcing frequencies due to the turbine. Because of this a fatigue life of 3 years was calculated with use of ANSYS ASAS Offshore – FATJACK, a fatigue module of ANSYS. The module enables the engineer to perform a full linear and non-linear fatigue analysis of the jacket with generated waves and other applied loads. [53] However, the substructure designer was unwilling to share the model and any specific details about their calculations, except for mentioning that the designer had used 1% critical damping, as stated in the literature.

It is worth mentioning that a 3rd party involved was also not able to identify this low estimated fatigue life due to resonance. They were unsuccessful in finding resonance in the structure. However, since the substructure designer was highly convinced this would be an issue, mitigation measurements were implemented to avoid this problem. Since the company Seaway Heavy Lifting was still interested to obtain more detailed information regarding this, further investigation was requested.

During this research it was found that the excitation of the external forces due to the turbine is apparent in the frequency range of 2 – 2.5 Hz. This was demonstrated with the use of Fourier analysis shown in section 5.1.

The local modal analysis showed that the damped eigen-frequencies of the cross braces of bay 3 are 2.5Hz and could possibly cause resonance, which could result in a short estimated fatigue life. This is what the substructure designer found as well. Bay 4 however, demonstrated that the damped natural frequency of 2.9 Hz would not cause resonance, which is different from the designer's findings.

Form the global analysis performed in this research showed that the breathing mode, with a damped natural frequency of 2.2 Hz, is in the same frequency region as the forcing frequencies. This outcome was similar to that of the substructure designer, causing it to resonate. However the designer also found that the sway modes, mode 6 and 7, would also be in the forcing frequency range, which was not obtained in this research. The sway modes would according to this investigation not cause any resonance having a damped eigen-frequency of 2.77 Hz.

5.3.2. RESONANCE BEHAVIOUR

The dictionary states that resonance is “the state of a system in which an abnormally large vibration is produced in response to an external stimulus, occurring when the frequency of the stimulus is the same, or nearly the same, as the natural vibration frequency of the system.” [52] In other words, due to resonance large amplification occurs which induces large stresses on the system. When the forcing frequency and the natural frequency are the same, the frequency ratio equals one.

Figure 5-11 shows the frequency ratio vs the amplification ratio. It can be seen that when the frequency ratio equals one, the amplification factor increases dramatically and is depending on the critical damping factor, ζ, which is defined as the ratio of the damping, C, divided by the critical damping, Cc. When no damping is considered the amplification ratio goes to infinity. For most cases a damping of 1% of the critical damping is used which results in a damping factor ζ of 0.01. More background information regarding this graph can be found in ‘Dynamics, Slender Structures and an Introduction to Continuum Mechanics CT 4145’, by A. V. Metrikine. [54]

Estimating damping of a structure is an important but also challenging aspect. When a structure is analysed, damping should be incorporated in the model. This is because it has an effect on the amplitude and phase of the generated excitation and thus on the estimated fatigue life.

The onset of resonance has a negative effect on the fatigue life of a structure. Due to the large stresses which are caused by the movement amplification of the brace, the accumulated fatigue damage increases rapidly when analysing the suitable S-N curve. This is why the investigation of resonance is of great importance.

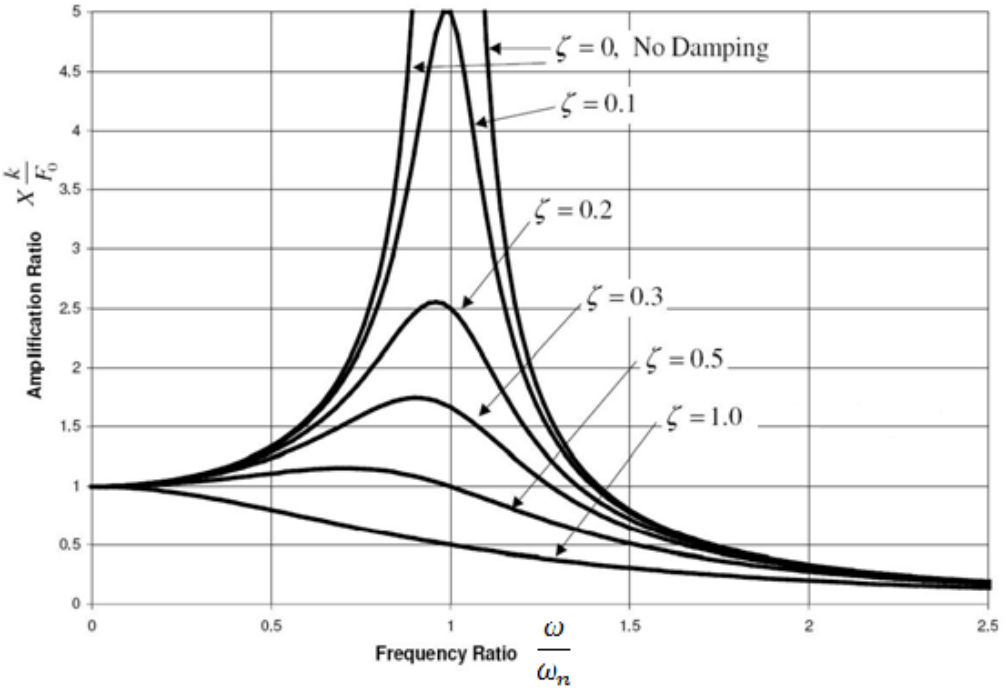

FIGURE 5-11 AMPLIFICATION RATIO VS FREQUENCY RATIO [51]

6. CONCEPT STUDY

In the previous sections the vibration amplification problem of the braces of the OWT jackets of the reference project are identified. It was found that the eigen-frequencies of the cross braces are in the same frequency range as those generated by the turbine loads. Also noted from the Fourier analysis is that forcing frequencies of other external forces occur in the frequency region from 0 to 2.5 Hz. Therefore to obtain a cross brace that is completely out of the forcing frequency regions, it is required to generate an eigen-frequency above 2.5 Hz. As mentioned in section 3.1.3 there are different options to obtain an increase in frequency shift.

This section describes possible jacket configurations that could be implemented to create this increase of eigen-frequency shift and to reduce the fatigue issues. It focusses on complete new concepts that could be designed had the vibration issue been found in an earlier stage of the project. Also adjustments to the current jacket structure are considered that can be applied before the jacket is be placed on the seabed or when the jacket has already been installed and the fatigue issues arise.

After the concepts are deliberated and the (dis)-advantages are summarized, a multi-criteria analysis (MCA) is used to obtain the top most suitable concepts. The selected concepts are finally analysed in more detail in section 6.2.

6.1. METHOD

To select the most appropriate concept for this challenge, several steps are done. First different concepts are described with each having advantages and disadvantages. From this the MCA is implemented; the MCA is a decision making tool to compare different options with regards to a variety of criteria. The different criteria are standardized and weighted. The total amount of points obtained for each option can then be compared. This is done to provide a good overview which option is most suitable. [41]

6.1.1. CONCEPT OVERVIEW

This section provides an overview of all the concepts considered with their (dis)-advantages. The concept overview includes both complete new design lay outs (1 – 4) and adjustments to the existing structure (5 - 9). This also obtains concepts that have no positive effect on the natural frequency shift. During the selection process these inappropriate concepts will be disqualified and not considered in the MCA.

TABLE 6-1 CONCEPT OVERVIEW

	Concept	Advantage	Disadvantage
1	Adding extra bay, 5 bays in total. *New design*	Reduces the length of the braces per bay, which results in an increase of local natural frequency per bay.	The extra bay would result in overall extra amount of steel which increases the costs of steel required. It increases the weight which could results in I&T issues. Due to the extra amount of steel the hydrodynamic forces shall increase, especially in the splash zone. However since this vibration problem is not caused due to the wave loads it does have a negative effect.
2	Increasing diameter *New Design*	This increases the stiffness of the brace, resulting in an increase of natural frequency.	The hydrodynamic drag forces increases and the added mass of water. This would result in a decrease in NF. However the increase of stiffness will provide an overall increase in NF. The diameter can only increase a certain diameter otherwise it is unable to connect the braces to the legs. If so the leg diameter has to increase which creates a new design loop.
3	Higher steel grade *New Design*	Structural jacket lay out does not have to change	Does not have an effect on the natural frequency NOT EFFECTIVE
4	Z-braces *New Design*	Less steel required which results in decrease of costs.	Has a negative effect on the NF. This lay out increases the length of the cross braces which results in a decrease of frequency, in to the critical zone. NOT EFFECTIVE

5	Water damping mechanism *Adjustment*	Steel costs stay the same. Able to keep the design as it is, no need to redesign the whole structure but just make local adjustments. The sloshing thank will damp the amplitude of the excitation of braces and creates a period phase shift. No added installation and transportation costs, since the construction weight will not increase much.	Most likely increases the weight of the in-place structure. New concept which is not developed into detail yet. Unsure if this has optimal use.
6	Diamond bracing *Adjustment*	Reduces brace length which results in an increase of frequency shift. This mechanism will restrict the braces to go in sway and breathing mode, which are the modes that create the main issues This adjustment can be added before the jackets are lowered onto the seabed but can also be implemented when the jacket is already been installed and fatigue issues do seem to occur.	Create a challenging connection with 3 members in one node. Extra steel increases the material costs.
7	Marine growth removing measures in combination with removing anodes *Adjustment*	Structural jacket lay out does not have to change	Most likely not sufficient enough, known from previous investigations With these implementations the welds had to be improved as well which added extra unforeseen costs. The marine growth remove measurements require maintenance. Frequent examination if the marine growth thickness is more than allowed is necessarily. This adds costs to the project.
8	Flooding braces *Adjustment*	Structural jacket lay out does not have to change. The added mass of water will create a natural frequency shift.	Create a frequency shift in a different direction , however it still shifts into the forcing frequencies region NOT EFFECTIVE

9	Tension Cables in between the bays *Adjustment*	Does not add reasonable amount of mass to the total structure	It is difficult to tension the cables. It will require a lot of maintenance to constantly keep the cables in appropriate tension Does not add value in the breathing mode. NOT EFFECTIVE

6.1.2. MCA

As mentioned before, the MCA is a decision making tool to compare different options with regards to a variety of criteria. First, the concepts described in Table 6-1 are evaluated on a variety of criteria. The concepts considered are 1, 2, 5, 6, 7. Each criterion is divided in its own grading, which is described in Table 6-2. This grading is described for the difficulty, the resulting increase or decrease and the effect of the implementation.

TABLE 6-2 GRADING LEGEND

Difficulty		Increase / Decrease		Effect	
--	Very difficult	↑↑	Large increase	--	Very negative
-	Difficult	↑	Increase	-	Negative
-/+	Maybe difficult	0	No change	-/+	No
+	Little difficult	↓	Decrease	+	Positive
++	Not difficult	↓↓	Large decrease	++	Very positive

In Table 6-3 the concept options are set out against the criteria in a matrix. The first column is with regards of the difficulty grade to design and the optimal use of the option. The columns 'influence of ω_n', 'm', 'k' and 'L' demonstrate if this implementation will result in an increase or decrease. Finally the last columns show what sort of effect the concept has on the specified criteria.

TABLE 6-3 OPTION VS CRITERIA

option	criteria	Difficulty	Influence ω_n	Weight (m) per bay	Stiffness (k)	Length (L)	I&T	Costs ($)	Maintenance	Decommission	Safety	Environment	Labour force
1	**Extra bay**	++	↑↑	↓	↑	↓↓	-/+	-	-/+	-/+	-/+	-/+	-
2	**Increasing diameter**	+	↑	↑	↑↑	0	-	-	-/+	-/+	-/+	-/+	-/+
5	**Water damping mech.**	-/+	↑	↓	0	0	-	-/+	-	-	-/+	-/+	-
6	**Diamond brace**	+	↑↑	↓	↑↑	↓↓	-/+	-	+	-/+	-/+	-/+	-
7	**Remove mg + annodes**	-	0	↓	0	0	--	+	--	-/+	-/+	-/+	-

The different grading's of the criteria are standardized to specific values. This is done so a comparison between the criteria can be made. It is grated in five equal steps from 0.2 to 1, with '1' representing the most desirable outcome and '0.2' the least.

TABLE 6-4 GRADING VALUES

Grading	Difficulty	Influence ω_n	Weight (m) per bay	Stiffness (k)	Length (L)	Effect
0.2	--	↓↓	↑↑	↓↓	↑↑	--
0.4	-	↓	↑	↓	↑	-
0.6	-/+	0	0	0	0	-/+
0.8	+	↑	↓	↑	↓	+
1	++	↑↑	↓↓	↑↑	↓↓	++

TABLE 6-5 OPTION VS CRITERIA GRADING VALUES

	weight	50	50	40	40	40	30	30	20	20	40	40	10
option	criteria	Difficulty	Influence ω_n	Weight (m) per bay	Stiffness (k)	Length (L)	I&T	Costs ($)	Maintenance	Decommission	Safety	Environment	Labour force
1	**Extra bay**	1.0	1.0	0.8	0.8	1.0	0.6	0.4	0.6	0.6	0.6	0.6	0.4
2	**Increasing diameter**	0.6	0.8	0.4	1.0	0.6	0.4	0.4	0.6	0.6	0.6	0.6	0.4
5	**Water damping mech.**	0.6	0.8	0.8	0.6	0.6	0.4	0.6	0.4	0.4	0.6	0.6	0.4
6	**Diamond brace**	0.8	1.0	0.8	1.0	1.0	0.6	0.4	0.8	0.6	0.6	0.6	0.4
7	**Remove mg + annodes**	0.4	0.2	0.8	0.6	0.6	0.2	0.8	0.2	0.6	0.6	0.6	0.2

Not all the criteria are of the same importance. To express the importance of each criteria a weighted value is determined varying from 10 – 50, with 50 indicating the most important criteria. The weighted importance for each criterion is shown in the top row of the table. Finally, the weighted importance is multiplied by the grading values of each option, shown in Table 6-6. This value is demonstrating the total standardized amount of graded importance. The summations of all the criteria for the options can be ranked to illustrate which options would be most suitable solutions. This is shown in Table 6-7.

TABLE 6-6 OPTIONS VS CRITERIA WEIGHTED TOTAL

option	criteria	Difficulty	Influence ω_n	Weight (m) per bay	Stiffness (k)	Length (L)	I&T	Costs ($)	Maintenance	Decommission	Safety	Environment	Labour force
1	**Extra bay**	50	60	32	32	40	18	12	12	12	24	24	4
2	**Increasing diameter**	30	48	16	40	24	12	12	12	12	24	24	4
5	**Water damping mech.**	30	48	32	24	24	12	18	8	8	24	24	4
6	**Diamond brace**	40	60	32	40	40	18	12	16	12	24	24	4
7	**Remove mg + annodes**	20	12	32	24	24	6	24	4	12	24	24	2

TABLE 6-7 CONCEPT PREFERENCE

	Option		Total
1	*6*	Diamond brace	322
2	*1*	Extra bay	320
3	*2*	Increasing diameter	258
4	*5*	Water damping bucket	256
5	*7*	Remove MG + annodes	208

6.2. RESULTS

Three concepts from the MCA are selected for further investigation and described in this section. These concepts are; ‘the diamond brace’, ‘the five bay jacket’ and ‘the water damping mechanism’.

6.2.1. CONCEPT – DIAMOND BRACE

The figure below demonstrates the diamond brace connected to the crossings of the diagonal braces of bay 4. The diamond brace has an outer diameter of 730 mm and a wall thickness of 10 mm. The diamond brace is especially useful in restraining the breathing and sway modes of bay 4. This concept can be applied in the fabrication yard, before lowering the jacket to the seabed, but also when the jacket is already been installed and fatigue issues do occur.

The natural frequencies obtained by ANSYS are analysed and adjusted just as done in the previous sections to take in to account the added masses and 1% of critical damping is applied. Detailed calculations are found in Appendix H and the final results are shown in Table 6-8. First the results are discussed followed by and explanation of installation methods and extra steel costs.

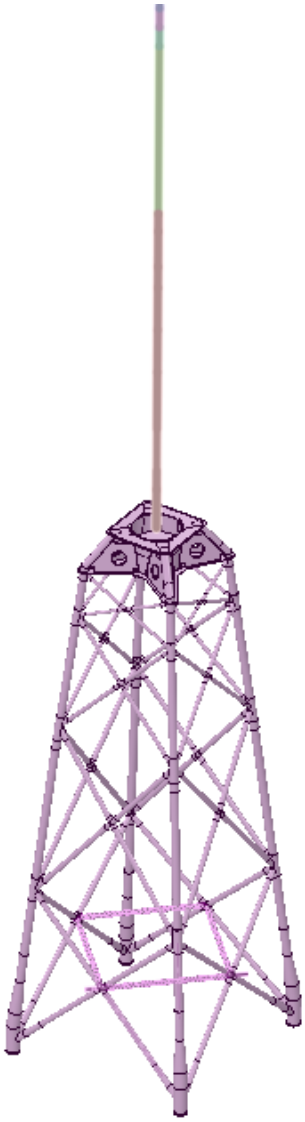

FIGURE 6-1 JACKET WITH DIAMOND BRACE

TABLE 6-8 JACKET WITH DIAMOND BRACE DAMPED GLOBAL EIGEN FREQUENCIES

n	OWT-Diamond [Hz]		OWT [Hz]		Mode shape
	ωn_air	ωn_water+MG	ωn_air	ωn_water+MG	
1	1.61	1.21	1.62	1.23	Global sway mode
2	1.61	1.21	1.62	1.23	Global sway mode
3	1.66	1.25	1.66	1.26	Jacket extend mode
4	2.60	1.96	2.61	2.00	Torsion mode - braces
5	3.12	2.36	2.87	2.19	Breathing mode - alternating bays - bay 3 and 4 same direction
6	4.16	3.14	3.60	2.76	Braces sway mode – bay 3
7	4.16	3.14	3.63	2.78	Braces sway mode – bay 3
8	4.43	3.34	4.46	3.40	Breathing mode - alternating bays - bay 3 and 4 opposite direction
9	4.89	3.68	-	-	Breathing mode - bay 3
10	4.94	3.73	-	-	Braces sway mode – bay 3
11	4.95	3.73	-	-	Braces sway mode – bay 3
12	5.08	3.83	-	-	Torsion mode - jacket
13	6.36	4.80	-	-	Breathing mode - alternating bays - bay 2

RESULTS DISCUSSION

The effect that the diamond brace has on the breathing and sway modes is illustrated in Figure 6-2 and Figure 6-3. When analysing the results the following can be said; the amplitude of the cross braces of bay 4 are effectively restricted and are not dominantly active in the breathing and sway modes anymore. More detailed information about the modes is provided below;

Breathing mode; 5

Figure 6-4 demonstrates both breathing modes with and without the diamond brace for comparison. Mode number 5, the breathing mode for bay 3 and 4, shows an eigen-frequency of 2.36 Hz which suggest it could cause complications. However, the diamond brace is restricting the bay in this specific movement, so the amplitude of the cross braces is limited. This ensures that the stresses in the leg-brace connection generated are smaller with the diamond brace compared to when the diamond brace is not been installed. Due to this an increase in fatigue life could be obtained.

It is worth noting that by adding the diamond brace, the stresses obtained in the diamond brace connections increase. This could result in a shift of the problem into another node.

Sway mode; 6,7

The sway modes (6, 7) of the original jacket, having a frequency of roughly 2.76 Hz have increased to a frequency around 3.14 Hz, which won't cause any fatigue issues. It is worth mentioning that the initial sway mode without diamond brace was already, found in this research, out of the critical frequency range of 2 - 2.5Hz

Global sway modes; 1,2

Furthermore it is worth mentioning that the damped natural frequencies of the global sway modes (mode 1, 2) are almost identical for the jacket including the diamond brace compared to the original jacket. This can

be explained since the diamond brace provides no restriction to these mode shapes, meaning that the stiffness for these mode shapes are the same for both jackets.

Overall it can be concluded that this concept is a successful implementation for this particular challenge.

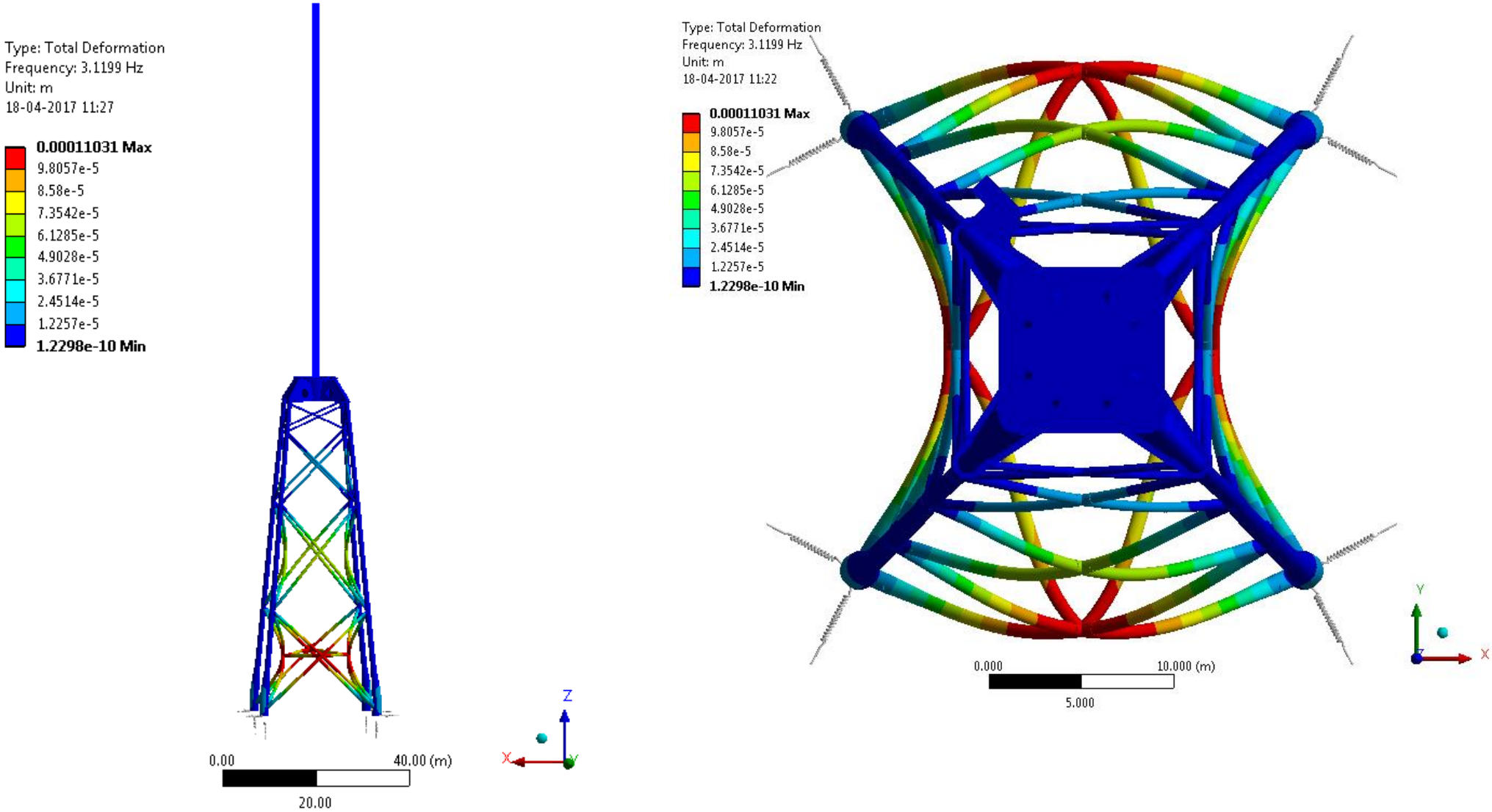

FIGURE 6-2 DIAMOND BRACE - BREATHING MODE 5

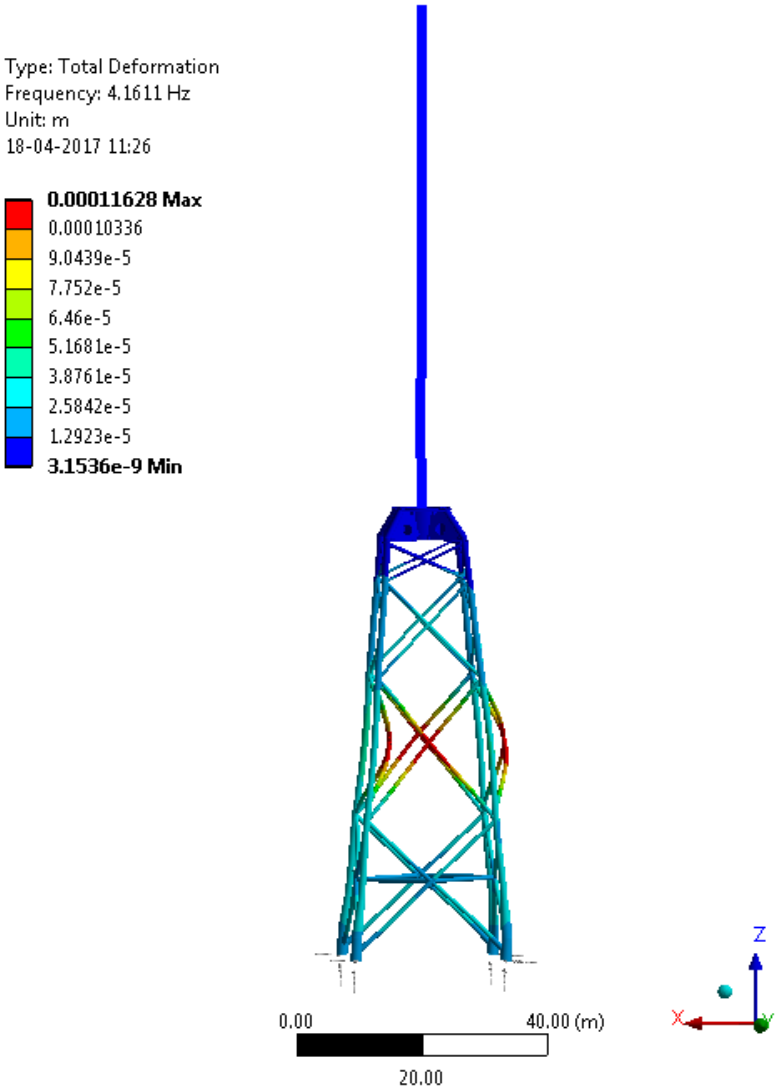

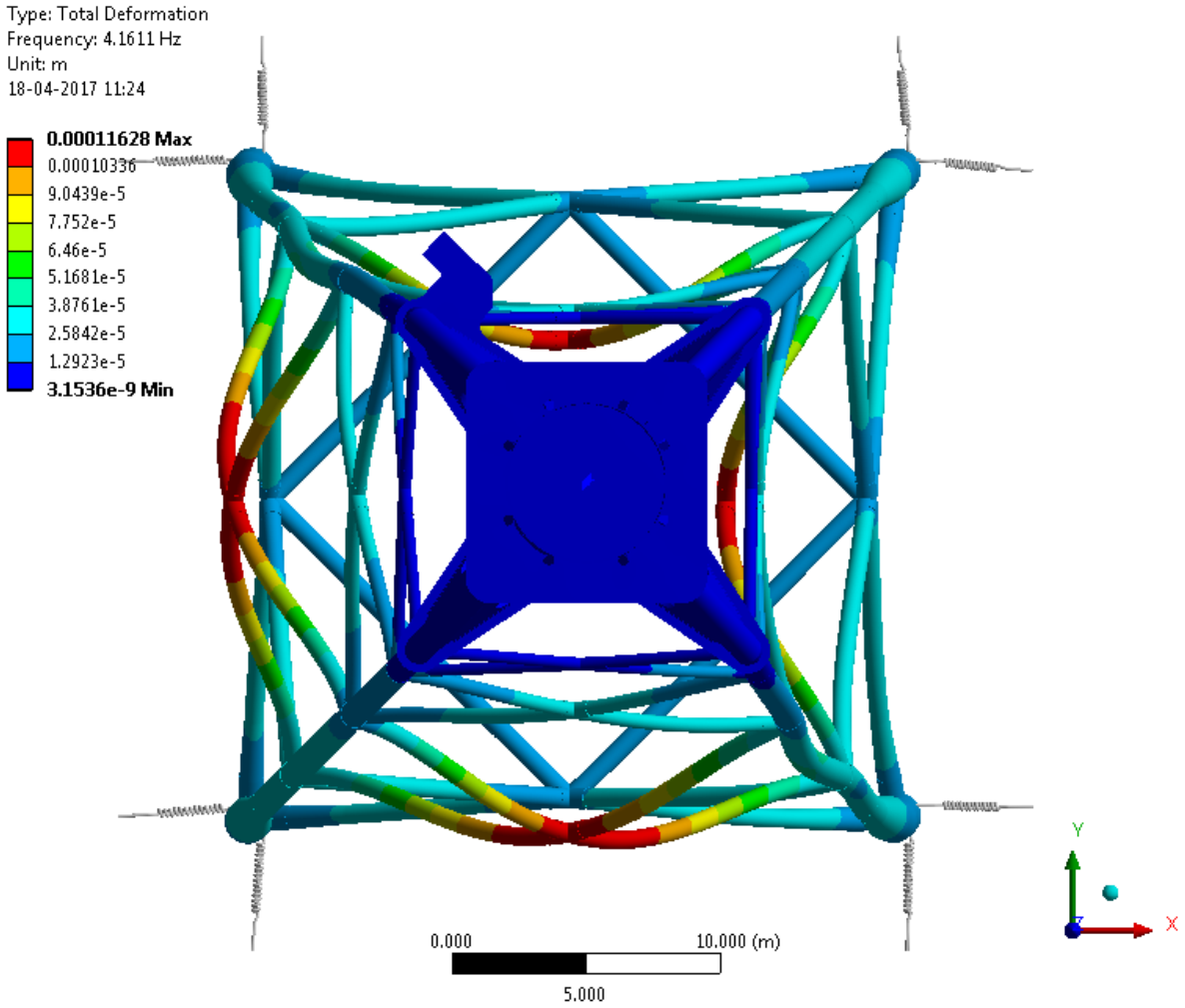

FIGURE 6-3 DIAMOND BRACE - SWAY MODE 6

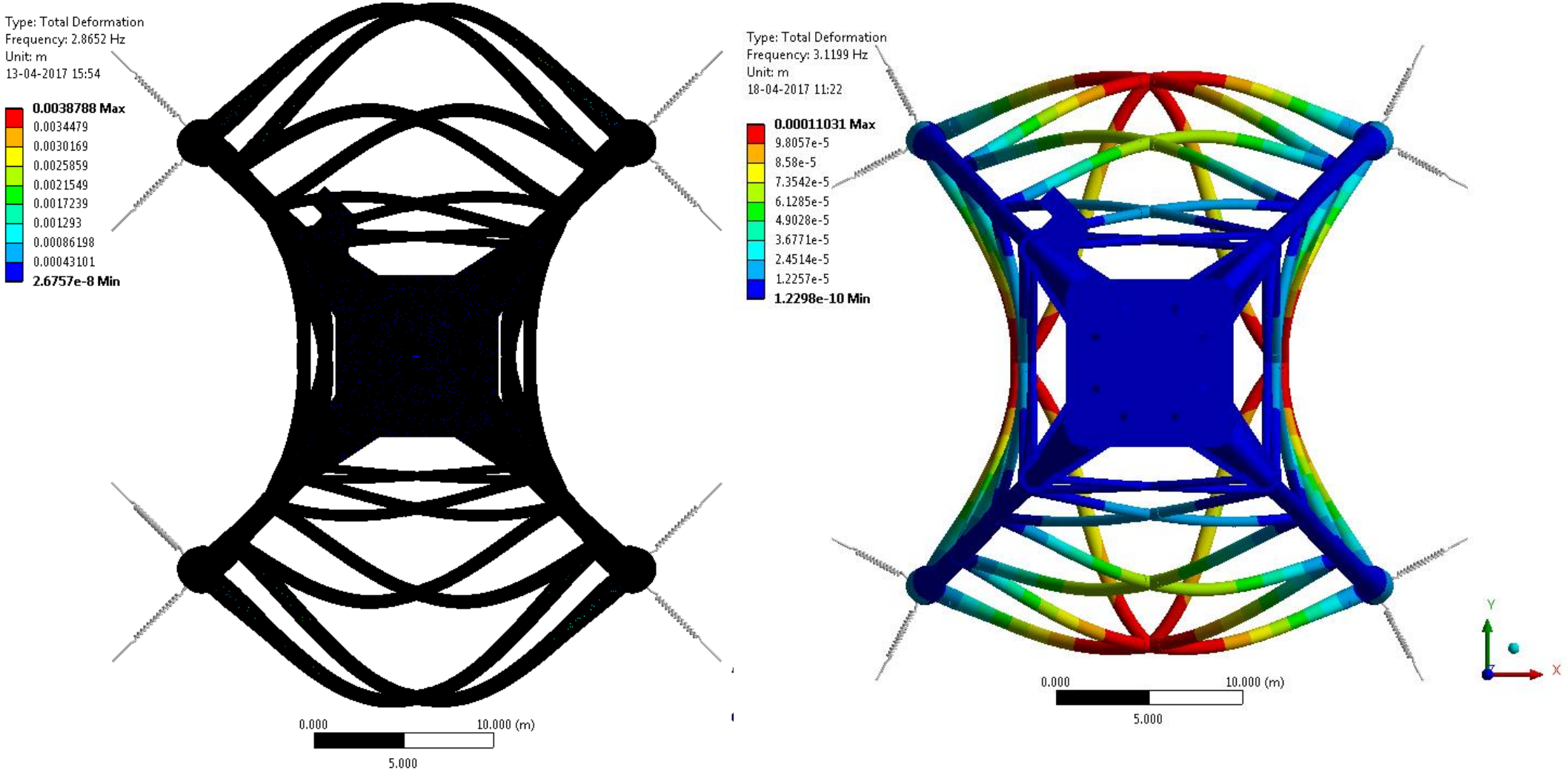

FIGURE 6-4 BREATHING MODE COMPARISON

Application of the diamond brace can be done before the jacket is lowered in the sea as well as after the jacket has been installed. When considering the adjustment of the jacket when the OWT jacket is already been placed on the seabed, there are different methods to do so. The preferred method to apply the steel braces to the bottom bay is by the use of clamps rather than welding. The quality of underwater welding is not always up to standards and proper inspection of the weld is difficult, due to the poor visibility in water. Three clamped connections that could be implemented for fatigue problems are 'unstressed grouted connection', 'stressed mechanical clamp' and the 'stressed grouted clamp'. These connections are now explained in more detail. [49]

When applying the unstressed grouted connection, the bolds are tightened before the grout is injected into the annular space. Hence the grout and steel interface connection is not stressed. An advantage regarding this connection is that it allows for large tolerances in applying the clamp on the correct position due to the grout. A disadvantage however is that a long connection is required for appropriate load transfer capacity.

Moreover the stressed mechanical clamp; with this clamp the force transfer is based on the friction capacity between the two tubulars and is connected by tension stud-bolds. The steel friction is obtained by the compressive force normal to the tubular and clamp interface. Usual installation times are somewhere between 2 to 6 days and are depending on the size and complexity of the clamp. A benefit of this method is that it can transfer large forces over a small clamp length compared to unstressed grouted connection. It is worth noting that this method cannot be used for the repair of tubular joints. A disadvantage regarding this is that the clamp offers small tolerances between the clamp and the member face and high accuracy in placing the clamp is required. Furthermore, the clamp needs regular inspection to ensure sufficient bold tension is still applied, this is since the connection between the clamp and the member is corrosion sensitive.

Furthermore an explanation about the stressed grouted clamp; this is a combination between the unstressed grouted connection and the stressed mechanical clamp. The connection is formed by first injecting and curing the grout in the annular space between the clamp and the member, followed by then applying the stud-bolds onto a tubular member. The advantages are that it can transfer high loads over a small clamp length, just like the stressed mechanical clamp, as well as it is able to have large tolerances in applying the clamp as the unstressed grouted connection. Because of these reasons the stressed grouted clamp connection is mainly used in the industry. [50]

To install the clamped connection deep sea divers as well as ROVs could be used. Since the bottom bays of the cluster 5 jackets are at a depth of 55 meters, the deep sea divers require a decompression tank to do so. Deep sea divers do have the advantage to attach the bolts with more ease compared to ROVs. On the other hand the use of ROVs is a safer option compared to the use of deep sea divers. Which option to use is project specific.

This section provides a rough estimate of the steel cost of the cross brace. To calculate the costs the following equations are used;

$$mass_{steel} = volume_{steel} \cdot \rho_{steel}$$

$$mass_{steel} = \frac{\pi(Do^2 + Di^2)}{4} \cdot L \cdot \rho_{steel} \quad (31)$$

$$Costs = mass_{steel} \cdot rate\ per\ kg \quad (32)$$

TABLE 6-9 COST DIAMOND BRACE

Name	Symbol	Value	Unit
Length	*L*	14000	[mm]
Outer diameter	*Do*	730	[mm]
Wall thickness	*WT*	10	[mm]
Inner diameter	*Di*	710	[mm]
Area	*A*	22619	[mm2]
volume	*vol*	316672539	[mm3]
Density	ρ_{steel}	7.85E-06	[kg/mm3]
mass	*m*	2486	[kg]
Rate	€/*kg*	€ 4.00	[€/kg]
Price brace	€ *brace*	€ 9,944	[€]
Price diamond brace	€ *diamond*	€ 39,774	[€]

Table 6-9 demonstrate the values obtained for the cost calculation. From reference projects a steel rate of 4 euro per kg is used. It can be conclude that the price per diamond brace would be roughly €40,000.

It is worth mentioning that these are only the steel costs, also the transportation and installation costs need to be added to obtain an overview of the total costs of this implementation. This all, results in an expensive solution.

6.2.2. CONCEPT – FIVE BAY JACKET

This concept is based on the idea that adding an extra cross brace to the current jacket design will result in a decrease of the diagonal length of the cross braces. This is desirable since a decrease in length creates an increase in natural frequency. This concept could therefore possibly create a natural frequency shift out of the forcing vibrations. Figure 6-5, demonstrates a jacket structure with five bays of cross braces.

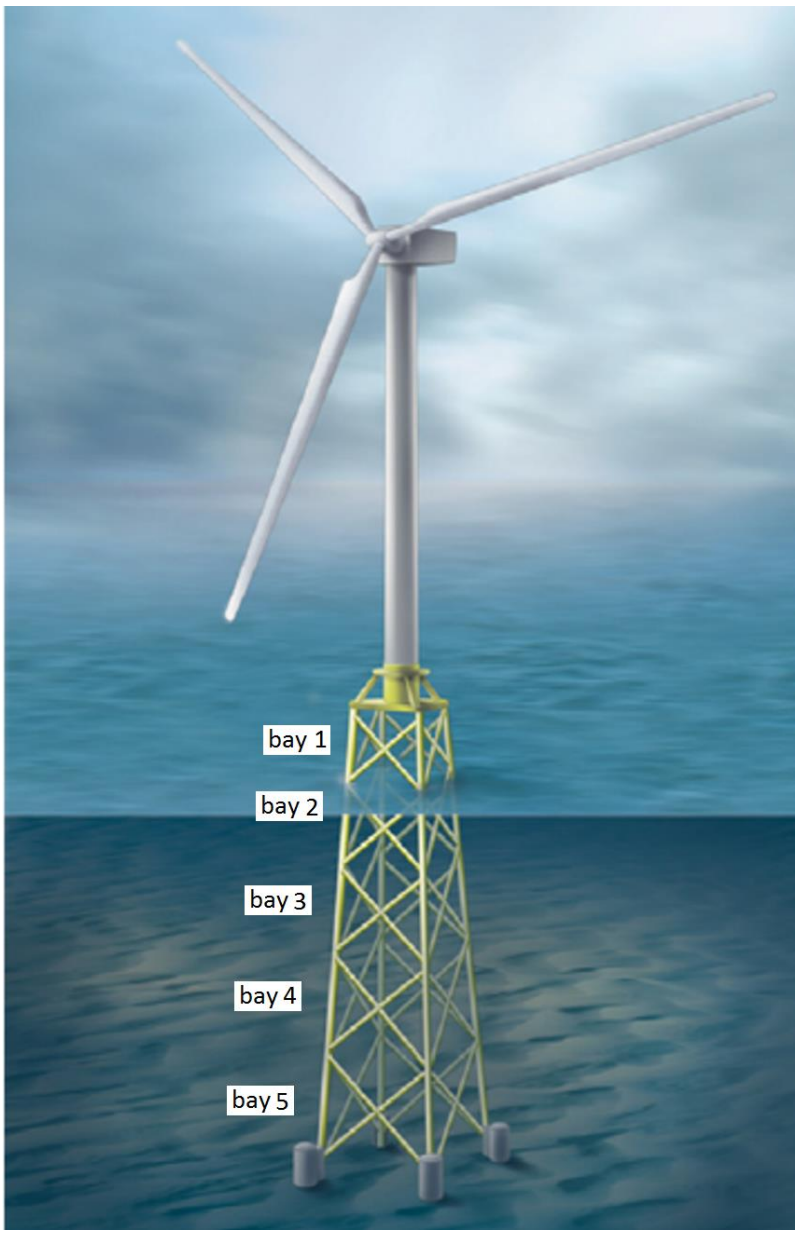

FIGURE 6-5 CONCEPT - 5 BAY JACKET [55]

There are multiple bays lengths possible when designing the jacket consisting of five bays. The aim of this concept is to select the bay lengths in such manner that the damped eigen-frequencies of all the bays are above 2.5Hz. This is to avoid resonance by ensuring no overlapping with forcing frequency regions occurs. A boundary condition to consider in designing the cross brace grid is that the angle between the braces has to be a minimum of 30 degrees. This is a requirement to ensure the weld can still be made. It is worth mentioning that the angle of the legs is consistent all along the jacket and no change in batter is present as in the OWT jackets of the reference project.

First the definition of the horizontal, vertical and diagonal lengths of the bays are provided. For these calculations the horizontal length of the bay is specified as the bottom length of each bay. A schematic view of the length definitions is illustrated in Figure 6-6. The purpose is to obtain an optimal cross brace framework. The lengths of the bays for a particular case are defined in Table 6-10.

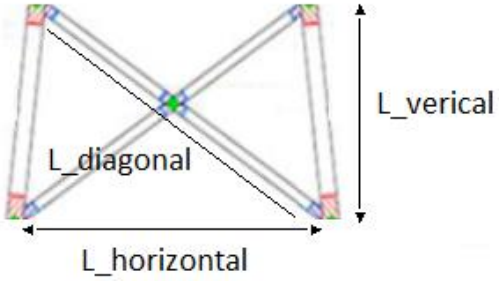

FIGURE 6-6 BAY LENGTHS DEFINITIONS

TABLE 6-10 BAY LENGTHS

bay	L_vertical [mm]	L_horizontal [mm]	L_diagonal [mm]	Do [mm]	Di [mm]
1	9000	12875	15087	600	570
2	12600	15023	18797	650	610
3	11000	16899	19384	690	650
4	15000	19456	23567	700	650
5	16800	22320	26806	710	660

For these cross brace lengths the eigen-frequencies are calculated. This is done with the same equation as explained in section 5.2.2.2; a CHS with a mass in the middle, equation (20). These calculations are executed for both fixed and pinned boundary conditions. The constant, c, for the first mode in the equation is 22.4 and 9.87 for the fixed and pinned connection respectively. Furthermore the Young's modulus, E, is 2E11 MPa and the density of the steel, ρ_{steel}, equals 7850 kg/m^3. The obtained natural frequencies for the fixed and pinned conditions are demonstrated in Table 6-11.

TABLE 6-11 CROSS BRACE FREQUENCIES

bay	Do [m]	Di [m]	A [m^2]	Do_node [m]	Di_node [m]	A_node [m^2]	I [m^4]	*Fixed* ωn [Hz]	*Pinned* ωn [Hz]
1	0.6	0.57	0.028	0.65	0.6	0.049	0.0012	15.2	6.7
2	0.65	0.61	0.040	0.67	0.65	0.021	0.0020	11.1	4.9
3	0.69	0.65	0.042	0.71	0.69	0.022	0.0024	11.1	4.9
4	0.7	0.65	0.053	0.73	0.7	0.034	0.0030	7.6	3.3
5	0.71	0.66	0.054	0.76	0.71	0.058	0.0032	5.9	2.6

The generated natural frequencies of the cross braces are for the steel brace only. When the jacket is installed on the seabed, marine growth will attach to the structure, which is increasing the mass. Furthermore the added hydrodynamic masses also need to be considered, since it has an effect on the natural frequency as well. Therefore the volume and the added mass of the marine growth and the water

are calculated as done in equations (26) and (27). A marine growth of 100mm is assumed and a Ca value of 1 for the hydrodynamic added mass. Table 6-12 shows the obtained values for each cross brace.

TABLE 6-12 MASSES CROSS BRACE

bay	volume steel [mm^3]	mass steel [kg]	volume MG [mm^3]	mass MG [kg]	volume hydro [mm^3]	mass hydro [kg]
1	8.32E+08	6530	6.64E+09	9290	1.52E+10	14768
2	1.49E+09	11682	8.86E+09	12401	2.13E+10	20773
3	1.63E+09	12812	9.62E+09	13471	2.41E+10	23485
4	2.50E+09	19616	1.18E+10	16585	3.00E+10	29198
5	2.88E+09	22642	1.36E+10	19099	3.49E+10	33953

With the use of these values, the adjusted natural frequencies for the pinned and fixed conditions can be calculated. The same equations and calculation steps as done in section 5.2.2.6 are executed. The generated values are shown in Table 6-13 and Table 6-14 for the fixed and pinned condition respectively.

TABLE 6-13 CROSS BRACE NATURAL FREQUENCIES - FIXED

bay	***Fixed*** **ωn [Hz]**	***Fixed*** **β [-]**	**mass steel [kg]**	**k [N/m]**	**mass steel + MG +hydro [kg]**	***Fixed*** **ωn_ water+MG [Hz]**
1	15.2	3.6	6530	117648	30588	7.0
2	11.1	3.6	11682	113632	44856	5.7
3	11.1	3.6	12812	124775	49768	5.7
4	7.6	3.6	19616	88787	65399	4.2
5	5.9	3.6	22642	61965	75694	3.2

TABLE 6-14 CROSS BRACE NATURAL FREQUENCIES - PINNED

bay	***Pinned*** **ωn [Hz]**	***Pinned*** **β [-]**	**mass steel [kg]**	**k [N/m]**	**mass steel + MG +hydro [kg]**	***Pinned*** **ωn_ water+MG [Hz]**
1	6.7	1.57	6530	117648	30588	3.1
2	4.9	1.57	11682	113632	44856	2.5
3	4.9	1.57	12812	124775	49768	2.5
4	3.3	1.57	19616	88787	65399	1.8
5	2.6	1.57	22642	61965	75694	1.4

As mentioned before, the leg-brace connection has roughly 70% fixity. When analysing the natural frequencies with this connection the following frequencies for the bays are the obtained with 1% of the critical damping;

TABLE 6-15 CROSS BRACE DAMPED NATURAL FREQUENCIES - 70% FIXITY

bay	*70% fixity* ωn_ water+MG [Hz]
1	5.8
2	4.7
3	4.7
4	3.5
5	2.7

The aim was to obtain an optimal cross brace framework of the current jacket, with the damped eigen-frequencies of all the bays above 2.5Hz. As presented in Table 6-15, this is the case for this particular jacket lay out and hence no resonance would occur.

Overall it can be concluded that this concept is a successful implementation for this particular challenge.

6.2.3. CONCEPT – WATER DAMPING MECHANISM

This concept that has not been implemented to underwater jacket structures having this brace amplification problem. The idea originates from a system which is used to damp vibrating movements of high rise buildings. In this concept the braces are connected with a bucket of water to the middle of the brace. When the braces vibrate the bucket with water starts to vibrate as well. The tank is filled for 70% of water which enables it to slosh. The sloshing of the tank acts as a dynamic absorber. This can be represented as a simple 2DOF mass-spring-damping system illustrated in Figure 6-7. The primary system, 1, represents the cross brace of the jacket and the dynamic absorber, 2, embodies the bucket filled with water.

The aim of the absorber is to have the same frequency as the eigen-frequency of the primary system. This way the vibration of the primary system is damped most effectively.

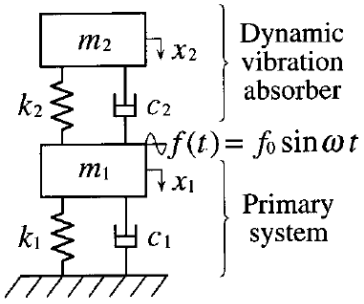

FIGURE 6-7 DYNAMIC ABSORBER [42]

First the mass, stiffness and natural frequency of the cross brace bay 4 needs to be determined. For this the pinned connection is selected, having the eigen-frequency of 2.15[Hz] and a mass of 84238[kg] which is including the marine growth and the hydrodynamic added mass. This is gathered from the calculations shown in the previous section 5.2.2.6 of Table 5-10.

The eigen-frequency 2.15[Hz] of the pinned system includes the β coefficient. For the mass absorber calculations the equivalent stiffness, $k_{e,}$ is used which is obtained the following;

$$\omega_1 = \beta \sqrt{\frac{k_1}{m_1}} = \frac{1}{2\pi} \sqrt{\frac{k_{e1}}{m_1}}$$

$$\beta \sqrt{k_1} = \frac{1}{2\pi} \sqrt{k_{e1}} \tag{33}$$

$$k_{e1} = \left[\beta \sqrt{k_1}\, 2\pi\right]^2$$

TABLE 6-16 PRIMARY SYSTEM - JACKET

Primary system – Jacket			
Symbol	**Value**	**Unit**	**Description**
m1	84238	[kg]	*Mass steel brace + mass MG + Hydrodynamic added mass*
k1	82562	[N/m]	*Stiffness brace - Table 4.11*
ω1	2.15	[Hz]	*Pinned connection*
β	2.18	[-]	*Table 4.11*
ke1	15490031	[N/m]	*Equivalent stiffness - Equation 32*

The eigen-frequency of the sloshing tank is determined by the dimensions of the bucket. A simple approach to obtain this natural frequency is by using the following equation [44];

$$\omega_2 = \frac{1}{2\pi}\sqrt{\frac{g\,\pi}{b}\,tanh\left(\frac{\pi h}{b}\right)} \tag{34}$$

The purpose is to design the bucket in such manner that the eigen-frequency of the bucket system is identical to that of the primary cross brace system. In this case dimensions are selected that obtain a frequency of 2.15[Hz]. Finally the mass and stiffness of the bucket are determined by;

$$m_2 = \rho_w b^2 h \cdot 0.7 \tag{35}$$

$$k_2 = \omega_2^2 m_2 \tag{36}$$

TABLE 6-17 ABSORBER - BUCKET

Absorber – Bucket			
Symbol	**Value**	**Unit**	**Description**
b	0.168	[m]	*Width bucket*
h	3	[m]	*Height bucket*
ρw	1025	[kg/m^3]	*Density water*
ω2	2.156	[Hz]	*Eigen frequency bucket*
m2	60.75	[kg]	*Mass bucket*
k2	11145	[n/m]	*Stiffness bucket*

Analysing the system the optimal width dimension of the bucket to obtain a frequency of 2.15[Hz] is 0.168[m]. It is worth mentioning that the eigen-frequency of the bucket is not so much depending on the height of the water bucket. The height mainly effect's the total mass and therefore stiffness of the bucket. More detail regarding this is provided later on in this section.

The purpose of the dynamic mass absorber is to reduce the amplitude of the primary system. Once all data regarding the mass-spring 2DOF system, illustrated in Figure 6-7, is known the differential equations of motion can be set up for this particular system. For this an assumed damping of 1% critical damping for the primary system is selected and for the dynamic absorber a damping of 2%.

$$\begin{bmatrix} m1 & 0 \\ 0 & m2 \end{bmatrix}\begin{Bmatrix} \ddot{x}1 \\ \ddot{x}2 \end{Bmatrix} + \begin{bmatrix} c1+c2 & -c2 \\ -c2 & c2 \end{bmatrix}\begin{Bmatrix} \dot{x}1 \\ \dot{x}2 \end{Bmatrix} + \begin{bmatrix} k1+k2 & -k2 \\ -k2 & k2 \end{bmatrix}\begin{Bmatrix} x1 \\ x2 \end{Bmatrix} = \begin{Bmatrix} f1(t) \\ f2(t) \end{Bmatrix} \tag{37}$$

This matrix equation can be simplified as follows;

$$[M]\{\ddot{x}\} + [C]\{\dot{x}\} + [K]\{x\} = \{fi\}\sin(\omega t) \tag{38}$$

Where i = 1,2.

From this the steady state of the solution can be written as;

$$x_{iss} = x_{is}\sin(\omega t) + x_{ic}\cos(\omega t) \tag{39}$$

Where i = 1,2.

Substituting the x1 and x2 of the system, the original matrix differential equation results in a single matrix equation given by;

$$\begin{bmatrix} -\omega^2[M]+[K] & \omega[C] \\ -\omega[C] & -\omega^2[M]+[K] \end{bmatrix} \begin{Bmatrix} x_{ic} \\ x_{is} \end{Bmatrix} = \begin{Bmatrix} 0 \\ fi \end{Bmatrix} \tag{40}$$

The amplitude of the system is defined as;

$$X_i = \sqrt{|x_{ic}|^2 + |x_{is}|^2} \tag{41}$$

Finally, the DAF of the system is obtained by;

$$DAF = \frac{X_i}{F_i/k_i} \tag{42}$$

To plot the DAF vs the frequency [Hz] MATLAB was used. The MATLAB script is written in such manner that there are 2 cases; case 1 with just the primary system 1 and case 2 the primary system including the absorber. This way the two graphs can easily be compared showing the effect the dynamic absorber has on the system. The MATLAB script is found in Appendix I. [43]

The DAF for case 1 (red) and 2 (blue) are illustrated in the graphs shown in Figure 6-8 for a bucket height of 3[m]. It can be seen that the amplification is roughly reduced by half. Figure 6-9 demonstrates the amplitude of the dynamic absorber.

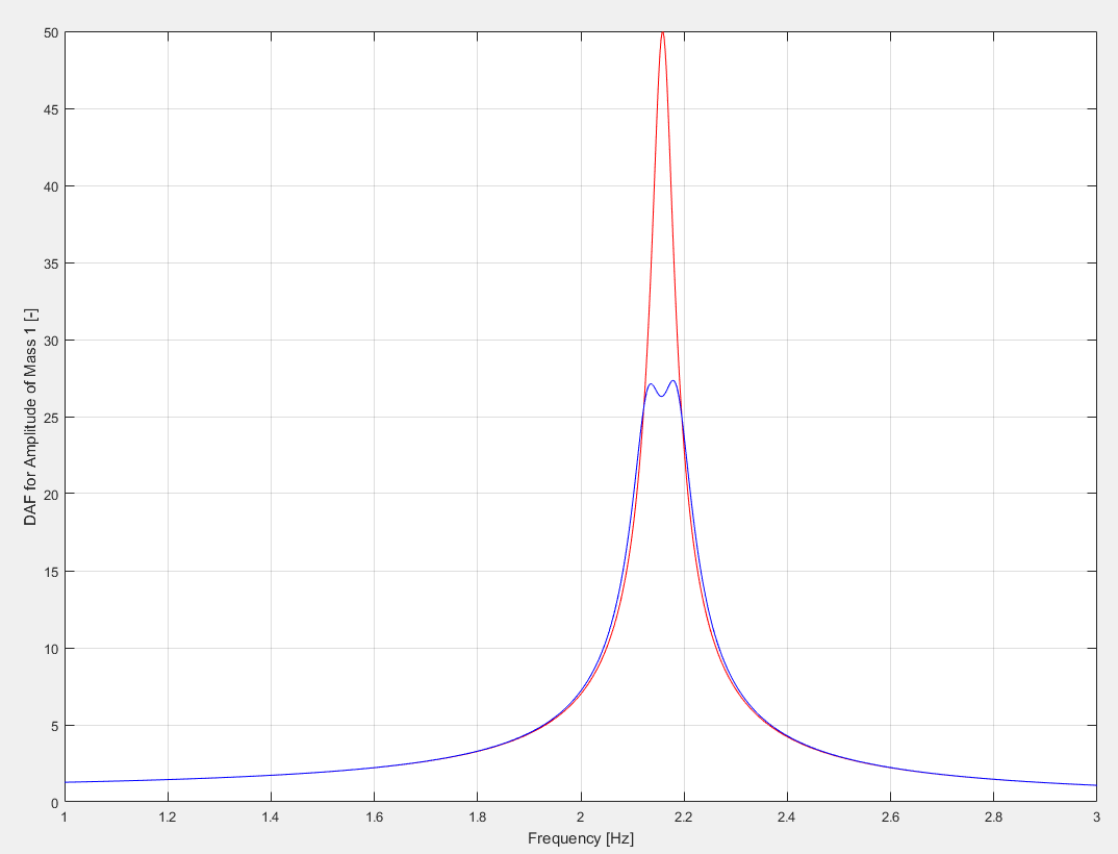

FIGURE 6-8 DAF CASE 1 AND 2 - H=3[M]

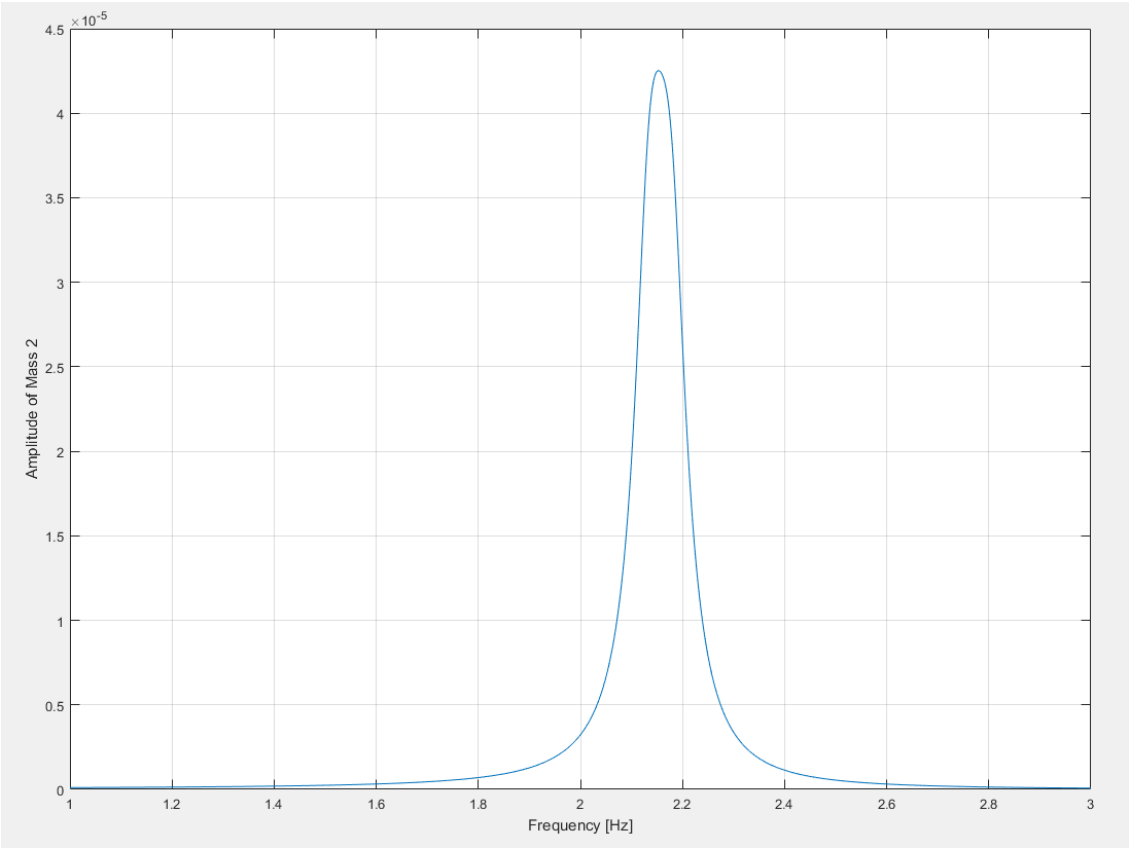

FIGURE 6-9 AMPLITUDE OF MASS 2

As mentioned before, the bucket height does not influence the natural frequency of the sloshing system. It does however have an effect on the total mass and stiffness of the dynamic absorber and therefor on the amount of amplitude damping. The graph below demonstrates the damping ratio effect vs the height of the water bucket.

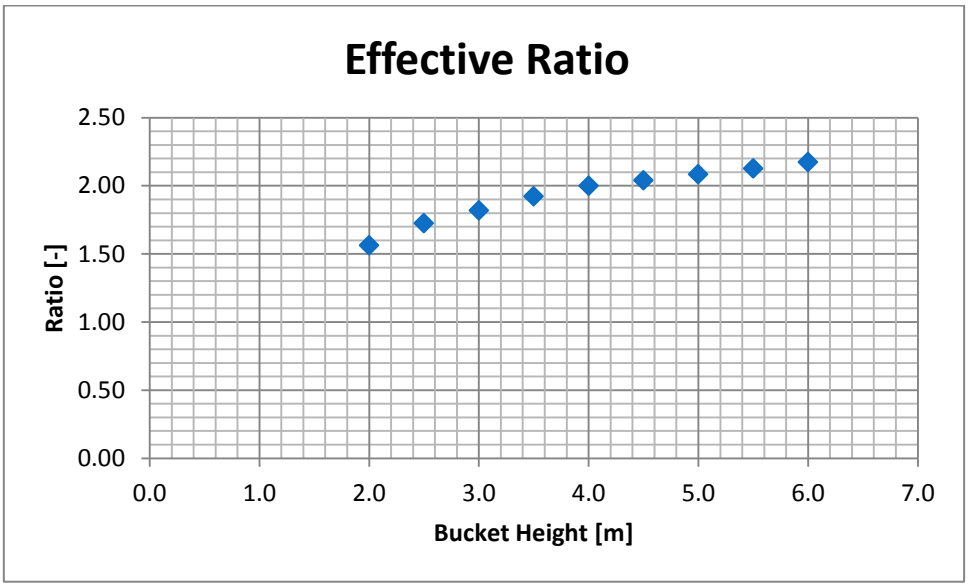

FIGURE 6-10 EFFECTIVE RATIO VS BUCKET HEIGHT

From the graph it shows that a bucket of 2[m] high will damp the system by 1.5 times. It can be seen that an increase in bucket height as only little effect on the effective ratio. By increasing the bucket dimensions, the hydrodynamic added masses become more dominant which will have a negative decreasing effect on the overall natural frequency.

Theoretically the required bucket dimensions can accurately be calculated to obtain the optimal damping of the cross brace. However, the practical implementation of the system is more challenging. From the calculations shown it can be determined that relative large buckets filled with water are required to obtain proper damping. The connection between the cross brace and the bucket will be a challenging aspect as well. Furthermore, the fatigue life of the bucket system needs to be up to standard which will also be a difficult task.

Overall it can be concluded that the implementation of this damping system is unrealistic.

7. CONCLUSIONS

This thesis is based on a project having OWT structures with the foundation consisting of a jacket design having a framework of four bays of cross braces. In a late stage of the project it was found by the substructure designer that fatigues issues in the jacket structure would occur, since it was found that the applied external forces on the structure are in the same frequency range as the natural frequency of particular cross braces in the jackets. Due to this, large brace excitation was found in the computational model, due to resonance, which results in a low expected fatigue life. To mitigate this, double sided welds and external toe grinding were implemented.

However, no clear explanation regarding this perceived fatigue issue was provided and not all parties involved obtained the same results and conclusions. Therefore further investigation regarding this academic fatigue issue was requested.

The goal of this research is to identify and provide a clear explanation of the amplification of the brace vibration movement and thus independently assess if there is a fatigue problem with the OWT jackets of the reference project.

This research can be separated into two main sections.

1. Identification of the overlapping of eigen-frequencies of the substructure and the forcing frequencies, resulting in the short estimated fatigue life due to resonance.
2. Alternative solutions to this problem, had the vibration issue been found in an earlier stage of the project.

This thesis also provides a procedure with regards to identifying the potential for resonance at an early stage of the design process. This procedure is expressed in a flowchart shown in Appendix K and described in chapter 4.

After investigation the following conclusions can be made;

1. Identification of the overlapping of eigen- frequencies of the substructure and the forcing frequencies, resulting in the short estimated fatigue life due to resonance.

In this section the (a) forcing frequencies and the (b) eigen-frequencies of the cross braces were analysed. The outcomes of both studies were (c) compared to determine if this results in a low fatigue life.

a. Analysis of the forcing frequencies

From the power density spectra graph excitations around 2 - 2.5 Hz are visible. These excitations are due to the turbine forces caused by the eigen-frequencies of the tower and the blades.

b. Analysis of the eigen-frequencies of the cross braces of bay 3 and 4 of cluster 5

With the use of ANSYS modal analysis were the local eigen-frequencies obtained of bay 3 and 4. The leg-brace connection was analysed and it was estimated that the connections behaves for 70% as a fixed connection. The obtained damped natural frequencies are the following for bay 3 and 4 when considering 1% of critical damping;

TABLE 7-1 BAY 3 AND 4 DAMPED NATURAL FREQUENCIES WITH DIFFERENT BOUNDARY CONDITIONS

damped ωn_water+MG	**Bay 4**	**Bay 3**	**[unit]**
Pinned	2.2	2.1	[Hz]
70%	2.9	2.5	[Hz]
Fixed	3.5	2.7	[Hz]

The global analysis demonstrates that the breathing mode (5) and the sway modes (6, 7) have a damped eigen- frequency of 2.19 Hz and 2.76 Hz respectively.

c. Comparison of forcing frequencies and eigen-frequencies

When assuming the brace-leg connection has 70% fixity, the damped natural frequency for bay 4 is out of the critical forcing frequency range of 2 – 2.5Hz. This would suggest no resonance would occur for this particular cross brace. The local damped natural frequency of bay 3 is determined as 2.5 Hz, meaning this could overlap with the forcing frequency and the occurrence of resonance is possible, which could result in a low estimated fatigue life.

From the global analysis was found that the breathing mode (5) has a damped natural frequency of 2.19 Hz and is in the critical frequency zone, 2 – 2.5 Hz, for the occurrence of resonance. The 'all braces bays sway modes' (mode 6, 7) are out of the critical frequency range, with an damped eigen-frequency of 2.76 Hz.

This is different compared to the substructure designer's findings. Their analysis showed that the damped natural frequency of both bay 3 and 4 would overlap with the forcing frequencies. Furthermore the sway and the breathing modes were determined to be in the critical frequencies by the substructure designer.

2. Alternative solutions to this problem, had the vibration issue been found in an earlier stage of the project.

Different concepts were described with each having advantages and disadvantages. With these concepts a MCA was executed and three concepts were investigated in more detail;

a. Concept 1 – Diamond brace

This concept aims to increase the eigen-frequencies of the sway and breathing mode and to restrict these movements from amplification.

Mode number 5, the breathing mode for bay 3 and 4, shows an eigen-frequency of 2.36 Hz which suggest it could cause complications. However, the diamond brace is restricting the bay in this specific movement, so the amplitude of the cross braces is limited. This ensures that the stresses in the leg-brace connection generated are smaller and an increase in fatigue life is obtained by this implementation. However, by adding the diamond brace, the stresses obtained in the diamond brace connections increase. This could result in simply shifting the problem into another node.

The sway modes (6, 7) of the original jacket, having a natural frequency of roughly 2.77 Hz have increased to a frequency around 3.14 Hz. It is worth mentioning that the sway mode without diamond brace was, found in this research, out of the critical frequency range of 2 - 2.5Hz

Overall it can be concluded that this concept is a successful implementation for this particular challenge.

b. Concept 2 – Five bay jacket

This concept aims to increase the eigen-frequency of the cross braces by physically decreasing the brace length by adding an extra bay. By obtaining an optimal cross brace framework of the current jacket, eigen-frequencies of all the five bays should be above 2.5Hz. As presented in Table 6-15, this is the case for this particular jacket lay out and hence no resonance would occur.

Overall it can be concluded that this concept is a successful implementation for this particular challenge.

c. Concept 3 – Water damping mechanism

In this concept the braces are connected with a bucket of partly filled with water to the middle of the brace. The sloshing of the tank acts as a dynamic absorber which goal is to suppress the motion brace vibration.

Theoretically the required bucket dimensions can be calculated to obtain the optimal damping of the cross brace. However, the practical implementation of the system is more challenging. From the calculations shown it can be determined that relatively large buckets filled with water are required to obtain a reasonable decrease in amplitude. The connection between the cross brace and the bucket will be a challenging aspect as well. Furthermore, the fatigue life of the bucket system needs to satisfy the requirements which will also be an ambitious task.

Overall it can be concluded that the implementation of this damping system is unrealistic.

8. RECOMMENDATIONS

The following recommendations are suggested for further investigation and improvement to this research.

- It was noticed that the selection of boundary conditions for the local brace modal analysis has a considerable effect on the eigen-frequency outcome and deciding if resonance would occur. In this research simple calculations provided a rough estimation of the leg-brace connection behaviour. Further investigation of the exact connection between the brace and jacket leg is recommended, to establish the exact local eigen-frequencies.

- It is recommended to apply motion sensors on the substructure braces of the referenced project to measure the movements. With the use of these accelerometer sensors, the amplification of the actual brace movements can be generated and be determined if the designed model predictions were correct. This is would be useful data for future projects.

- It is recommended for future projects that in the design process of the substructure the applied forcing frequencies are taken into account at an early stage of the design. Following the design steps that are described in the flowchart, Appendix K, is suggested to avoid resonance. Furthermore when performing the fatigue assessment it is of great importance that the correct amount of damping is applied to the model to obtain reliable results.

- For this particular project a four legged jacket foundation design was selected. Other foundation layouts such as a three-legged-jacket design should be examined, with the use of flowchart shown in appendix K, to observe if these designs are also susceptible to vibration issues.

- It was found that when no marine growth is present, no resonance would occur that could cause a short estimated fatigue life. The added mass due to the marine growth has an effect on the eigen-frequencies of the braces and determines if overlapping of forcing and eigen- frequencies of the braces occurs. Therefore it is recommended to make use of mechanisms that prevent marine growth from attaching to the structure. It is suggested to apply specially designed rings around the members that move up and down due to the wave forces, which prevent marine growth from attaching.

9. REFERENCING

[1] 4C Offshore. "Events on XXX" accessed September 27, 2016. http://www.4coffshore.com/windfarms/project-dates-for-XXX-uk53.html

[2] SSE. "XXX," accessed September 27, 2016. http://sse.com/whatwedo/ourprojectsandassets/renewables/XXX/

[3] Subhamoy Bhattacharya, "Challenges in Design of Foundations for Offshore Wind Turbines," *IET The Institute of Engineering and Technology* (2014) accessed September 13, 2016. doi; 10.1049/etr.2014.0041

[4] Dale S. L. Dolan and Peter W. Lehn, "Simulation Model of Wind Turbine 3p Torque Oscillation due to Wind Shear and Tower Shadow." IEEE Transactions on energy conversion (2006). Vol 21, no.3

[5] Muhammed Arshad and Brendan C. O'Kelly, "Analysis and Design of Monopile Foundations for Offshore Wind-Turbines Structures," Marine Georesources & Geotechnology (2016), 34;6, 503-525, doi:10.1080/1064119X.2015.1033070

[6] Det Norske Veritas, "Environmental Conditions and Environmental Loads," DNV-RP-C205 (2010).

[7] "IEV Offshore Engineering Sector." Accessed October 26, 2016. http://www.iev-group.com/index.php?p=contents-item&id=9536

[8] Live Salvesen Fevag, "Influence of marine growth on support structure design for offshore wind turbines," *Norwegian University of Science and Technology Department of Civil and Transport Engineering* (2012)

[9] Det Norske Veritas, "Design of Offshore Wind Turbine Structures," DVN_OS_J101 (2014)

[10] J. Lee, J. Seo, M. Kim, S. Shin, M. Han, J. Park5,and M. Mahendran, "Comparison of hot spot stress evaluation methods for welded structures," *Society of Naval Architects of Korea* (2010), 2:200 - 210

[11] P.J. Haagensen and S.J. Maddox, "IIW Recommendations of Post Weld Improvement of Steel and Aluminium Structures," *The International Institute of Welding* (2001). IIW Commision XII, XIII-1815-00

[12] M. Damgaards, J.K.F. Andersen, L.B. Ibsen, L. V. Andersen, "Natural Frequency and Damping Estimation of an Offshore Wind Turbine Structure," *International Offshore an Pilar Engineering Conference* (2012), ISBN 978-1-880653-94–4.

[13] Jin-wei Huang, "Development of modified p-y curves for Winkler Analysis to characterize the lateral load behaviour of a single pile embedded in improved soft clay," *IOWA State University* (2011)

[14] M. C. Ong, O. D. Okland, E. E. Bachynski, E. Passano, "Dynamic Response of a Jacket-type Offshore Wind Turbine using Decoupled and Coupled Models." *ASME 2014 33rd International Conference on Ocean, Offshore and Arctic Engineering* (2014). OMAE2014-24246

[15] "OrcaFlex Rayleigh Damping" accessed December 9, 2016. https://www.orcina.com/SoftwareProducts/OrcaFlex/Documentation/Help/Content/html/RayleighDamping,Guidance.htm

[16] I. Chowdhury and S. P. Dasgupta. "Computation of Rayleigh Damping Coefficients for Large Systems," *Petrofac International Limited and Indian Institute of Technology* (?)

[17] Kareem, A., and K. Gurley. "Damping in Structures; Its Evaluation and Treatment of Uncertainty." *Journal of Wind Engineering and Industrial Aerodynamics* 59 (1996): 131-57

[18] Cai, C., H. Zheng, M. S. Khan, and K. C. Hung. "Modelling of Material Damping Properties in ANSYS." *Defense Systems Division, Institute of High Performance Computing*

[19] Lackner, Matthew A., and Mario A. Rotea. "Passive Structural Control of Offshore Wind Turbines." *Wind Energy*, 2010, 373-88. doi:10.1002/we.

[20] Colwell, Shane, and Biswajit Basu. "Tuned liquid column dampers in offshore wind turbines for structural control." *Elsevier Engineering Structures*, September 1, 2008, 358-68. doi:10.1016/j.engstruct.2008.09.001.

[21] Knowledge. 2016. "Evaluation of TLCD Damping Factor from FRF Measurement Due to Variation of The Fluid Viscosity." Accessed December 13, 2016 http://www.knepublishing.com/index.php/KnE-Engineering/article/view/481/1527.
[22] SweetHaven. “Fundamentals of Professional Welding.” Accessed December 29, 2016. http://www.free-ed.net/free-ed/Courses/05%20Building%20and%20Contruction/050205%20Welding/Welding00.asp?iNum=0302.
[23] Holthuijsen, Leo H. *Waves in Oceanice and Coastal Waters*. ISBN 978-0-521-86028. UK: Cambridge University Press, 2007.
[24] Gerven, Frank, Van. *Opstimising the Design of a Steel Substructure for Offshore Wind Turbines in Deepter Waters*. Delft: Delft University of Technology, 2011.
[25] DNV-GL. *Fatigue design of offshore steel structures*. DNVGL-RP-C203. 2016.
[26] SubTech. "Fatigue." *Knowledge source on Material Engineering* . 2014. Accessed January 2, 2017. http://www.substech.com/dokuwiki/doku.php?id=fatigue.
[27] eFatigue. "Rainflow Counting Technical Background." A trusted source for fatigue analsys. 2008. Accessed January 2, 2017. https://www.efatigue.com/variable/background/rainflow.html.
[28] Vocal Technologies. 2015. "The FFT: An Efficient Class of Algorithms." Accessed January 1, 2017. https://www.vocal.com/noise-reduction/fft-algorithms/.
[29] Spijkers, J. M. J., A. W. C. M. Vrouwenvelder, and E. C. Klaver. *Dynamics of Structures. Part 1 Vibration of Structures*. Series 06917300009. Delft: Delft University of Technology, 2006.
[30] Systemes, D. “Rayleigh Damping” accessed February 7, 2017. http://help.solidworks.com/2015/English/SolidWorks/cworks/c_Rayleigh_Damping.htm
[31] Det Norske Veritas, “Environmental Conditions and Environmental Loads,” DVN-RP-C205 (2010)
[32] XXX, XXX Offshore Wind Farm Clustering Strategy Report, LF000005-REP-139, Rev 2 (2014)
[33] XXX, XXX Offshore Wind Farm Analysis Design Brief, LF000005-REP-278, Rev 9 (2016)
[34] XXX, XXX Offshore Wind Farm Geotechnical Design Brief, LF000005-REP-276, Rev 7 (2016)
[35] XXX, XXX Offshore Wind Farm Hydrodynamic Load Design Brief, LF000005-REP-288, Rev 4 (2015)
[36] Siemens. SWT 7.0-154, T87.72-01 – XXX Tower Design Document, LF000005-REP-464, Ref 7 (2016)
[37] Siemens. SWT-7.0-154, Initial Offshore interface loads, jacket foundation. LF000005-REP-415, Ref 4 (2015)
[38] XXX, Cluster 5 Weak Iteration 1.6 – Description of ASAS Model for Couple Analysis, LF000005-REP-1031, Rev 1 (2016)
[39] ABP mer, (2014). *XXX Offshore Windfarm Metocean Criteria for Construction, Decommissioning, Operation and Maintenance*. Report R.2104.
[40] Journee, J.M.J. and W.W. Massie. 2001. *Offshore Hydromechanics*. 1st ed. TU Delft.
[41] “Multi-Criteria Analysis.” JRC European Commision. 2005. Accessed March 1, 2017. http://forlearn.jrc.ec.europa.eu/guide/4_methodology/meth_multi-criteria-analysis.htm
[42] Asami, Toshihiko, and Osamu Nishihara. "Closed-Form Exact Solution to H∞ Optimization of Dynamic Vibration Absorbers (Application to Different Transfer Functions and Damping Systems)." *Journal of Vibration and Acoustics* 125, no. 3 (2003): 398. doi:10.1115/1.1569514.
[43] Harihara, Parasuram, and Dara W. Childs. *Solving Problems in Dynamics and Vibrations Using MATLAB*. Texas A & M University, ?
[44] Mondal, Jitaditya , Harsha Nimmala, Shameel Abdulla, and Reza Tafreshi. "Tuned Liquid Damper." *Proceedings of the 3rd International Conference on Mechanical Engineering and Mechatronics*, August 2014, 68-74.
[45] Hansen, M. H. "Aeroelastic instability problems for wind turbines." *Wind Energy* 10, no. 6 (2007): 551-77. doi:10.1002/we.242.
[46] Hau, Erich. *Wind Turbines Fundamentals, Technologies, Application, Economics*. Berlin, Heidelberg: Springer Berlin Heidelberg, 2013.

[47] Chaviaropoulos, P. K. "Flap/lead-lag aeroelastic stability of wind turbine blades." *Wind Energy* 4, no. 4 (2001): 183-200. doi:10.1002/we.55.
[48] Burton, Tony. *Wind energy handbook*. Chichester, West Sussex: Wiley, 2011.
[49] FoundOcean. *Strengthening, Modification and Repair for Offshore Assets*. 2016. www.foundocean.com
[50] El-Reedy, Mohamed A. *Offshore structures: design, construction and maintenance*. Amsterdam: Elsevier, 2012.
[51] "Harmonically Excited Forced Vibration of a Single DOF System (Theory)" Virtual Labs for Mechanical Vibrations (M) : Mechanical Engineering : IIT GUWAHATI Virtual Lab. Accessed April 03, 2017. http://iitg.vlab.co.in/?sub=62&brch=175&sim=1084&cnt=1.
[52] "Resonance." Dictionary.com. Accessed April 03, 2017. http://www.dictionary.com/browse/resonance.
[53] "ANSYS ASAS Offshore." TDA Engineering. Accessed April 03, 2017. http://tda.as/services/training_and_events/ansys/_ansys_asas_offshore/.
[54] Metrikine, A. V. *Dynamics, Slender Structures and an Introduction to Continuum Mechanics - CT 4145*. Delft : Delft University of Technology, ?
[55] "Offshore wind turbine with jacket support structure." ResearchGate . 2017. Accessed April 5, 2017. https://www.researchgate.net/figure/262790782_fig1_Fig-1-Offshore-wind-turbine-with-jacket-support-structure-Artist-impressionB-jarne.
[56] Det Norske Veritas, "Design of Offshore Wind Turbine Structures," DVN-OS-J101 (2013)
[57] Mishra, Gopal. "LIMIT STATES OF STEEL DESIGN." The Constructor. December 11, 2012. Accessed May 04, 2017. https://theconstructor.org/structural-engg/limit-states-of-steel-design/6879/.
[58] Kooijman, H. J.T., C. Lindenburg, D. Winkelaar, and E. L. Hooft, Van Der. "DOWEC 6 MWPRE-DESIGN." *Aero-elastic modelling of the DOWEC 6 MW pre-design in PHATAS*, DOWEC-F1W2-HJK-01-046/9 (September 2003).
[59] Jonkman, J., S. Butterfield, W. Musial, and G. Scott. "Definition of a 5-MW Reference Wind Turbine for Offshore System Development." *NREL Innovation for Our Engergy Future* , NREL/TP-500-38060 (2009).
[60] Vorpahl, Fabian, Wojciech Popko, and Daniel Kaufer. "Fraunhofer IWES." *Description of a basic model of the 'UpWind reference jacket' for code comparison in the OC4 project under EIA Wind Annex 30*, OC4 Phase I - Jacket Model (2013). www.fraunhofer.iwes.de.
[61] Vugts, J. (2002). *Handbook of bottom founded offshore structures* (Vol. II, OE 4651). Delft: Eburon.
[62] Jia, J. (2014). *Essentials Of Applied Dynamic Analysis* (2195-4348). Bergen: Springer. doi:10.1007/978-3-642-37003-8
[63] Male, P. van der, K. N. van, Dalen, and A. V., Metrikine. "Aerodynamic Damping of Nonlinearily Wind-Excited Wind Turbine Blades." *Proceedings of 9th PhD Seminar on Wind Energy in Europe*, 2013.
[64] Carswell, W., J. Johansson, F. Løvholt, S. R. Arwade, C. Madshus, D. J. DeGroot, and A. T. Myers. "Foundation damping and the dynamics of offshore wind turbine Monopiles." *Renewable Energy* 0960-1481 (2015). http://dx.doi.org/10.1016/j.renene.2015.02.058.
[65] Carswell, Wystan. "Soil-Structure Modeling and Design Considerations for Offshore Wind Turbine Monopile Foundations." 2015. http://scholarworks.umass.edu/dissertations_2/531.
[66] Latini, C., V. Zania, and B. Johannesson. "Dynamic stiffness and damping of foundations for jacket structures." *6th International Conference on Earthquake Geotechnical Engineering*, November 2015.

APPENDIX A – MATLAB SCRIPT FFT

The following script was used to obtain the FFT results of the turbine loads.

```
clc
% Import XXX data into matlab
M_run22=importdata('.\..\Turbine Loads
XXX\HT__bhr_BOW_DLC12_240011_000075_07502_#m05.dat');
%

% Wind Speed     24[m/s]
% Wind Direction 75[deg]
% Wave Direction 75[deg]

% Sampling Data
t_run22=M_run22(:,1);            %time [s]
N = length(t_run22);             %Length signal / number of samples N [#]
n = 0.04;                        %bins / time steps [s]
Fs = 1/n;                        %sampling frequency [Hz]
f = Fs*(0:(N/2))/N;              %frequency [Hz]

% Turbine Loads
V_run22=M_run22(:,2);              %speed [m/s]
Fx_run22 = M_run22(:,4);           %Fx [kN]
Fy_run22 = M_run22(:,5);           %Fy [kN]
Fz_run22 = M_run22(:,6);           %Fz [kN]
Fxy_run22 = M_run22(:,7);          %Fxy [kN]
Mx_run22 = M_run22(:,8);           %Mx [kNm]
My_run22 = M_run22(:,9);           %My [kNm]
Mz_run22 = M_run22(:,10);          %Mz [kNm]
Mxy_run22 = M_run22(:,11);         %Mxy [kNm]


% Fx Fourier Analysis
Fx = fft(Fx_run22);               %Fourier Transform [Hz]
P2x = abs(Fx/N);                 %magnitude
P1x = P2x(1:N/2+1);              %Magnitude
P1x(2:end-1) = 2*P1x(2:end-1);   %Magnitude
%
figure;
subplot(4,1,1)
plot(f,P1x);
title('Fx vs Frequency [Hz]')
axis([0 4 0 30])

% Fy Fourier Analysis
Fy = fft(Fy_run22);               %Fourier Transform [Hz]
P2y = abs(Fy/N);                 %magnitude
P1y = P2y(1:N/2+1);              %Magnitude
P1y(2:end-1) = 2*P1y(2:end-1);   %Magnitude
%
subplot(4,1,2)
plot(f,P1y);
title('Fy vs Frequency [Hz]')
axis([0 4 0 30])

% Fz Fourier Analysis
```

```
Fz = fft(Fz_run22);              %Fourier Transform [Hz]
P2z = abs(Fz/N);                %magnitude
P1z = P2z(1:N/2+1);             %Magnitude
P1z(2:end-1) = 2*P1z(2:end-1);  %Magnitude
%
subplot(4,1,3)
plot(f,P1z);
title('Fz vs Frequency [Hz]')
axis([0 4 0 30])

% Fxy Fourier Analysis
Fxy = fft(Fxy_run22);              %Fourier Transform [Hz]
P2xy = abs(Fxy/N);                %magnitude
P1xy = P2xy(1:N/2+1);             %Magnitude
P1xy(2:end-1) = 2*P1xy(2:end-1);  %Magnitude
%
subplot(4,1,4)
plot(f,P1xy);
title('Fxy vs Frequency [Hz]')
axis([0 4 0 30])

% Mx Fourier Analysis
Mx = fft(Mx_run22);                %Fourier Transform [Hz]
P2mx = abs(Mx/N);                 %Magnitude
P1mx = P2mx(1:N/2+1);             %Magnitude
P1mx(2:end-1) = 2*P1mx(2:end-1);  %Magnitude
%
figure;
subplot(4,1,1)
plot(f,P1mx)
title('Mx vs Frequency [Hz]')
axis([0 4 0 100])

% My Fourier Analysis
My = fft(My_run22);               %Fourier Transform [Hz]
P2my = abs(My/N);                 %Magnitude
P1my = P2my(1:N/2+1);             %Magnitude
P1my(2:end-1) = 2*P1my(2:end-1);  %Magnitude
%
subplot(4,1,2)
plot(f,P1my)
title('My vs Frequency [Hz]')
axis([0 4 0 100])

% Mz Fourier Analysis
Mz = fft(Mz_run22);               %Fourier Transform [Hz]
P2mz = abs(Mz/N);                 %Magnitude
P1mz = P2mz(1:N/2+1);             %Magnitude
P1mz(2:end-1) = 2*P1mz(2:end-1);  %Magnitude
%
subplot(4,1,3)
plot(f,P1mz)
title('Mz vs Frequency [Hz]')
axis([0 4 0 100])

% Mxy Fourier Analysis
Mxy = fft(Mxy_run22);               %Fourier Transform [Hz]
P2mxy = abs(Mxy/N);                 %Magnitude
P1mxy = P2mxy(1:N/2+1);             %Magnitude
P1mxy(2:end-1) = 2*P1mxy(2:end-1);  %Magnitude
```

```
%
subplot(4,1,4)
plot(f,P1mxy)
title('Mxy vs Frequency [Hz]')
axis([0 4 0 100])
```

APPENDIX B – POWER DENSITY SPECTRA

Wind speed; 10[m/s]

Wind direction; 75[deg]

Wave direction 75[deg]

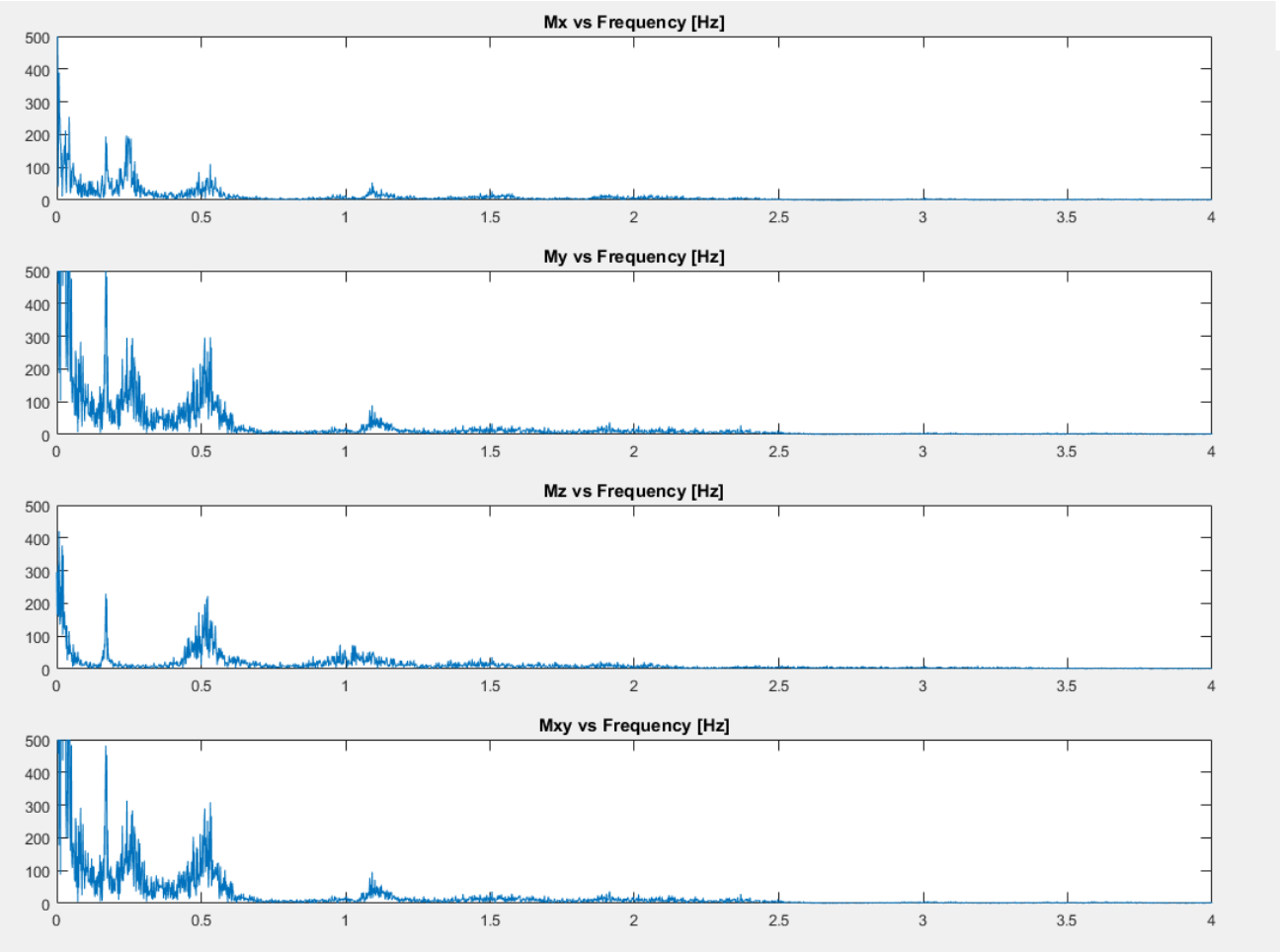

FIGURE B-0-1 FFT - WINDSPEED 10[M/S], WIND WAVE DIRECTION 75[DEG]

Wind speed; 16[m/s]

Wind direction; 75[deg]

Wave direction 75[deg]

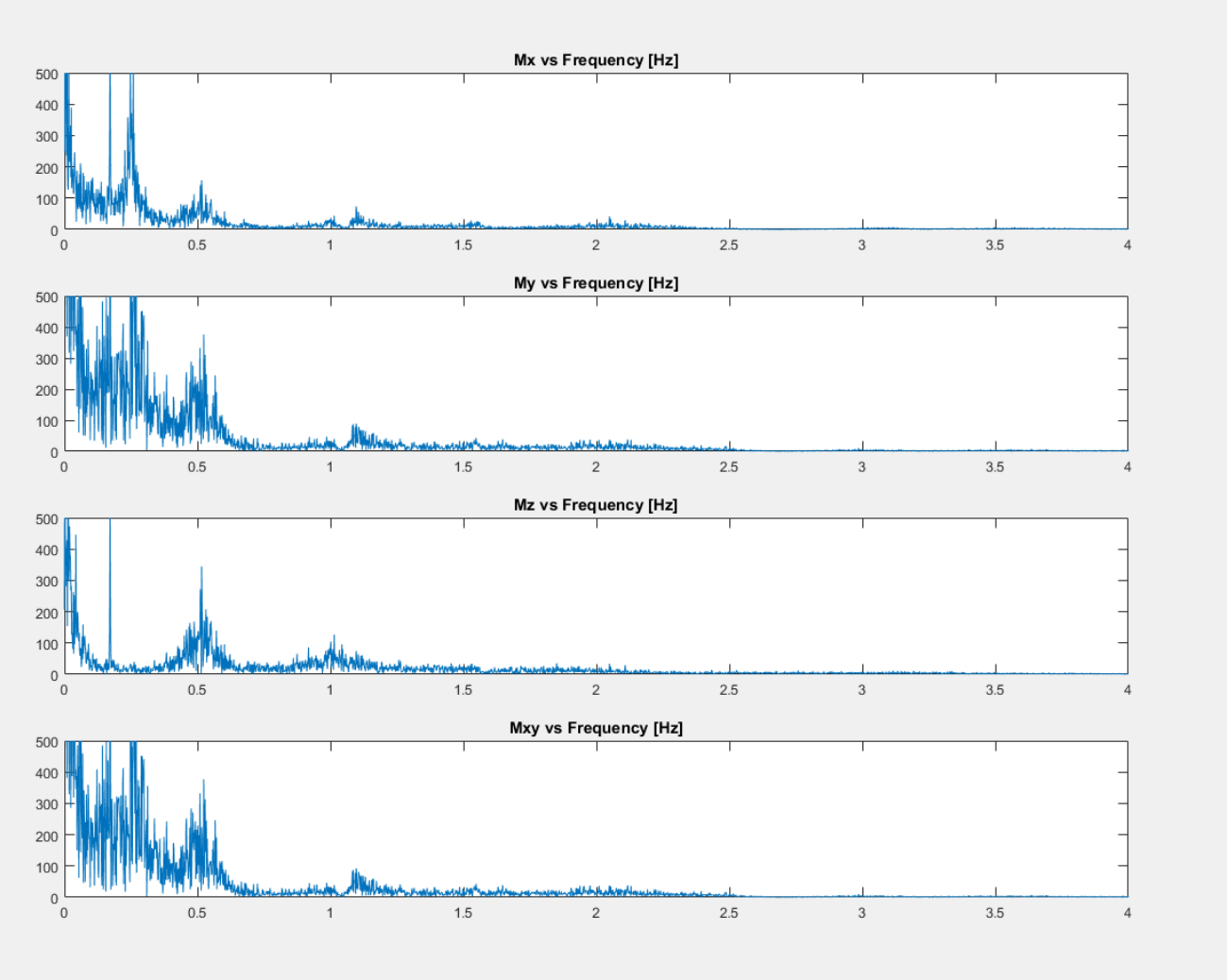

FIGURE B-0-2 FFT - WINDSPEED 16[M/S], WIND WAVE DIRECTION 75[DEG]

Wind speed; 18[m/s]

Wind direction; 75[deg]

Wave direction 75[deg]

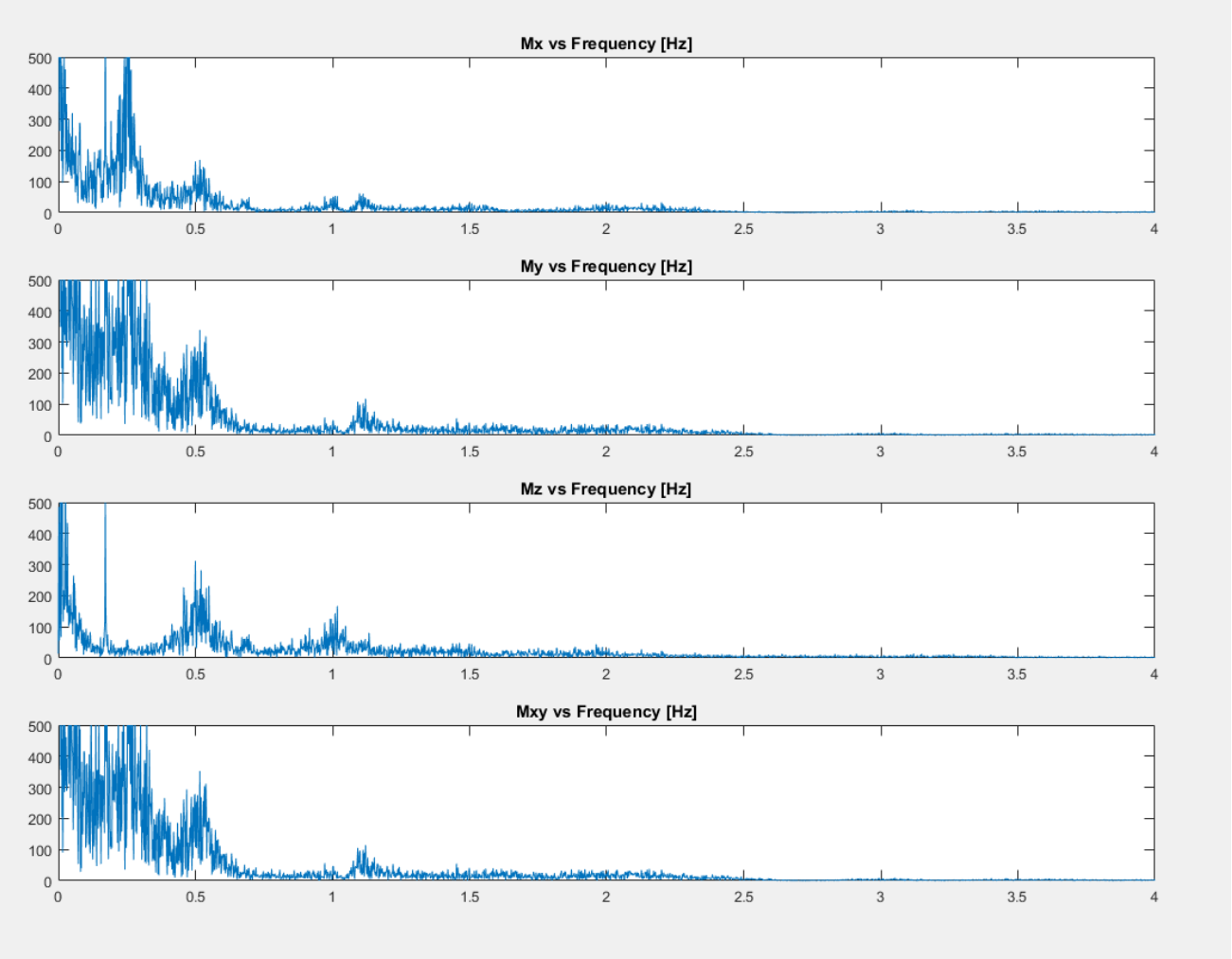

FIGURE B-0-3 FFT - WINDSPEED 18[M/S], WIND WAVE DIRECTION 75[DEG]

Wind speed; 24[m/s]

Wind direction; 75[deg]

Wave direction 75[deg]

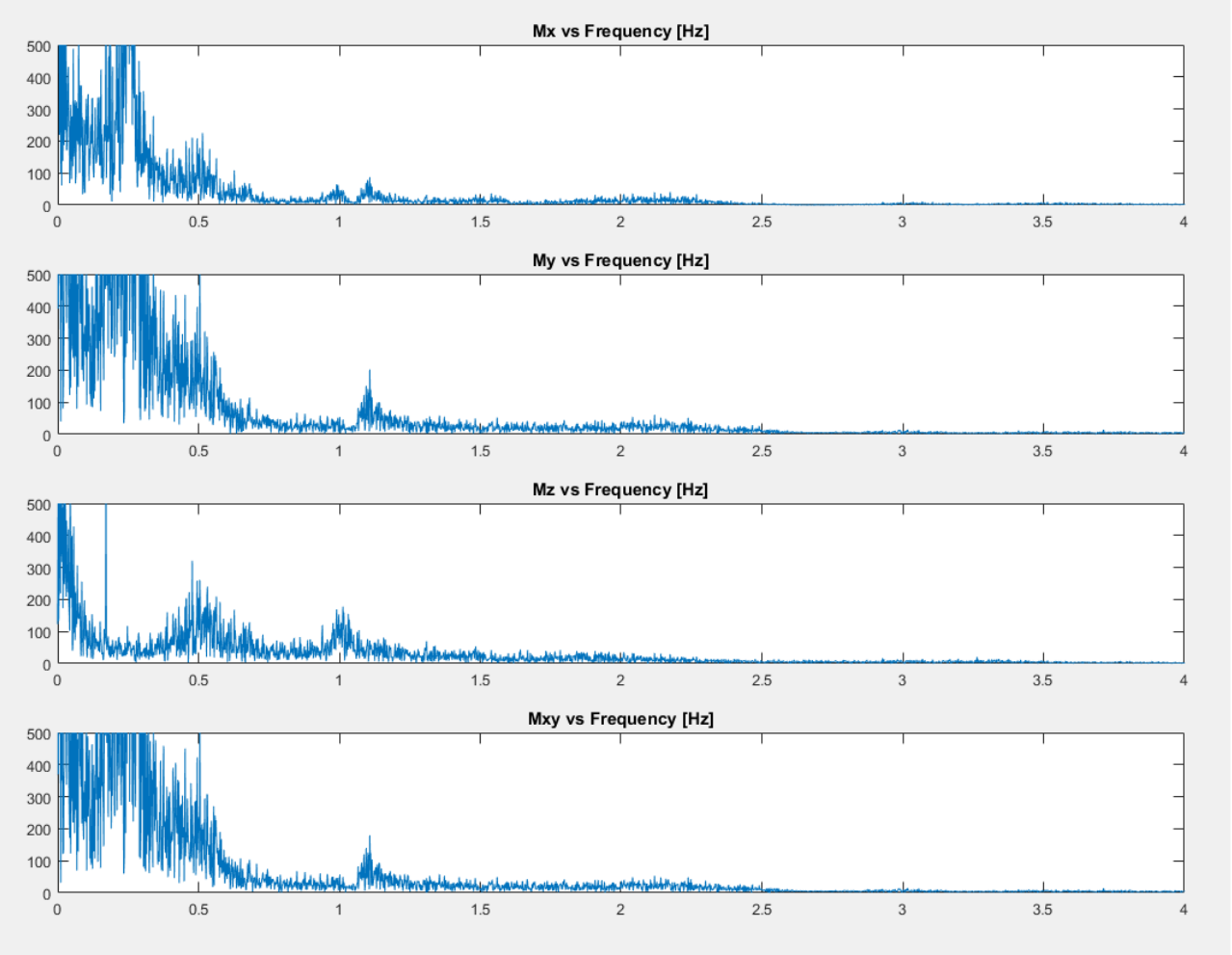

FIGURE B-0-4 FFT - WINDSPEED 24[M/S], WIND WAVE DIRECTION 75[DEG]

Wind speed; 28[m/s]

Wind direction; 75[deg]

Wave direction 75[deg]

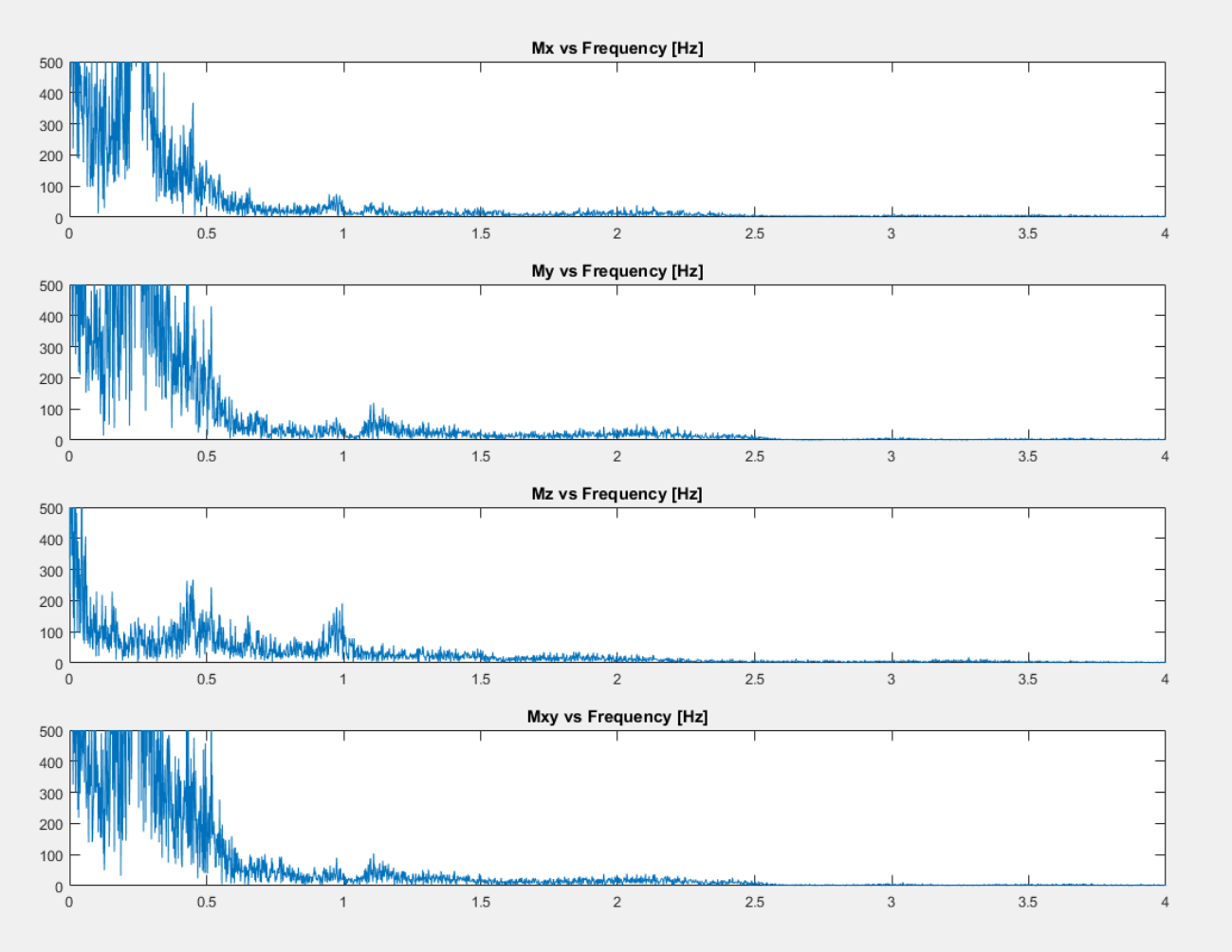

FIGURE B-0-5 FFT - WINDSPEED 28[M/S], WIND WAVE DIRECTION 75[DEG]

APPENDIX C – VOLUME CALCULATIONS

This appendix provides the marine growth calculations of bay 3 and 4 of the reference project. The following equation was used;

$$Volume = \frac{lenght\ \pi D^2}{4}$$

TABLE C-0-1 VOLUME BAY 3

Section	Length [mm]	Do [mm]	volume [mm^3]	MG wt [mm]	Do + MG [mm]	volume + MG [mm^3]	volume MG only [mm^3]
1	10496	680	3.81E+09	100	880	6.38E+09	2.57E+09
2	10196	680	3.70E+09	100	880	6.20E+09	2.50E+09
3	13391	680	4.86E+09	100	880	8.14E+09	3.28E+09
4	13091	680	4.75E+09	100	880	7.96E+09	3.21E+09
5	1485	720	6.04E+08	100	920	9.87E+08	3.82E+08
6	10084	720	4.11E+09	100	920	6.70E+09	2.60E+09
7	1380	690	5.16E+08	100	890	8.59E+08	3.42E+08
8	1380	690	5.16E+08	100	890	8.59E+08	3.42E+08
TOTAL			**2.29E+10**			**3.81E+10**	**1.52E+10**
Total 4x			**9.15E+10**			**1.52E+11**	**6.09E+10**

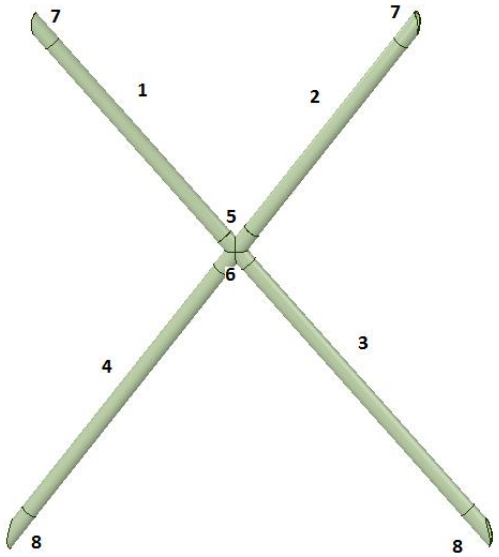

FIGURE C-0-1 BAY 3 SECTIONED

TABLE C-0-2 VOLUME BAY 4

Section	Length [mm]	Do [mm]	volume [mm3]	MG wt [mm]	Do + MG [mm]	volume + MG [mm3]	volume MG only [mm3]
1	11751	710	4.65E+09	100	910	7.64E+09	2.99E+09
2	11452	710	4.53E+09	100	910	7.45E+09	2.91E+09
3	10456	710	4.14E+09	100	910	6.80E+09	2.66E+09
4	10156	710	4.02E+09	100	910	6.61E+09	2.58E+09
5	1404	760	6.37E+08	100	960	1.02E+09	3.79E+08
6	1286	760	5.83E+08	100	960	9.31E+08	3.47E+08
7	1460	730	6.11E+08	100	930	9.92E+08	3.81E+08
8	1532	920	1.02E+09	100	1120	1.51E+09	4.91E+08
9	6002	815	3.13E+09	100	1015	4.86E+09	1.73E+09
TOTAL			**2.33E+10**			**3.78E+10**	**1.45E+10**
Total 4x			**9.33E+10**			**1.51E+11**	**5.79E+10**

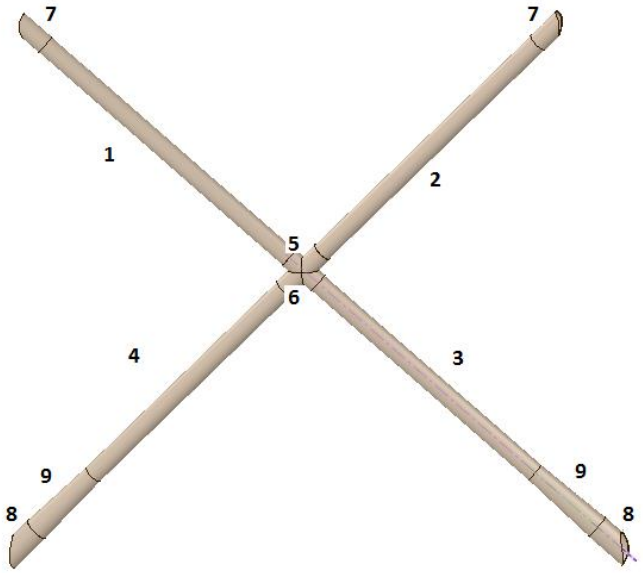

FIGURE C-0-2 BAY 4 SECTIONED

TABLE C-0-3 VOLUME LEG

section	Length [mm]	Do [mm]	volume [mm3]	MG wt [mm]	Do + MG [mm]	volume + MG [mm3]	volume MG only [mm3]
1	3600	1680	7.98E+09	100	1880	9.99 E+09	2.01 E+09
2	2000	1680	4.43 E+09	100	1880	5.55 E+09	1.12 E+09
3	4210	1385	6.34 E+09	100	1585	8.30 E+09	1.96 E+09
4	3800	1090	3.54 E+09	100	1290	4.96 E+09	1.42 E+09
5	7645	908	4.95 E+09	100	1108	7.37 E+09	2.42 E+09
6	3111	1100	2.95 E+09	100	1300	4.12 E+09	1.17 E+09
7	6849	1040	5.81 E+09	100	1240	8.27 E+09	2.45 E+09
8	1200	1080	1.10 E+09	100	1280	1.54 E+09	4.45 E+09
9	3305	1080	3.02 E+09	100	1280	4.25 E+09	1.23 E+09
TOTAL			**4.02E10**			**5.44E+10**	**1.42E+10**
Total 4x			**1.60E+11**			**2.18E+11**	**5.69E+10**

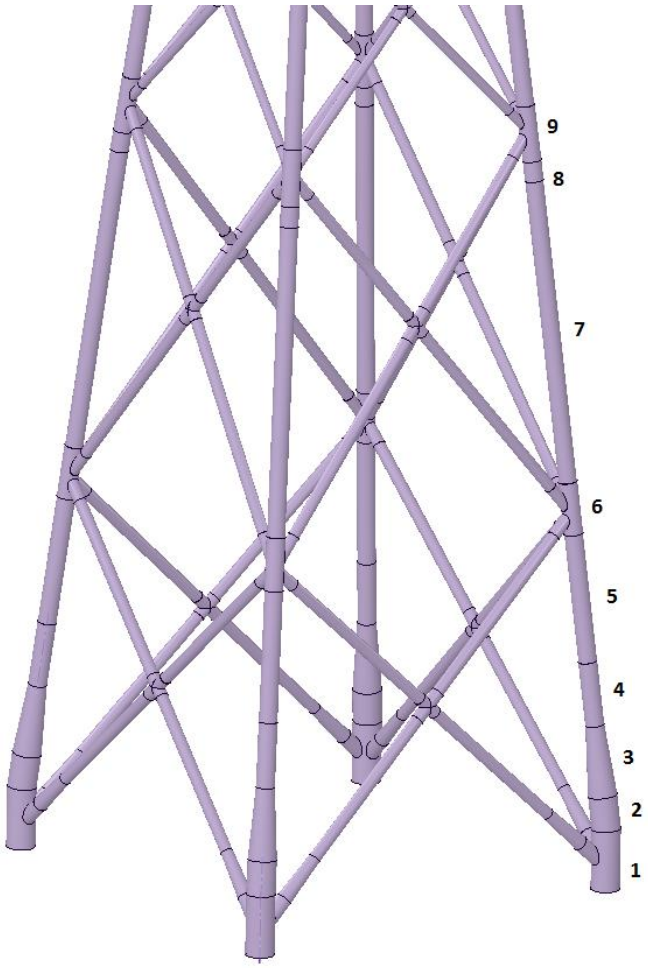

FIGURE C-0-3 LEG SECTIONED

APPENDIX D – ADDED MASS WATER CALCULATION - CA

This Appendix demonstrates the calculations in obtaining the Ca value for bay 3 and 4. The Ca value is gathered by;

$$Ca = Cm - 1$$

The graph below demonstrates the relation between the Cm and the KC value in combination with the surface roughness.

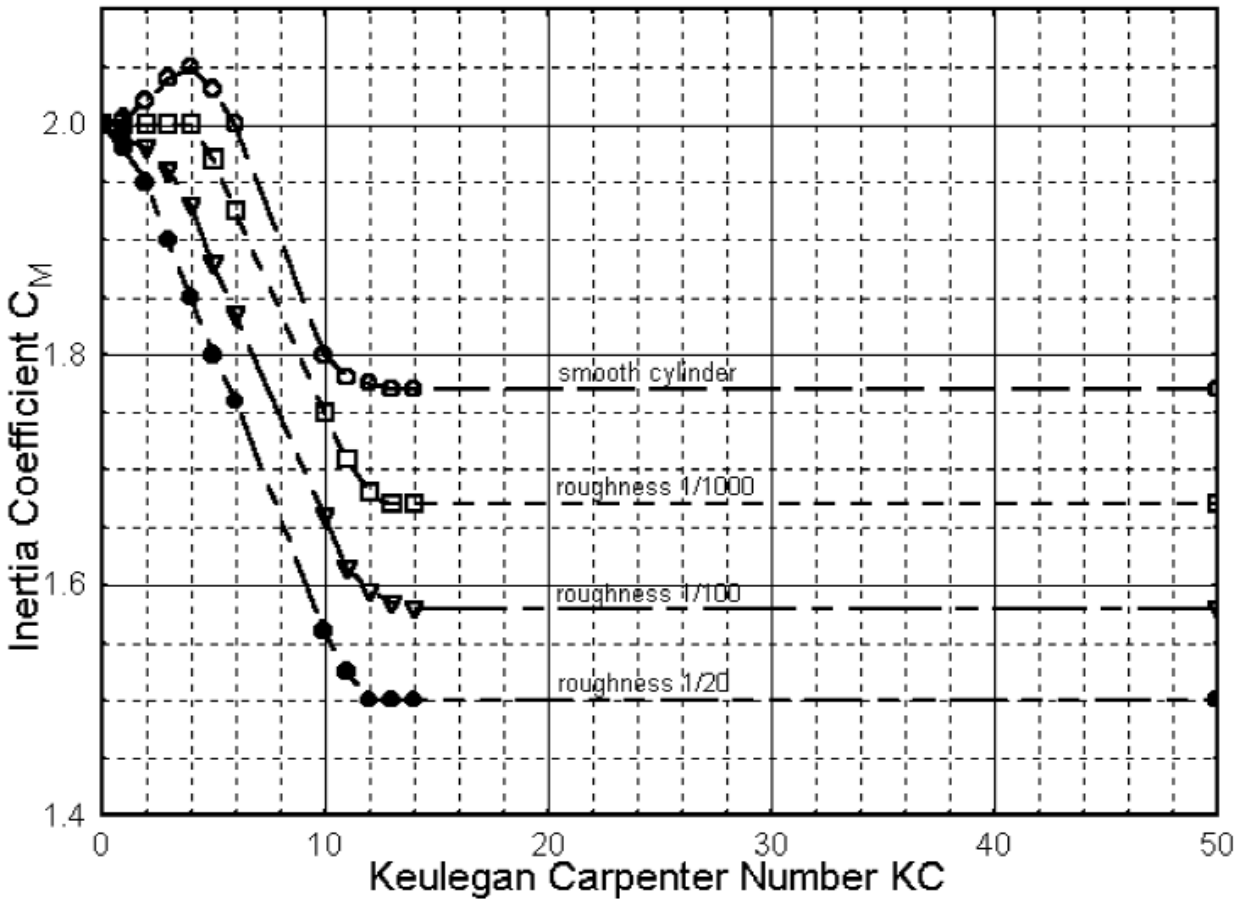

FIGURE D-0-1 CM VS KC [40]

Bay 3

This section demonstrates the calculations in obtaining the appropriate KC value for bay 3. A scatter of multiple wave heights and periods is selected to obtain a good overview. The wave height and period around 5 – 6 [m] and [m/s] is governing.

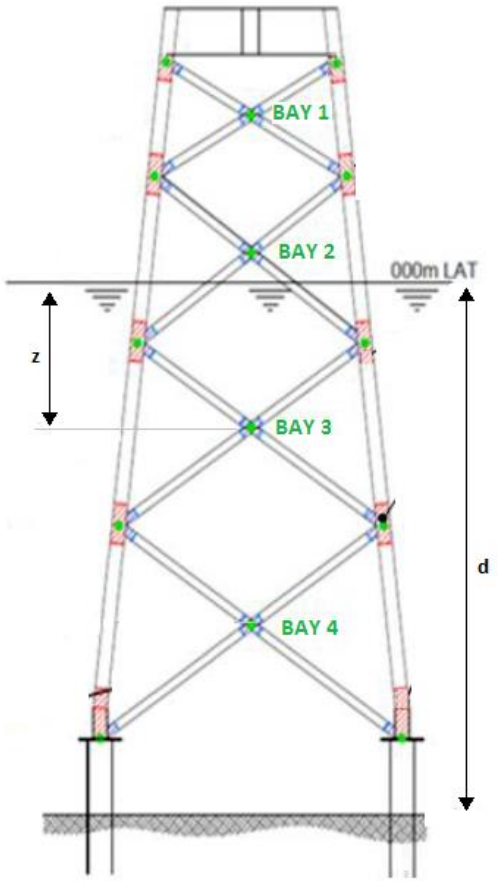

FIGURE D-0-2 BAY 3 DEPTH

Table D-0-1 provides the input values used to calculate the KC value for different flow periods. The equations used are demonstrated in section 5.2.2.6.

TABLE D-0-1 Input Ua Calculation - Bay 3

T	3	4	5	6	7	unit
λ (deep)	14.04	24.96	39.00	56.16	76.44	[m]
k	0.45	0.25	0.16	0.11	0.08	[-]
d	48.43	48.43	48.43	48.43	48.43	[m]
z	-16.09	-16.09	-16.09	-16.09	-16.09	[m]
cosh(k(z+d))	964784.46	1716.10	91.57	18.65	7.17	[-]
sinh(kd)	1293040122.29	98532.87	1223.27	112.75	26.77	[-]
cosh(k(z+d)) / sinh(kd)	0.001	0.017	0.075	0.165	0.268	[-]
ω	2.09	1.57	1.26	1.05	0.90	[rad/s]

TABLE D-0-2 Ua Calculation - Bay 3

Ua [m/s]	T [s]				
H [s]	3	4	5	6	7
3	0.0023	0.0410	0.1411	0.2598	0.3606
4	0.0031	0.0547	0.1881	0.3464	0.4809
5	0.0039	0.0684	0.2352	0.4330	0.6011
6	0.0047	0.0821	0.2822	0.5196	0.7213
7	0.0055	0.0958	0.3292	0.6062	0.8415
8	0.0063	0.1094	0.3763	0.6928	0.9617

The KC value is obtained for an outer diameter of 0.88[m] and 0.92[m]. These are the minimal and maximal outer diameters the cross brace in bay 3. This way a better understanding of selecting the appropriate KC value is obtained. An overview of all diameters in cross brace 3 is shown in Appendix C.

TABLE D-0-3 KC Calculation D0 = 0.88 - Bay 3

KC - Do = 0.88	T [s]				
H [m]	3	4	5	6	7
3	0.69	1.10	1.94	3.14	4.46
4	0.69	1.16	2.21	3.73	5.42
5	0.70	1.22	2.47	4.32	6.37
6	0.70	1.28	2.74	4.91	7.33
7	0.70	1.34	3.01	5.50	8.28
8	0.70	1.41	3.27	6.09	9.24

TABLE D-0-4 KC Calculation D0 = 0.92 - Bay 3

KC - Do = 0.92	T [s]				
H [m]	3	4	5	6	7
3	0.66	1.05	1.85	3.00	4.27
4	0.66	1.11	2.11	3.56	5.18
5	0.66	1.17	2.37	4.13	6.10
6	0.67	1.23	2.62	4.69	7.01
7	0.67	1.29	2.88	5.26	7.92
8	0.67	1.35	3.13	5.82	8.84

From the tables can be concluded that a KC of 3 will be used in Figure D-0-1 to obtain the Cm value. In combination with a surface roughness of 1/200 this results in a Cm value of 1.95, therefore a Ca value of 0.95.

Bay 4

This section demonstrates the calculations in obtaining the appropriate KC value for bay 4. A scatter of multiple wave heights and periods is selected to obtain a good overview. The wave height and period around 5 – 6 [m] and [m/s] is governing.

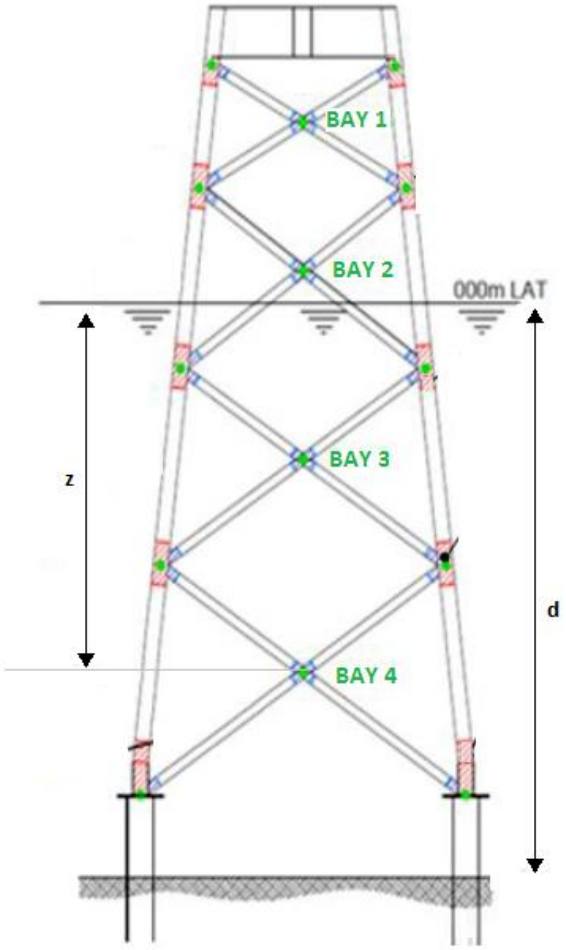

FIGURE D-0-3 BAY 4 DEPTH

Table D-0-5 provides the input values used to calculate the KC value for different flow periods. The equations used are demonstrated in section 5.2.2.6.

TABLE D-0-5 Input Ua Calculation - Bay 4

T	3	4	5	6	7	[s]
λ (deep)	14.04	24.96	39.00	56.16	76.44	[m]
k	0.45	0.25	0.16	0.11	0.08	[-]
d	48.43	48.43	48.43	48.43	48.43	[m]
z	-37.93	-37.93	-37.93	-37.93	-37.93	[m]
cosh(k(z+d))	54.92	7.06	2.81	1.77	1.40	[-]
sinh(kd)	1293040122.29	98532.87	1223.27	112.75	26.77	[-]
cosh(k(z+d)) / sinh(kd)	0.00000004	0.00007170	0.00229407	0.01572576	0.05215081	[-]
ω	2.09	1.57	1.26	1.05	0.90	[rad/s]

TABLE D-0-6 Ua Calculation - Bay 4

Ua [m/s]	T [s]				
H [m]	3	4	5	6	7
3	1.3E-07	1.7E-04	4.3E-03	2.5E-02	7.0E-02
4	1.8E-07	2.3E-04	5.8E-03	3.3E-02	9.4E-02
5	2.2E-07	2.8E-04	7.2E-03	4.1E-02	1.2E-01
6	2.7E-07	3.4E-04	8.6E-03	4.9E-02	1.4E-01
7	3.1E-07	3.9E-04	1.0E-02	5.8E-02	1.6E-01
8	3.6E-07	4.5E-04	1.2E-02	6.6E-02	1.9E-01

The KC value is obtained for an outer diameter of 0.91[m] and 1.2[m]. These are the minimal and maximal outer diameters the cross brace in bay 3. This way a better understanding of selecting the appropriate KC value is obtained. An overview of all diameters in cross brace 4 is shown in Appendix C.

TABLE D-0-7 KC Calculation D0 = 0.91 - Bay 4

KC - Do = 0.91	T [s]				
H [m]	3	4	5	6	7
3	0.66	0.88	1.12	1.48	2.08
4	0.66	0.88	1.13	1.54	2.26
5	0.66	0.88	1.14	1.59	2.44
6	0.66	0.88	1.15	1.64	2.62
7	0.66	0.88	1.15	1.70	2.80
8	0.66	0.88	1.16	1.75	2.98

TABLE D-0-8 KC Calculation D0 = 1.2 - Bay 4

KC - Do = 1.2	T [s]				
H [m]	3	4	5	6	7
3	0.50	0.67	0.85	1.12	1.58
4	0.50	0.67	0.86	1.16	1.71
5	0.50	0.67	0.86	1.21	1.85
6	0.50	0.67	0.87	1.25	1.99
7	0.50	0.67	0.88	1.29	2.12
8	0.50	0.67	0.88	1.33	2.26

From the tables can be concluded that a KC of 1 will be used in Figure D-0-1 to obtain the Cm value. In combination with a surface roughness of 1/200 this results in a Cm value of 1.95 and therefore a Ca value of 0.95.

APPENDIX E – GLOBAL EIGEN-FREQUENCY CALCULATIONS

TABLE E-0-1 UNDAMPED GLOBAL EIGEN FREQUENCY CALCULATIONS

	1	2	3	4	5	6	7	8	9	10	
volume steel	1.33E+11	1.33E+11	1.33E+11	1.33E+11	1.33E+11	1.33E+11	1.33E+11	1.33E+11	1.33E+11	1.33E+11	[mm3]
ρ steel	7.85E-06	7.85E-06	7.85E-06	7.85E-06	7.85E-06	7.85E-06	7.85E-06	7.85E-06	7.85E-06	7.85E-06	[kg/mm3]
mass steel	1.044E+06	1.044E+06	1.044E+06	1.044E+06	1.044E+06	1.044E+06	1.044E+06	1.044E+06	1.044E+06	1.044E+06	[kg]
β	1.57	1.57	11.93	11.93	12.26	19.30	21.16	26.62	26.79	32.91	[-]
ωn_air	**0.21**	**0.21**	**1.62**	**1.62**	**1.66**	**2.61**	**2.87**	**3.60**	**3.63**	**4.46**	[Hz]
k	1.9E+04	1.9E+04	1.9E+04	1.9E+04	1.9E+04	1.9E+04	1.9E+04	1.9E+04	1.9E+04	1.9E+04	[-]
volume water	5.2E+11	5.2E+11	5.2E+11	5.2E+11	5.2E+11	5.2E+11	5.2E+11	5.2E+11	5.2E+11	5.2E+11	[mm3]
ρ water	1.03E-06	1.03E-06	1.03E-06	1.03E-06	1.03E-06	1.03E-06	1.03E-06	1.03E-06	1.03E-06	1.03E-06	[kg/mm3]
Ca	0.9	0.9	0.9	0.9	0.9	0.9	0.9	0.9	0.9	0.9	[-]
mass water	4.81E+05	4.81E+05	4.81E+05	4.81E+05	4.81E+05	4.81E+05	4.81E+05	4.81E+05	4.81E+05	4.81E+05	[kg]
volume mg	1.76E+11	1.76E+11	1.76E+11	1.76E+11	1.76E+11	1.76E+11	1.76E+11	1.76E+11	1.76E+11	1.76E+11	[mm3]
ρ mg	1.40E-06	1.40E-06	1.40E-06	1.40E-06	1.40E-06	1.40E-06	1.40E-06	1.40E-06	1.40E-06	1.40E-06	[kg/mm3]
mass mg	2.46E+05	2.46E+05	2.46E+05	2.46E+05	2.46E+05	2.46E+05	2.46E+05	2.46E+05	2.46E+05	2.46E+05	[kg]
mass water + mg + steel	1.77E+06	1.77E+06	1.77E+06	1.77E+06	1.77E+06	1.77E+06	1.77E+06	1.77E+06	1.77E+06	1.77E+06	[kg]
ωn_water+MG	**0.16**	**0.16**	**1.24**	**1.24**	**1.27**	**2.01**	**2.20**	**2.77**	**2.79**	**3.42**	[Hz]

APPENDIX F – GLOBAL MODE SHAPES

This Appendix provides screenshot of the global mode shapes of the complete structure in ANSYS17.1. Modes 1 to 8 are illustrated in top and side view and demonstrate the following behaviour;

n	ωn_ansys [Hz]	Mode shape
1	1.62	Global sway mode
2	1.62	Global sway mode
3	1.66	Jacket extend mode
4	2.61	Braces torsion mode
5	2.87	Breathing mode - alternating bays
6	3.60	Braces all bays sway mode
7	3.63	Braces all bays sway mode
8	4.46	Breathing mode - alternating bays 3,4

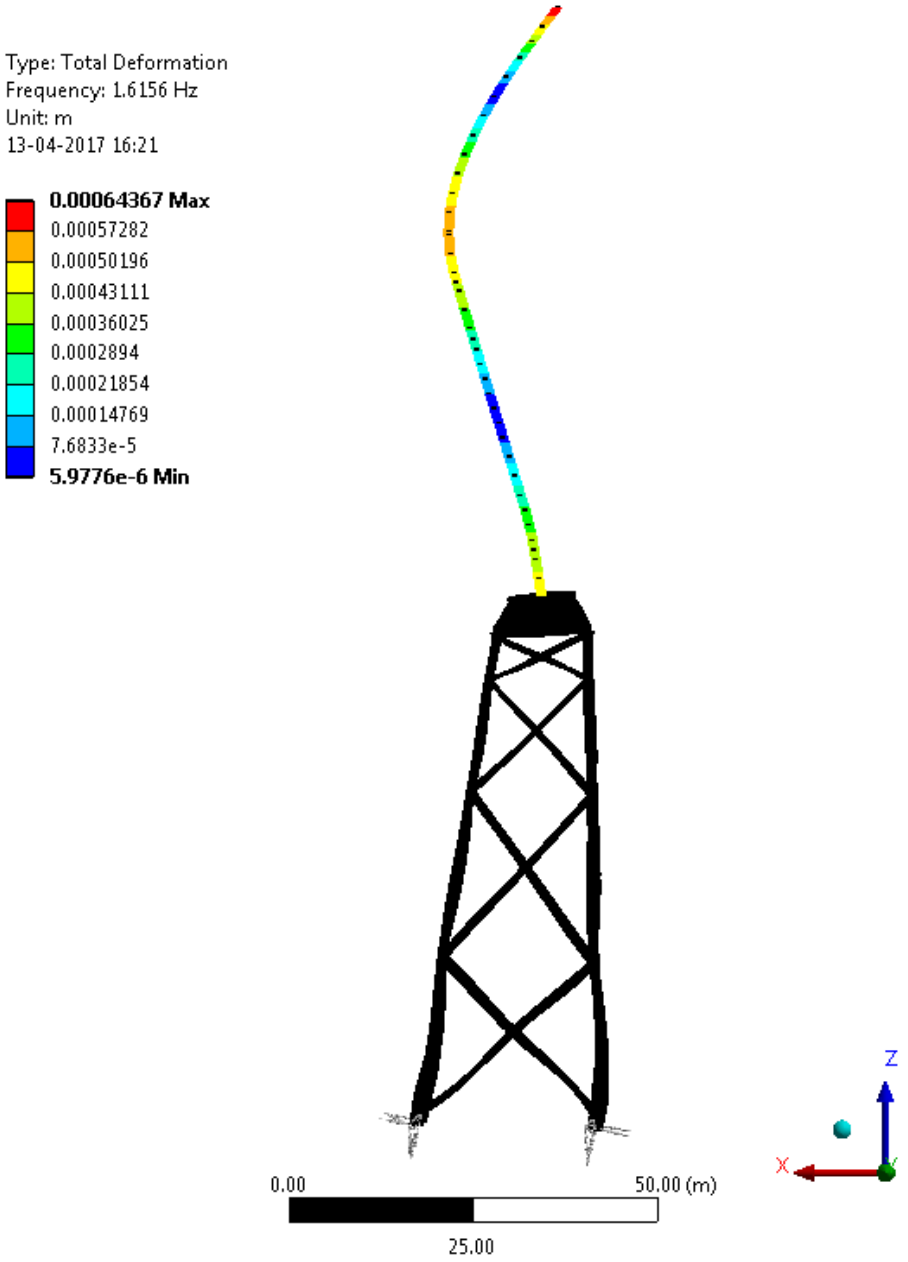
Type: Total Deformation
Frequency: 1.6156 Hz
Unit: m
13-04-2017 16:21
0.00064367 Max
0.00057282
0.00050196
0.00043111
0.00036025
0.0002894
0.00021854
0.00014769
7.6833e-5
5.9776e-6 Min
0.00
50.00 (m)
25.00
Z
X

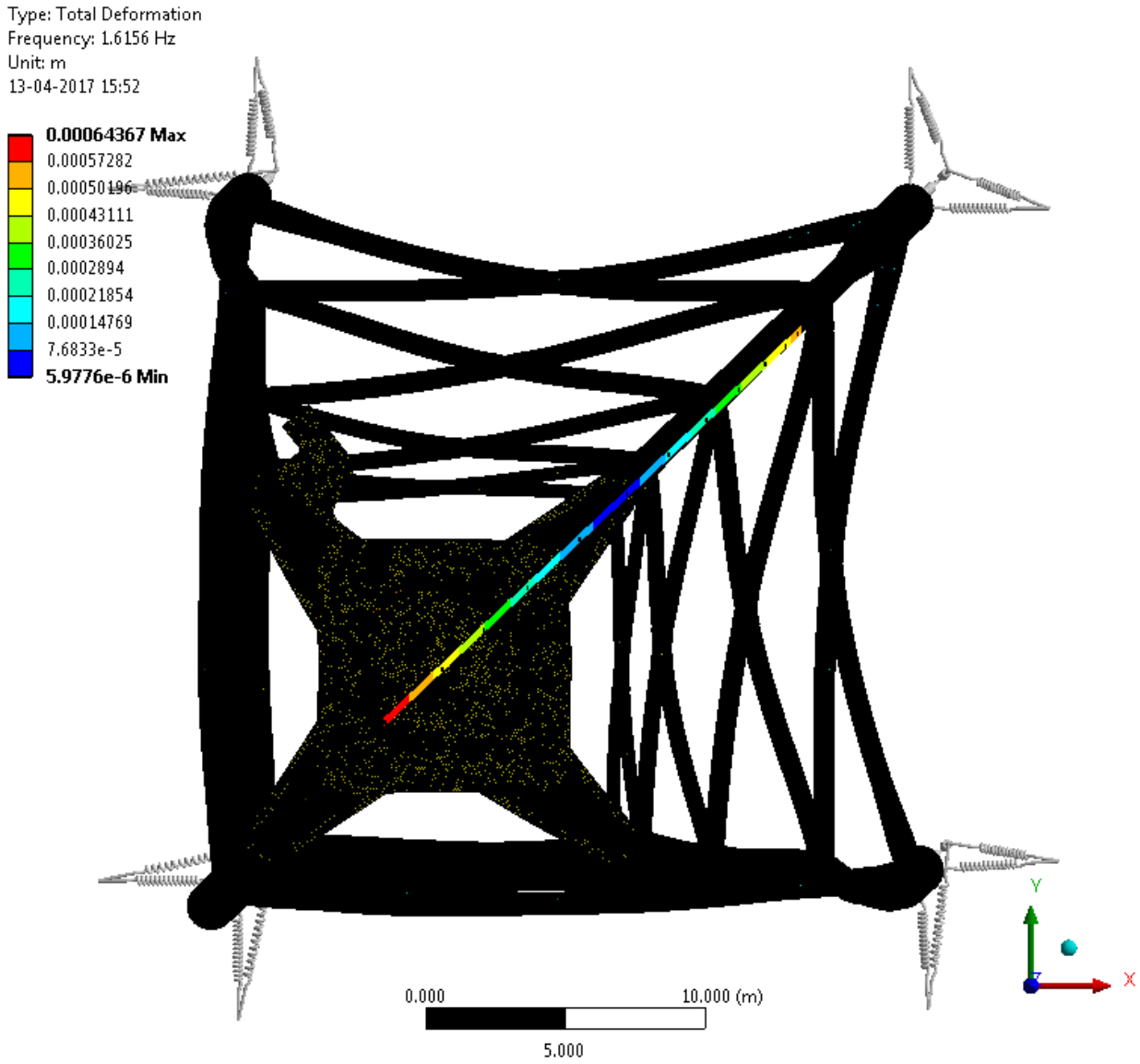
Type: Total Deformation
Frequency: 1.6156 Hz
Unit: m
13-04-2017 15:52
0.00064367 Max
0.00057282
0.00050196
0.00043111
0.00036025
0.0002894
0.00021854
0.00014769
7.6833e-5
5.9776e-6 Min
0.000
10.000 (m)
5.000
Y
X

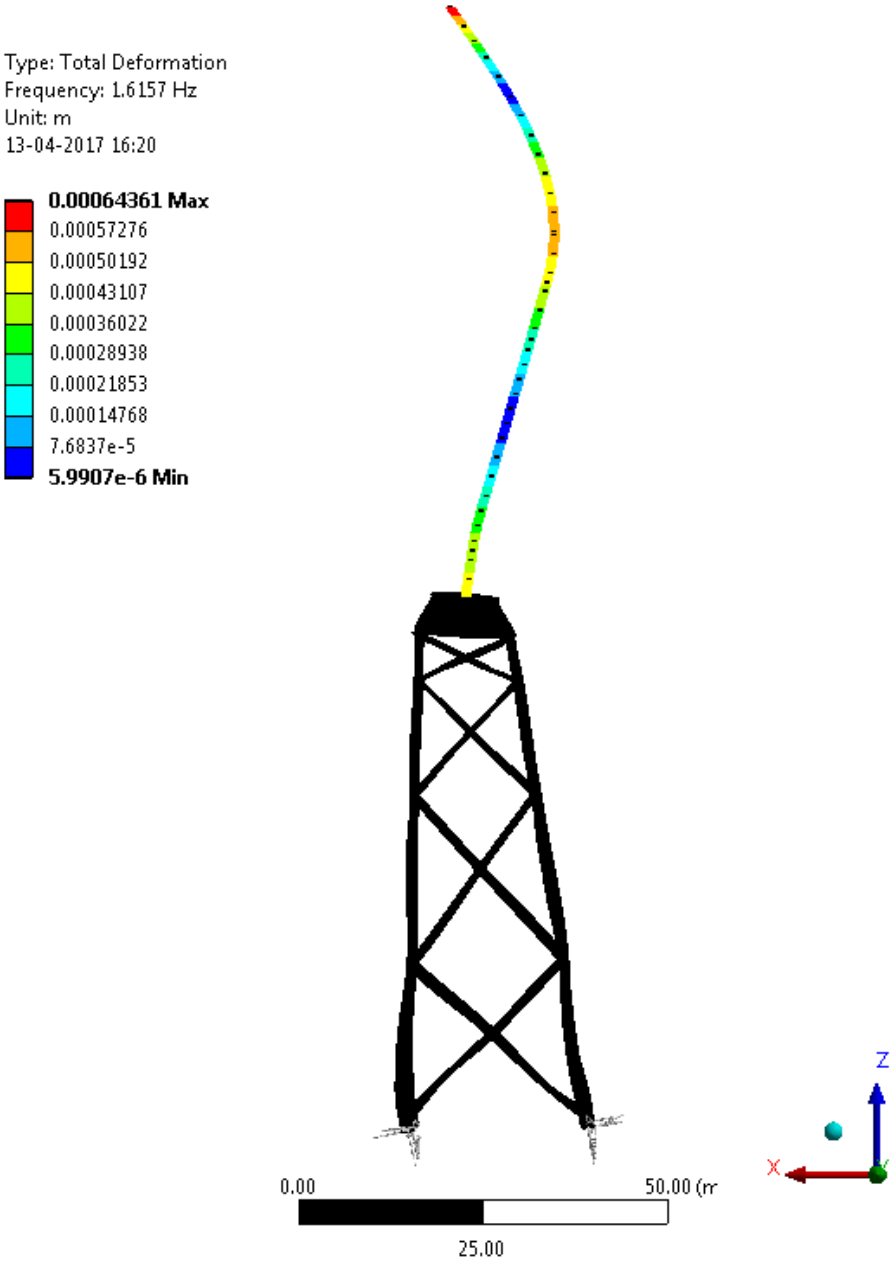
Type: Total Deformation
Frequency: 1.6157 Hz
Unit: m
13-04-2017 16:20
0.00064361 Max
0.00057276
0.00050192
0.00043107
0.00036022
0.00028938
0.00021853
0.00014768
7.6837e-5
5.9907e-6 Min
0.00
50.00 (m
25.00
Z
X

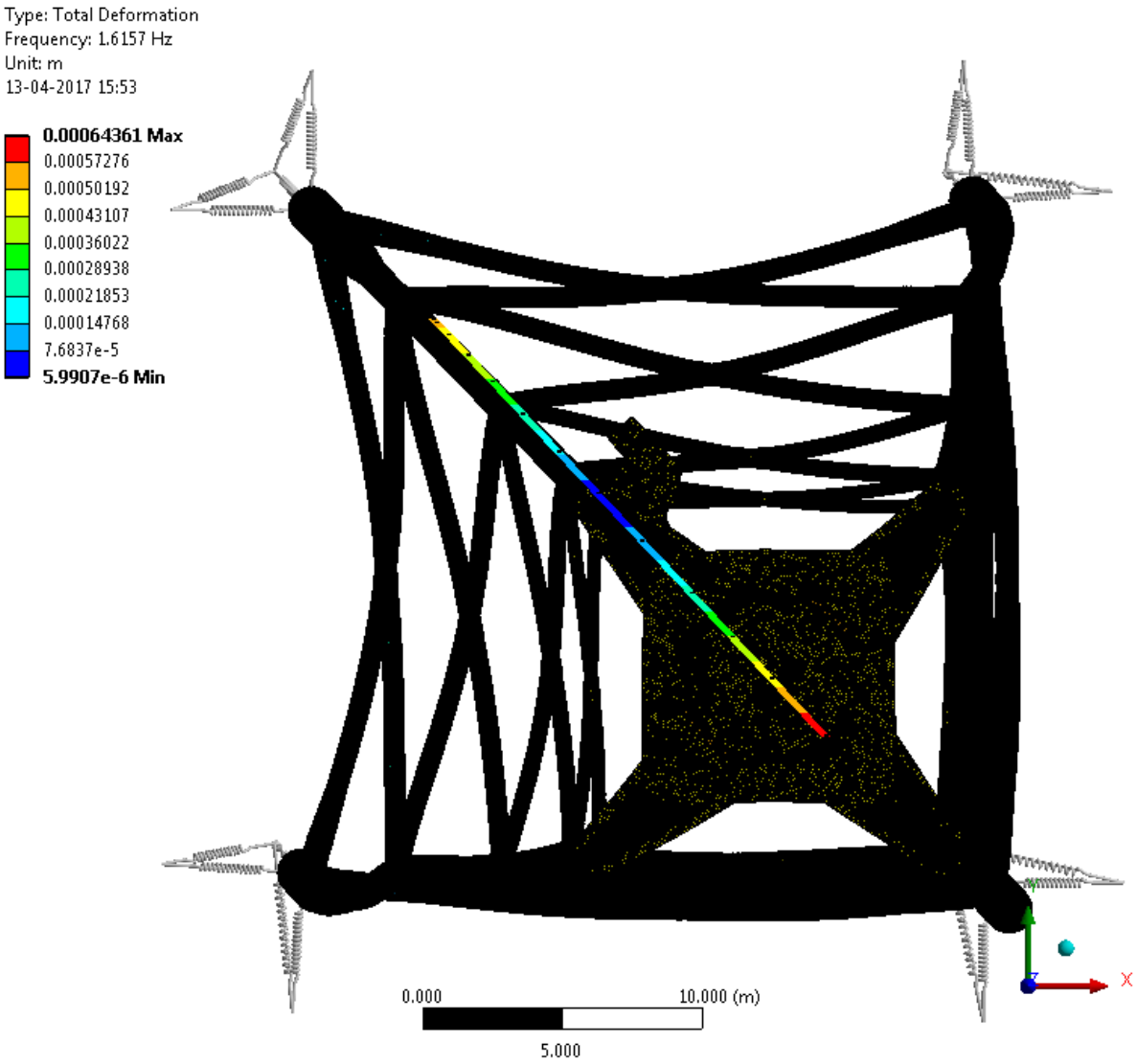
Type: Total Deformation
Frequency: 1.6157 Hz
Unit: m
13-04-2017 15:53
0.00064361 Max
0.00057276
0.00050192
0.00043107
0.00036022
0.00028938
0.00021853
0.00014768
7.6837e-5
5.9907e-6 Min
0.000
10.000 (m)
5.000
Z
X

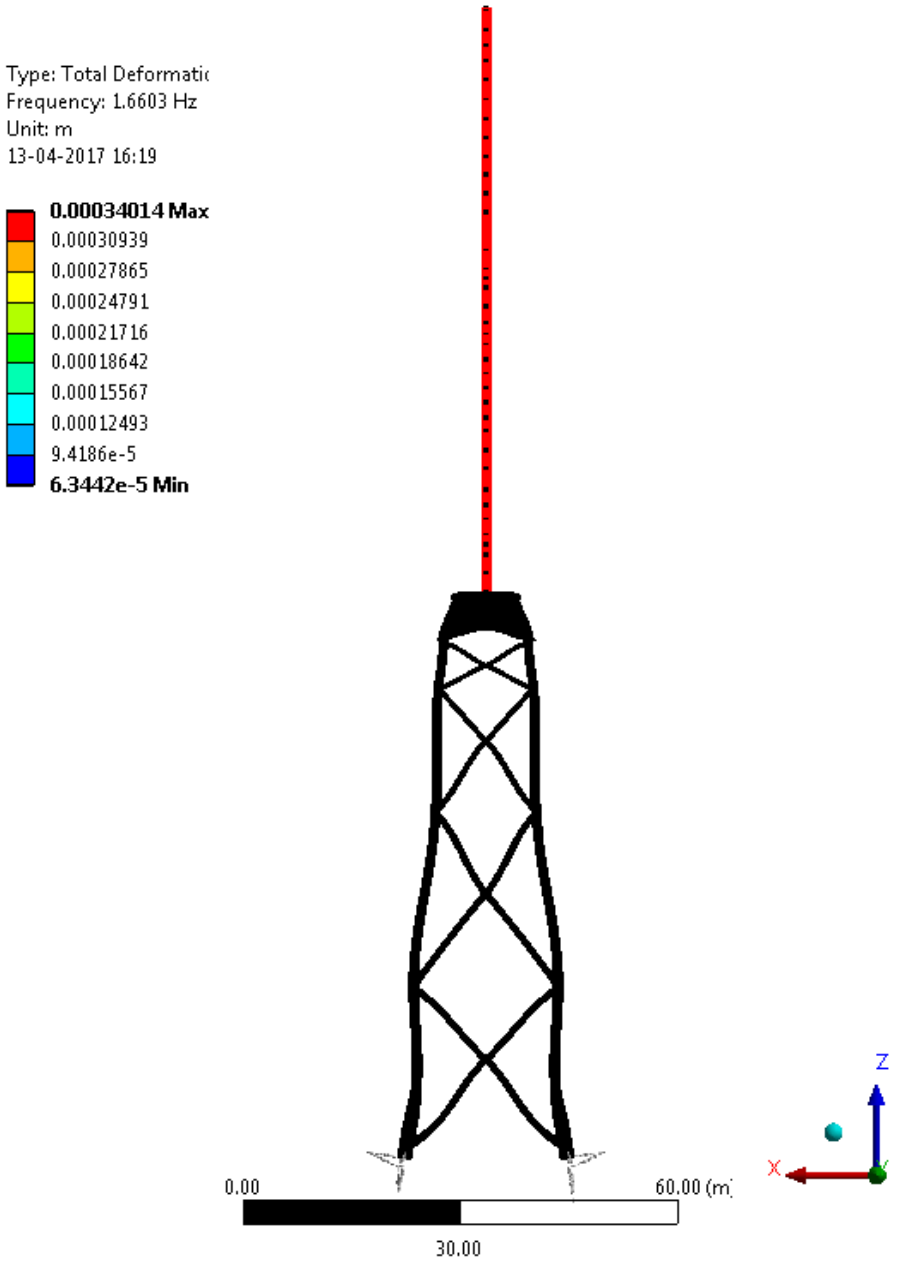
Type: Total Deformati
Frequency: 1.6603 Hz
Unit: m
13-04-2017 16:19
0.00034014 Max
0.00030939
0.00027865
0.00024791
0.00021716
0.00018642
0.00015567
0.00012493
9.4186e-5
6.3442e-5 Min
0.00
60.00 (m
30.00
Z
X

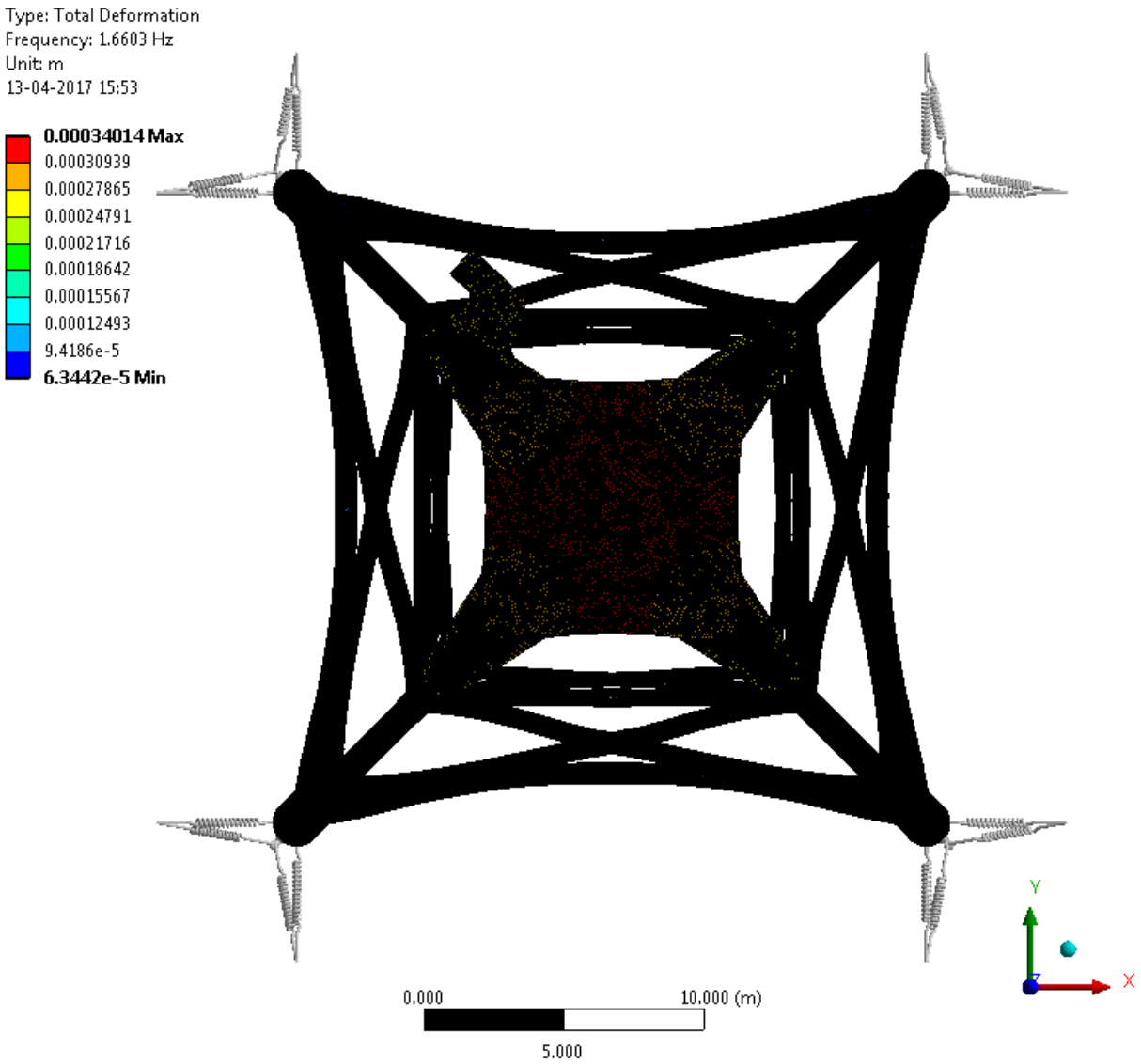
Type: Total Deformation
Frequency: 1.6603 Hz
Unit: m
13-04-2017 15:53
0.00034014 Max
0.00030939
0.00027865
0.00024791
0.00021716
0.00018642
0.00015567
0.00012493
9.4186e-5
6.3442e-5 Min
0.000
10.000 (m)
5.000
Y
X

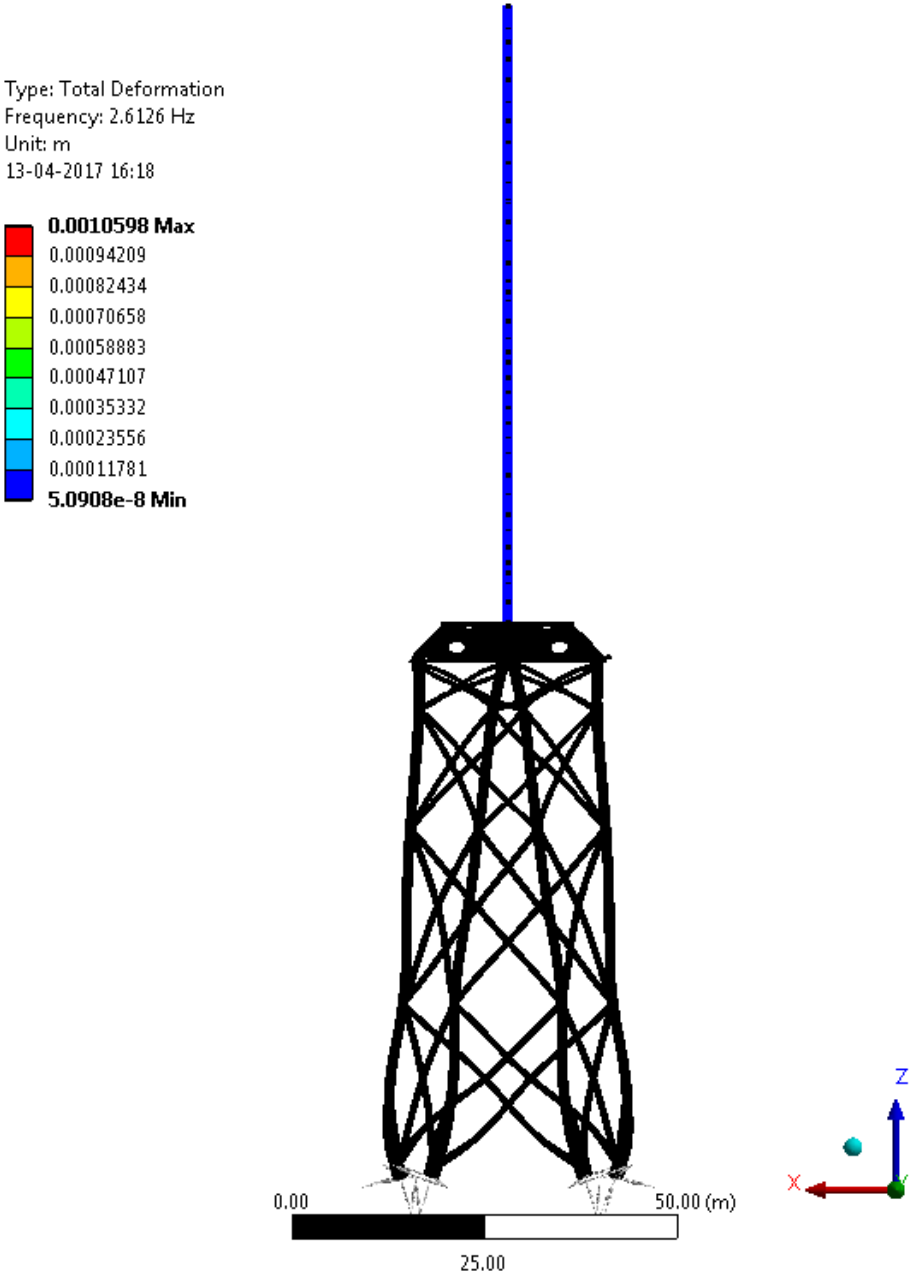
Type: Total Deformation
Frequency: 2.6126 Hz
Unit: m
13-04-2017 16:18
0.0010598 Max
0.00094209
0.00082434
0.00070658
0.00058883
0.00047107
0.00035332
0.00023556
0.00011781
5.0908e-8 Min
0.00
50.00 (m)
25.00
Z
X
Y

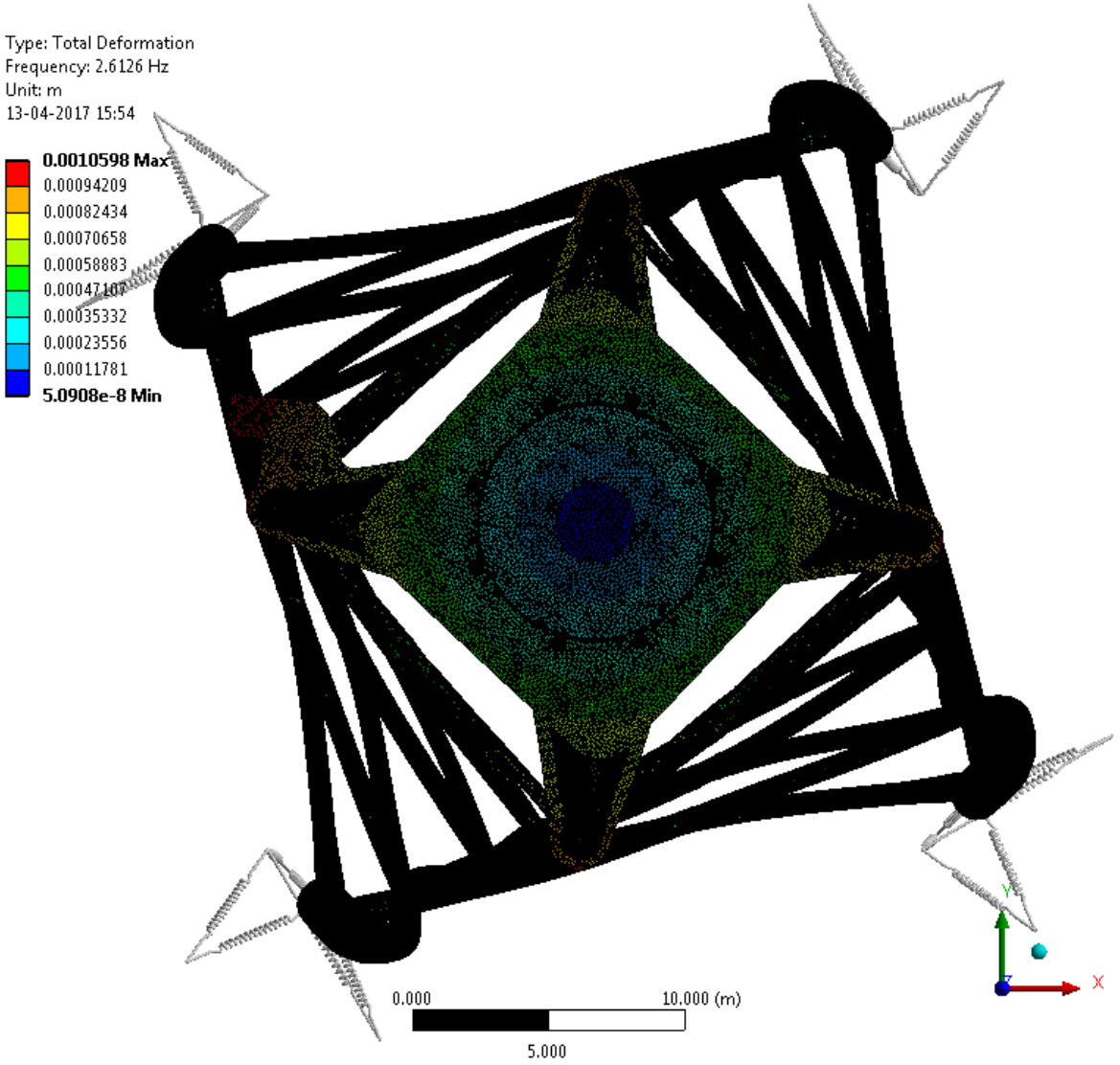
Type: Total Deformation
Frequency: 2.6126 Hz
Unit: m
13-04-2017 15:54
0.0010598 Max
0.00094209
0.00082434
0.00070658
0.00058883
0.00047107
0.00035332
0.00023556
0.00011781
5.0908e-8 Min
0.000
10.000 (m)
5.000
Y
X
Z

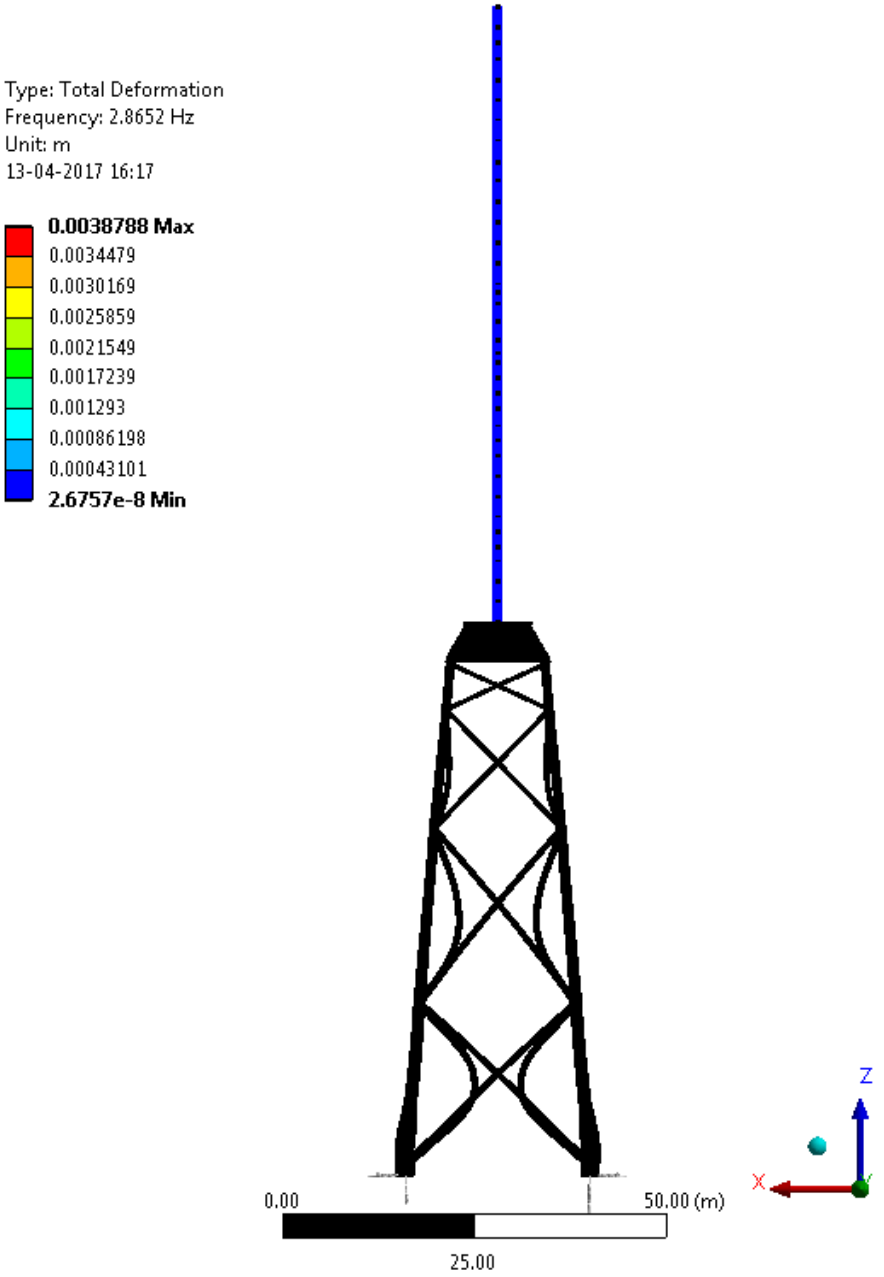
Type: Total Deformation
Frequency: 2.8652 Hz
Unit: m
13-04-2017 16:17
0.0038788 Max
0.0034479
0.0030169
0.0025859
0.0021549
0.0017239
0.001293
0.00086198
0.00043101
2.6757e-8 Min
0.00
50.00 (m)
25.00
Z
X

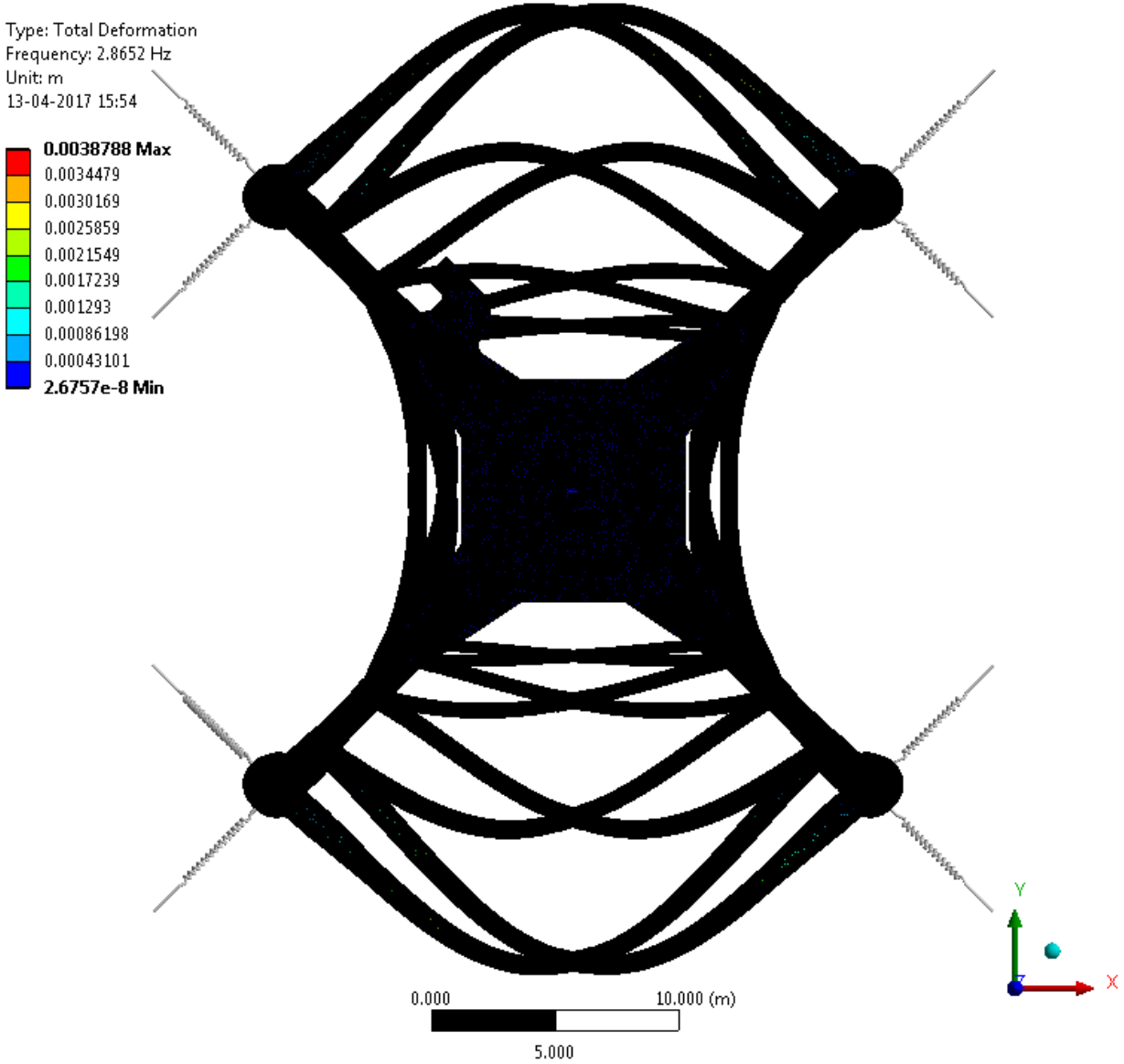
Type: Total Deformation
Frequency: 2.8652 Hz
Unit: m
13-04-2017 15:54
0.0038788 Max
0.0034479
0.0030169
0.0025859
0.0021549
0.0017239
0.001293
0.00086198
0.00043101
2.6757e-8 Min
0.000
10.000 (m)
5.000
Y
X

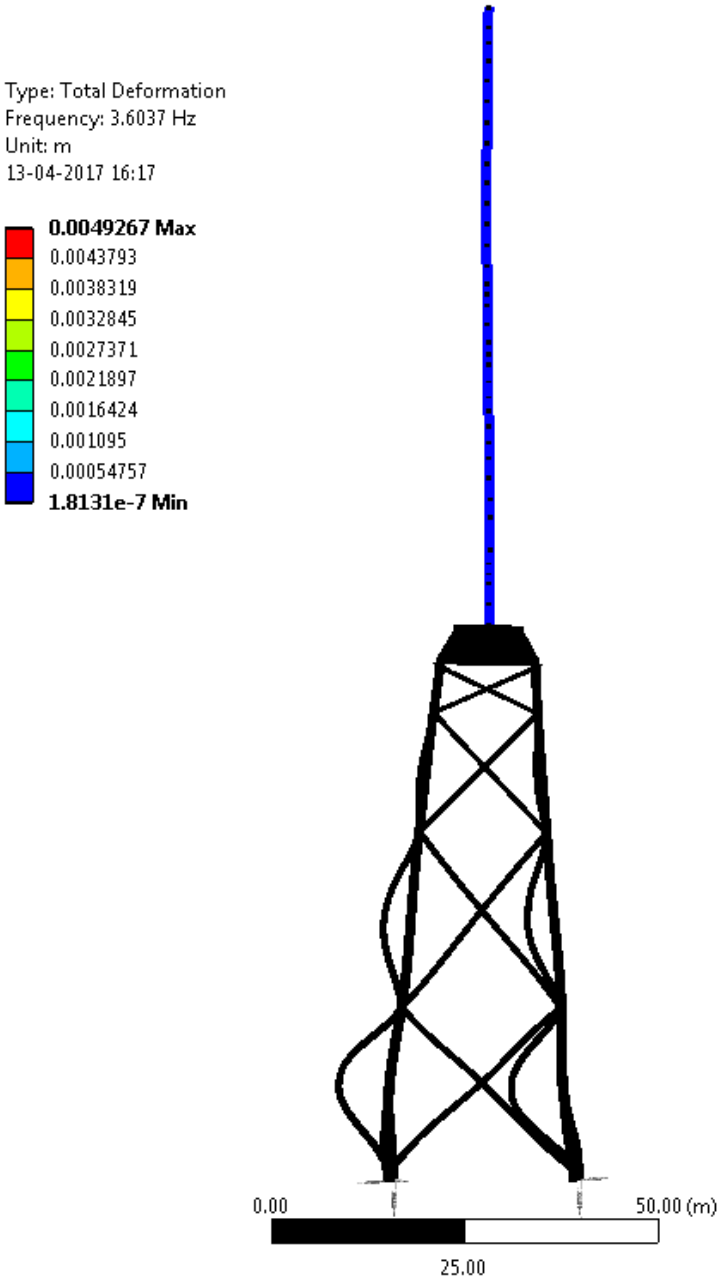
Type: Total Deformation
Frequency: 3.6037 Hz
Unit: m
13-04-2017 16:17
0.0049267 Max
0.0043793
0.0038319
0.0032845
0.0027371
0.0021897
0.0016424
0.001095
0.00054757
1.8131e-7 Min
0.00
50.00 (m)
25.00
Z
X
Y

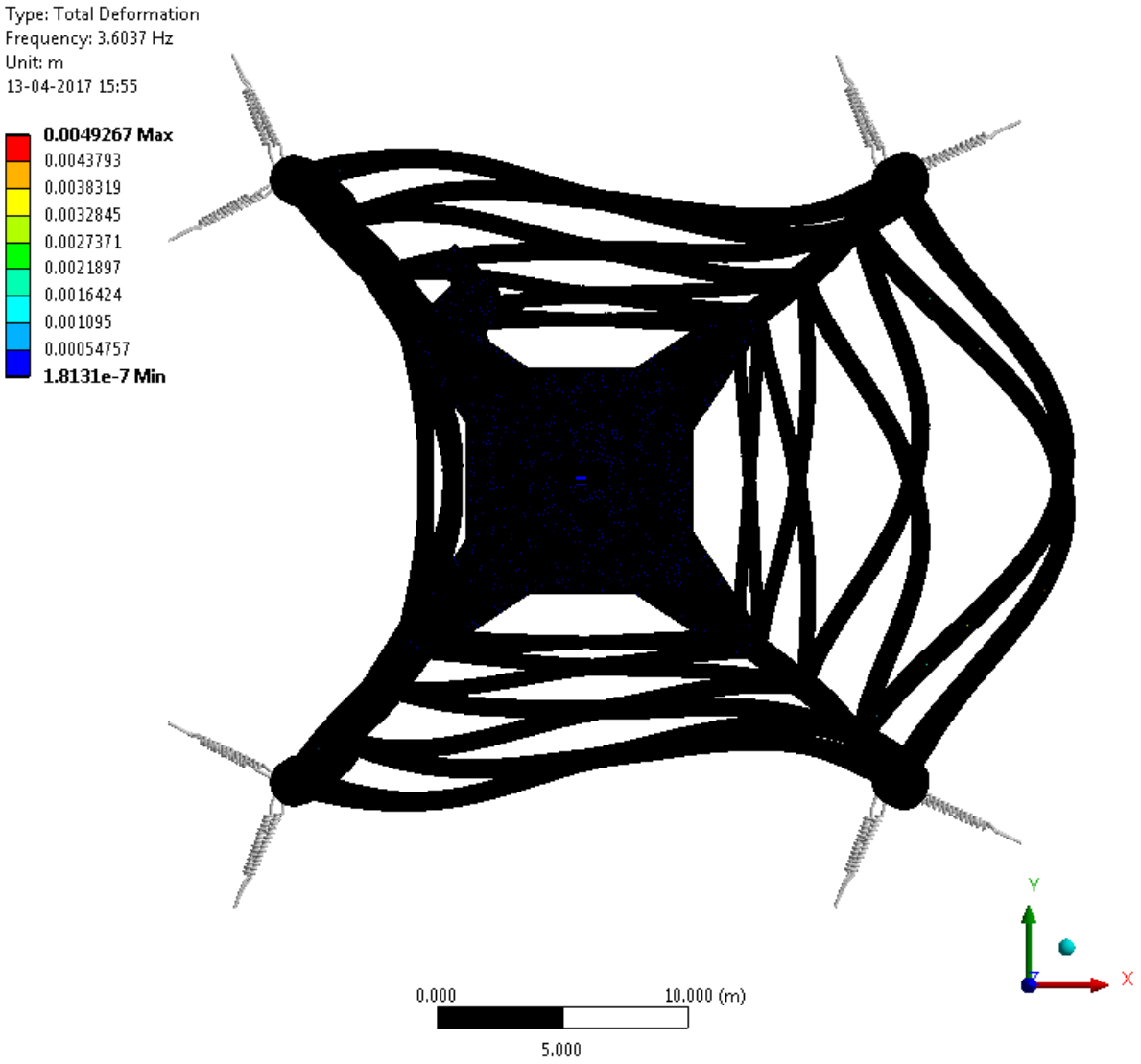
Type: Total Deformation
Frequency: 3.6037 Hz
Unit: m
13-04-2017 15:55
0.0049267 Max
0.0043793
0.0038319
0.0032845
0.0027371
0.0021897
0.0016424
0.001095
0.00054757
1.8131e-7 Min
0.000
10.000 (m)
5.000
Y
X

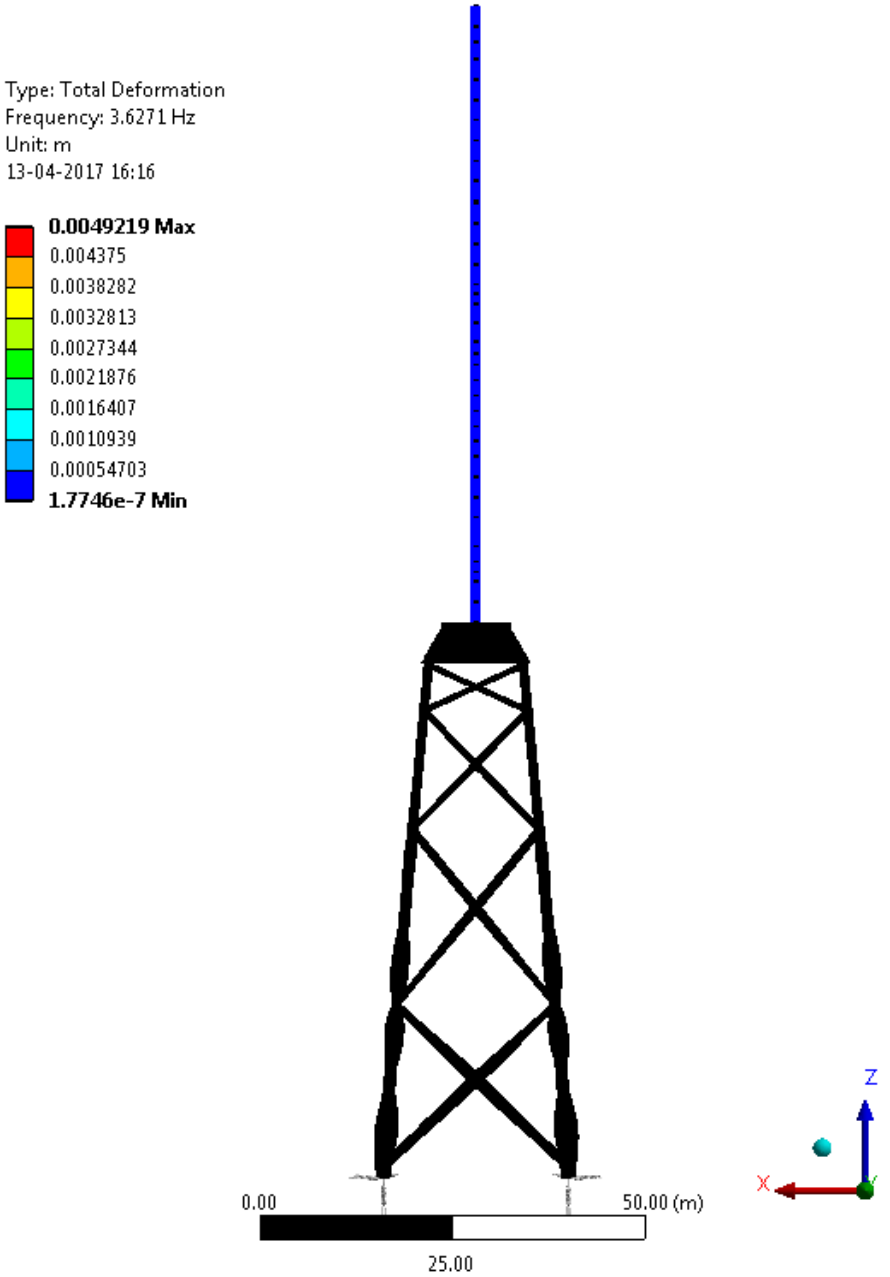
Type: Total Deformation
Frequency: 3.6271 Hz
Unit: m
13-04-2017 16:16
0.0049219 Max
0.004375
0.0038282
0.0032813
0.0027344
0.0021876
0.0016407
0.0010939
0.00054703
1.7746e-7 Min
0.00
50.00 (m)
25.00
Z
X

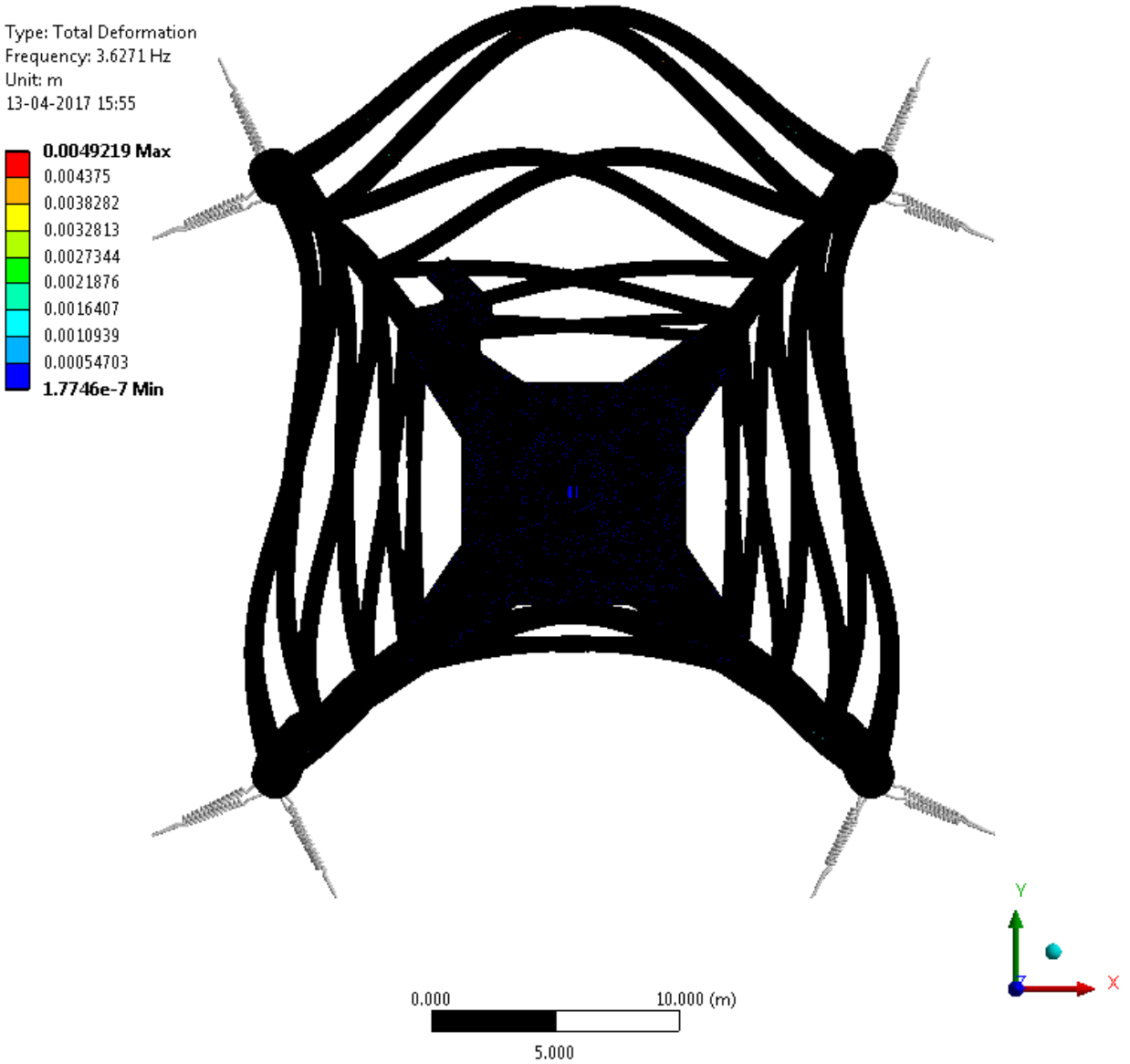
Type: Total Deformation
Frequency: 3.6271 Hz
Unit: m
13-04-2017 15:55
0.0049219 Max
0.004375
0.0038282
0.0032813
0.0027344
0.0021876
0.0016407
0.0010939
0.00054703
1.7746e-7 Min
0.000
10.000 (m)
5.000
Y
X

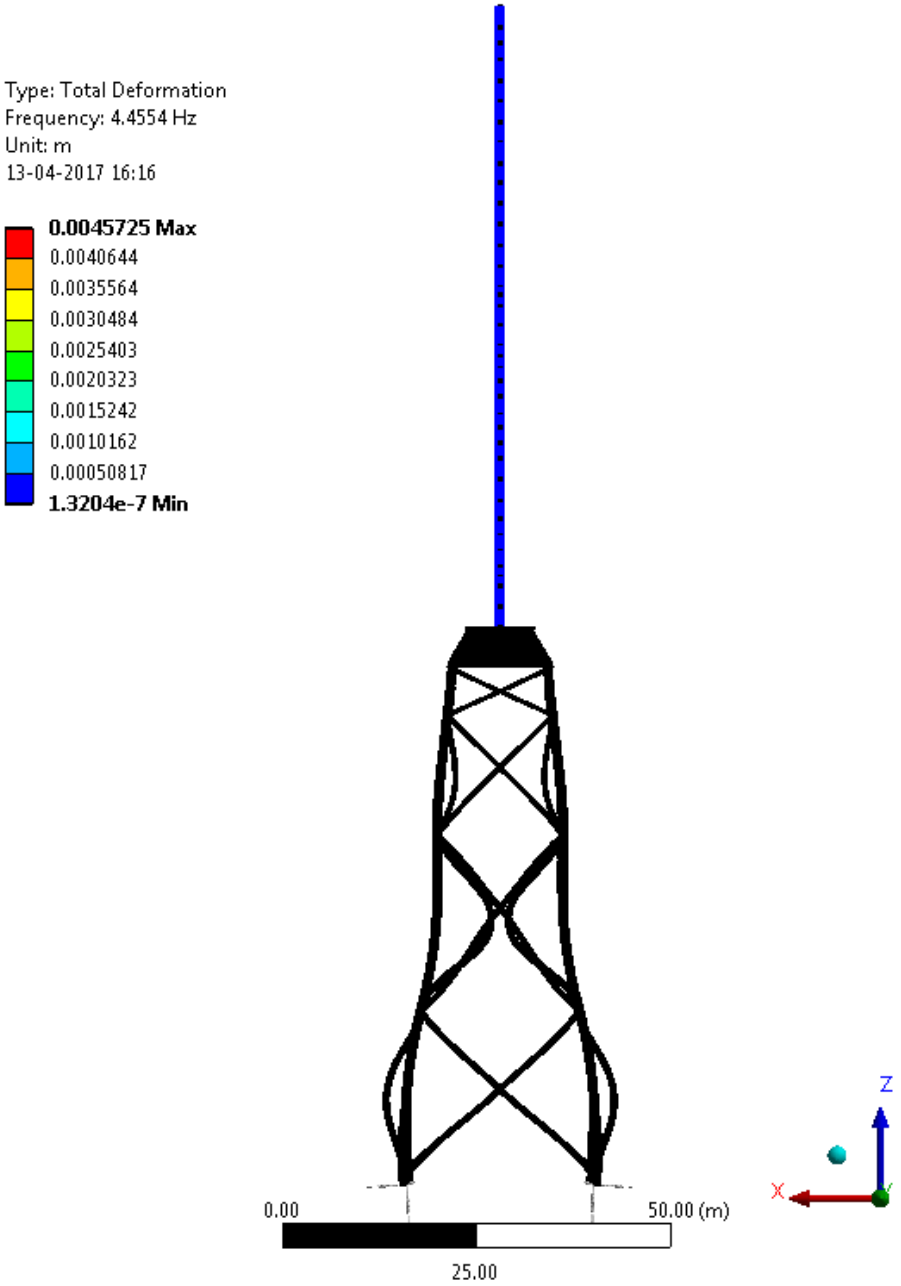
Type: Total Deformation
Frequency: 4.4554 Hz
Unit: m
13-04-2017 16:16
0.0045725 Max
0.0040644
0.0035564
0.0030484
0.0025403
0.0020323
0.0015242
0.0010162
0.00050817
1.3204e-7 Min
0.00
50.00 (m)
25.00
Z
X

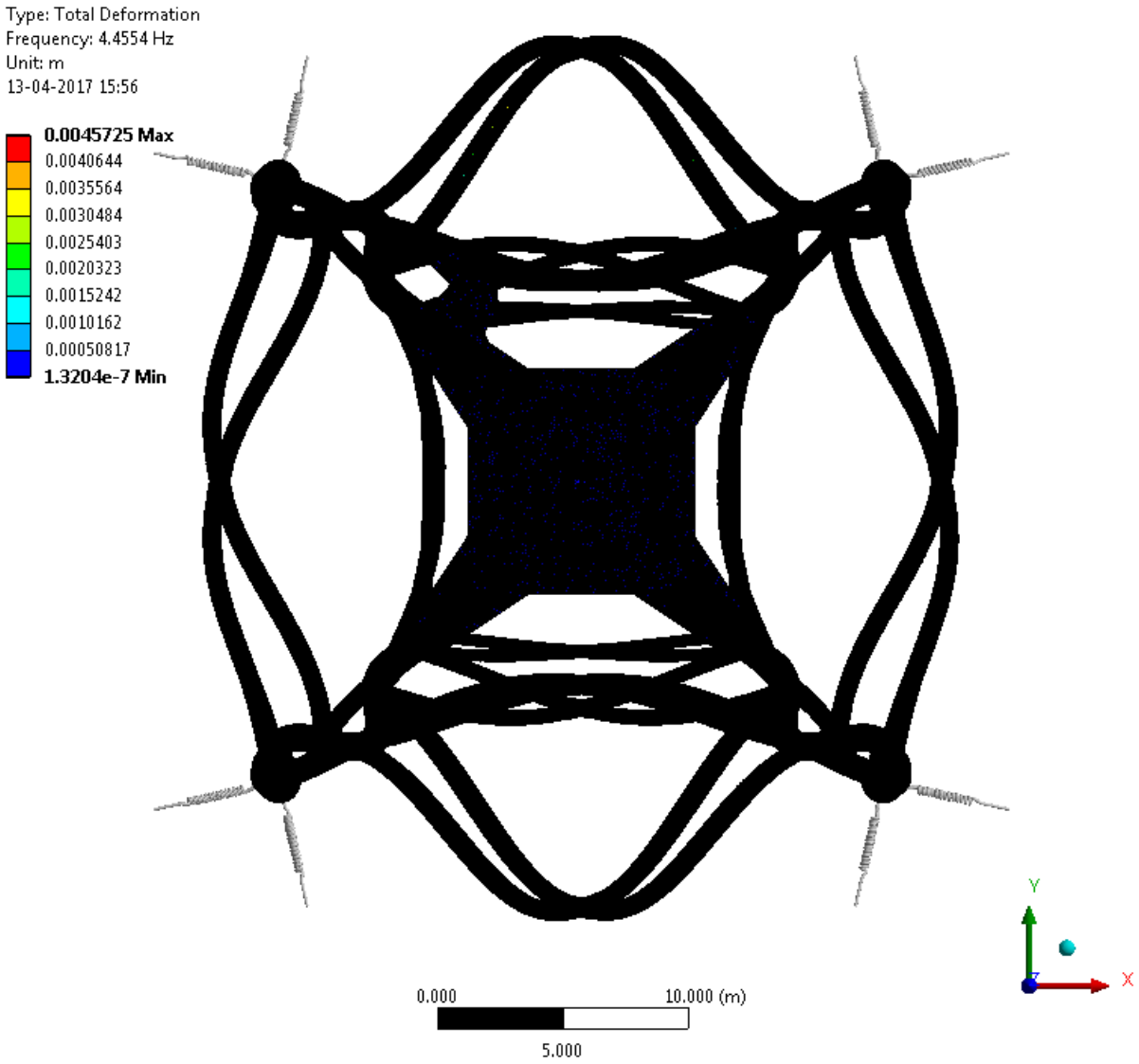
Type: Total Deformation
Frequency: 4.4554 Hz
Unit: m
13-04-2017 15:56
0.0045725 Max
0.0040644
0.0035564
0.0030484
0.0025403
0.0020323
0.0015242
0.0010162
0.00050817
1.3204e-7 Min
0.000
10.000 (m)
5.000
Y
X

APPENDIX G – S-N CURVE FOR TUBULAR JOINTS

Figure G-0-1 demonstrates the S-N curve for tubular joints used for the OWT jacket.

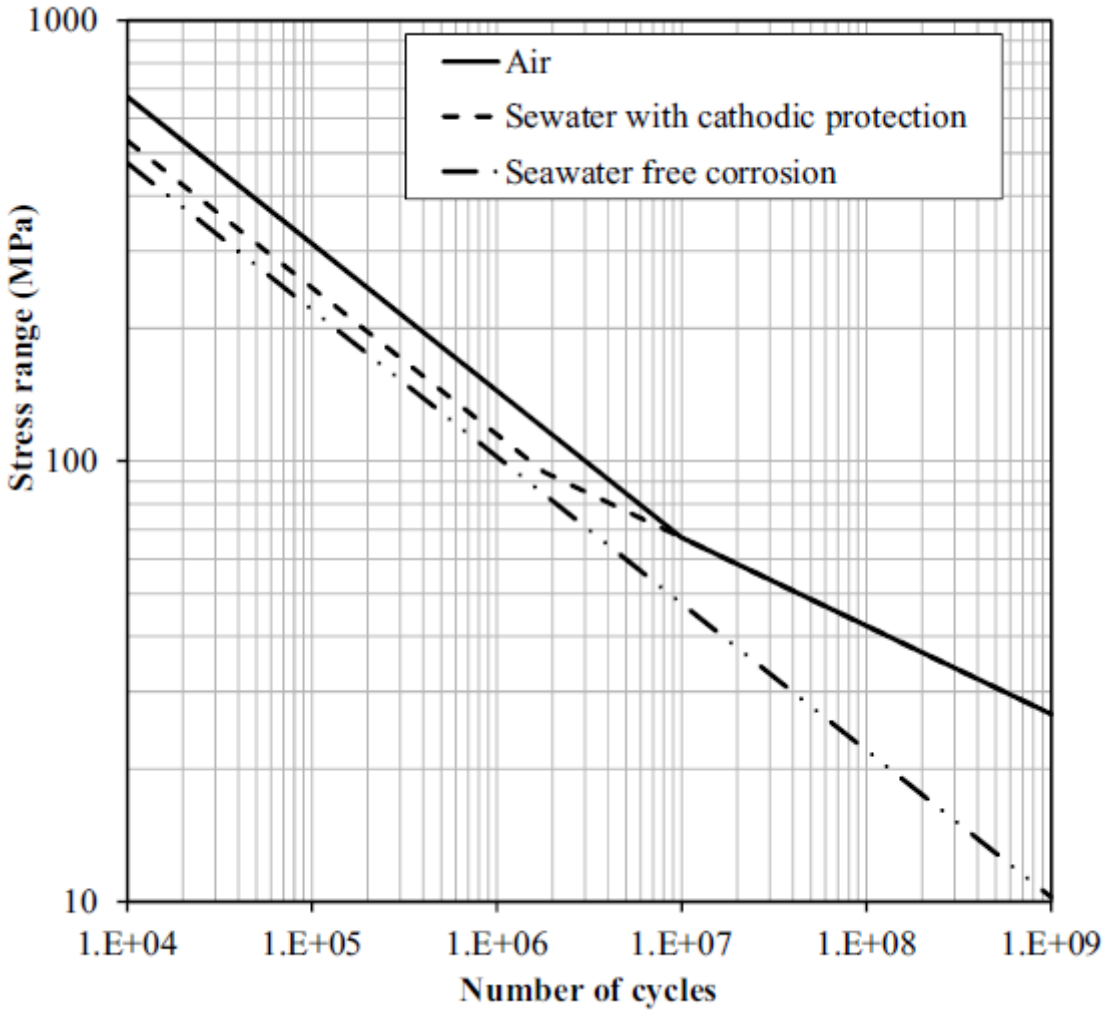

FIGURE G-0-1 S-N CURVE FOR TUBULAR JOINTS [25]

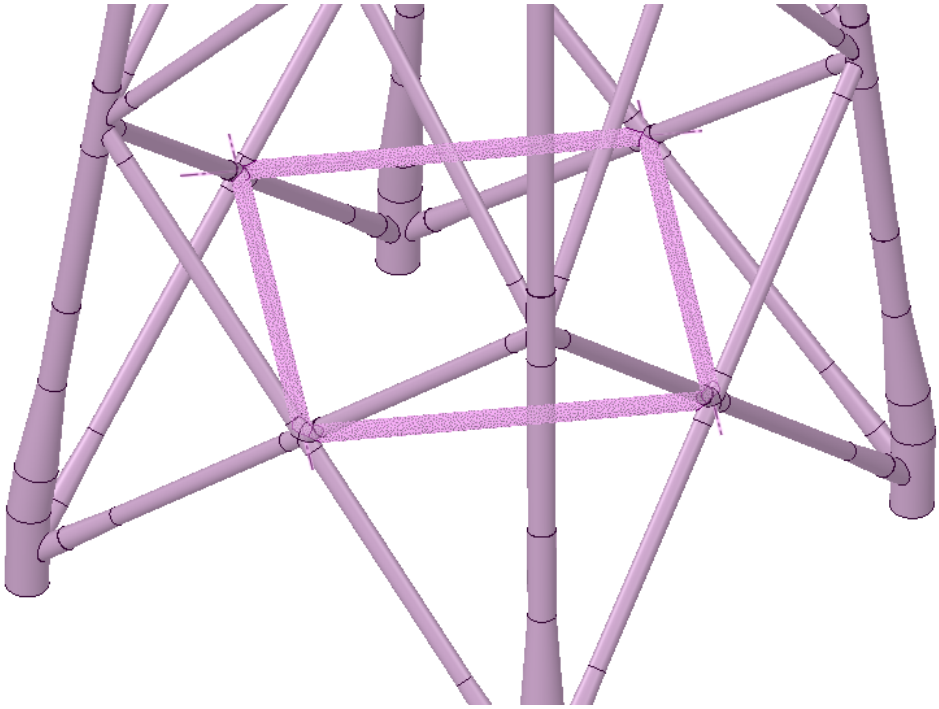

no	length [mm]	Do [mm]	volume [mm^3]	MG WT [mm]	Do + MG [mm]	area + MG [mm^2]	volume + MG [mm^3]	volume MG only [mm^3]	volume steel [mm^3]
1	14207	730	5946179045	100	930	41508324	9650685412	3.705E+09	321354769
TOTAL 4x						166033297	38602741647	1.482E+10	1285419077

	1	2	3	4	5	6	7	8	9	10	
volume steel	1.34E+11	1.34E+11	1.34E+11	1.34E+11	1.34E+11	1.34E+11	1.34E+11	1.34E+11	1.34E+11	1.34E+11	[mm3]
ρ steel	7.85E-06	7.85E-06	7.85E-06	7.85E-06	7.85E-06	7.85E-06	7.85E-06	7.85E-06	7.85E-06	7.85E-06	[kg/mm3]
mass steel	1.054E+06	1.054E+06	1.054E+06	1.054E+06	1.054E+06	1.054E+06	1.054E+06	1.054E+06	1.054E+06	1.054E+06	[kg]
β	1.57	1.57	5.41	5.41	11.93	11.94	12.26	19.20	23.07	30.77	[-]
ωn_air	**0.21**	**0.21**	**0.73**	**0.73**	**1.61**	**1.61**	**1.66**	**2.60**	**3.12**	**4.16**	[Hz]
k	1.9E+04	1.9E+04	1.9E+04	1.9E+04	1.9E+04	1.9E+04	1.9E+04	1.9E+04	1.9E+04	1.9E+04	[-]
volume water	5.6E+11	5.6E+11	5.6E+11	5.6E+11	5.6E+11	5.6E+11	5.6E+11	5.6E+11	5.6E+11	5.6E+11	[mm3]
ρ water	1.03E-06	1.03E-06	1.03E-06	1.03E-06	1.03E-06	1.03E-06	1.03E-06	1.03E-06	1.03E-06	1.03E-06	[kg/mm3]
Ca	0.9	0.9	0.9	0.9	0.9	0.9	0.9	0.9	0.9	0.9	[-]
mass water	5.14E+05	5.14E+05	5.14E+05	5.14E+05	5.14E+05	5.14E+05	5.14E+05	5.14E+05	5.14E+05	5.14E+05	[kg]
volume mg	1.89E+11	1.89E+11	1.89E+11	1.89E+11	1.89E+11	1.89E+11	1.89E+11	1.89E+11	1.89E+11	1.89E+11	[mm3]
ρ mg	1.40E-06	1.40E-06	1.40E-06	1.40E-06	1.40E-06	1.40E-06	1.40E-06	1.40E-06	1.40E-06	1.40E-06	[kg/mm3]
mass mg	2.65E+05	2.65E+05	2.65E+05	2.65E+05	2.65E+05	2.65E+05	2.65E+05	2.65E+05	2.65E+05	2.65E+05	[kg]
mass water + mg + steel	1.83E+06	1.83E+06	1.83E+06	1.83E+06	1.83E+06	1.83E+06	1.83E+06	1.83E+06	1.83E+06	1.83E+06	[kg]
ωn_water+MG	**0.16**	**0.16**	**0.55**	**0.55**	**1.22**	**1.22**	**1.26**	**1.97**	**2.37**	**3.16**	[hz]

	11	12	13	14	15	16	17	
volume steel	1.34E+11	1.34E+11	1.34E+11	1.34E+11	1.34E+11	1.34E+11	1.34E+11	[mm3]
ρ steel	7.85E-06	7.85E-06	7.85E-06	7.85E-06	7.85E-06	7.85E-06	7.85E-06	[kg/mm3]
mass steel	1.054E+06	1.054E+06	1.054E+06	1.054E+06	1.054E+06	1.054E+06	1.054E+06	[kg]
β	1.57	32.77	36.13	36.57	36.57	37.54	47.03	[-]
ωn_air	**4.16**	**4.43**	**4.89**	**4.94**	**4.95**	**5.08**	**6.36**	[Hz]
k	7.4E+06	1.9E+04	1.9E+04	1.9E+04	1.9E+04	1.9E+04	1.9E+04	[-]
volume water	5.6E+11	5.6E+11	5.6E+11	5.6E+11	5.6E+11	5.6E+11	5.6E+11	[mm3]
ρ water	1.03E-06	1.03E-06	1.03E-06	1.03E-06	1.03E-06	1.03E-06	1.03E-06	[kg/mm3]
Ca	0.9	0.9	0.9	0.9	0.9	0.9	0.9	[-]
mass water	5.14E+05	5.14E+05	5.14E+05	5.14E+05	5.14E+05	5.14E+05	5.14E+05	[kg]
volume mg	1.89E+11	1.89E+11	1.89E+11	1.89E+11	1.89E+11	1.89E+11	1.89E+11	[mm3]
ρ mg	1.40E-06	1.40E-06	1.40E-06	1.40E-06	1.40E-06	1.40E-06	1.40E-06	[kg/mm3]
mass mg	2.65E+05	2.65E+05	2.65E+05	2.65E+05	2.65E+05	2.65E+05	2.65E+05	[kg]
mass water + mg + steel	1.83E+06	1.83E+06	1.83E+06	1.83E+06	1.83E+06	1.83E+06	1.83E+06	[kg]
ωn_water+MG	**3.16**	**3.36**	**3.70**	**3.75**	**3.75**	**3.85**	**4.82**	[Hz]

APPENDIX I – WATER BUCKET DAMPING MECHANISM

Matlab script used to calculate the DAF of the mass absorber system [43];

```
close all;clear all;clc;
%*********************************************************%
%Defining the frequency vector and the mass matrix,
%damping matrix, the stiffness matrix and the amplitude of
%the excitation force.
%*********************************************************%
f=linspace(1,3,1000);    % [Hz] frequency

b_tk = 0.168;            % [m] dimension of water tank
h_tk = 3;                % [m] height of water tank
rho = 1025;              % [kg/m^3] water density
f_fill = 0.7;            % [-]
m_tk = f_fill*b_tk^2*h_tk*rho;  % [kg] mass of water tank
w_tk = sqrt(pi*9.81/b_tk*tanh(pi*h_tk/b_tk));   % [rad/s] natural frequency of
water tank
k_tk = w_tk^2*m_tk;      % [N/m] equivalent stiffness of water tank

k1 = 15490031.45;        % [N/m] equivalent linear stiffness of the braces
k2o = [0 k_tk];          % [N/m] stiffness with and without water tank
m=[8.42e4 0;0 m_tk];     % [kg] mass matrix
cc1 = 0.01*2*sqrt(k1*m(1,1));   % [kg/s] damping of the braces (structural +
hydrodynamic)
cc2o = [0, 0.02*2*sqrt(k2o(2)*m(2,2))]; % [kg/s] damping with and without the
water tank
fi=[1;0];                % [N] unit force on the braces
x0 = fi(1)/k1;           % [m] static displacement of the braces

for ii = 1:2

    k2 = k2o(ii);
    cc2 = cc2o(ii);
    k = [k1+k2 -k2;-k2 k2];
    c = [cc1+cc2 -cc2;-cc2 cc2];
%*********************************************************%
%Calculating the amplitude and the phase for each frequency
%defined by the frequency vector.
%*********************************************************%
for i = 1:1000
    omega(i)=2*pi*f(i); %omega in terms of frequency
    omega2(i)=omega(i)*omega(i); % squaring omega
    a11=-omega2(i)*m+k;
    a12=omega(i)*c;
    a21=-omega(i)*c;
    a22=-omega2(i)*m+k;
    a=[a11 a12;a21 a22];
    b=inv(a);
    c1=[0;0;fi];
    d(1,i)=b(1,:)*c1;
    d(2,i)=b(2,:)*c1;
    d(3,i)=b(3,:)*c1;
    d(4,i)=b(4,:)*c1;
    x(1,i)=sqrt(abs(d(1,i))^2+abs(d(3,i))^2);
```

```
    x(2,i)=sqrt(abs(d(2,i))^2+abs(d(4,i))^2);
    p(1,i)=atan(d(1,i)/d(3,i))*180/pi;
    if p(1,i)<0 % to check whether the angle is negative or not.
        p(1,i)=180+p(1,i);
    else
        p(1,i)=p(1,i);
    end
    p(2,i)=atan(d(2,i)/d(4,i))*180/pi;
    if p(2,i)<0
        if d(4,i)<0
            p(2,i) = -180 + p(2,i);
        else
            p(2,i)=180+p(2,i);
        end
    else
        p(2,i)=p(2,i);
    end
end

tmp(ii,:) = x(1,:)/x0;

end

figure(1)
plot(f,tmp(1,:),'r');hold on
plot(f,tmp(2,:),'b');grid
xlabel('Frequency [Hz]')
ylabel('DAF for Amplitude of Mass 1 [-]')
figure(2)
plot(f,x(2,:));grid
xlabel('Frequency')
ylabel('Amplitude of Mass 2')
```

APPENDIX J – WIND TURBINE FORCING FREQUENCIES

Figure J-0-1 shows the excitated frequencies of the turbine structure. It was found that the tower bending excitations are almost identical comparted to that of a stall-regulated 600kW wind turbine illustrated in Figure J-0-2

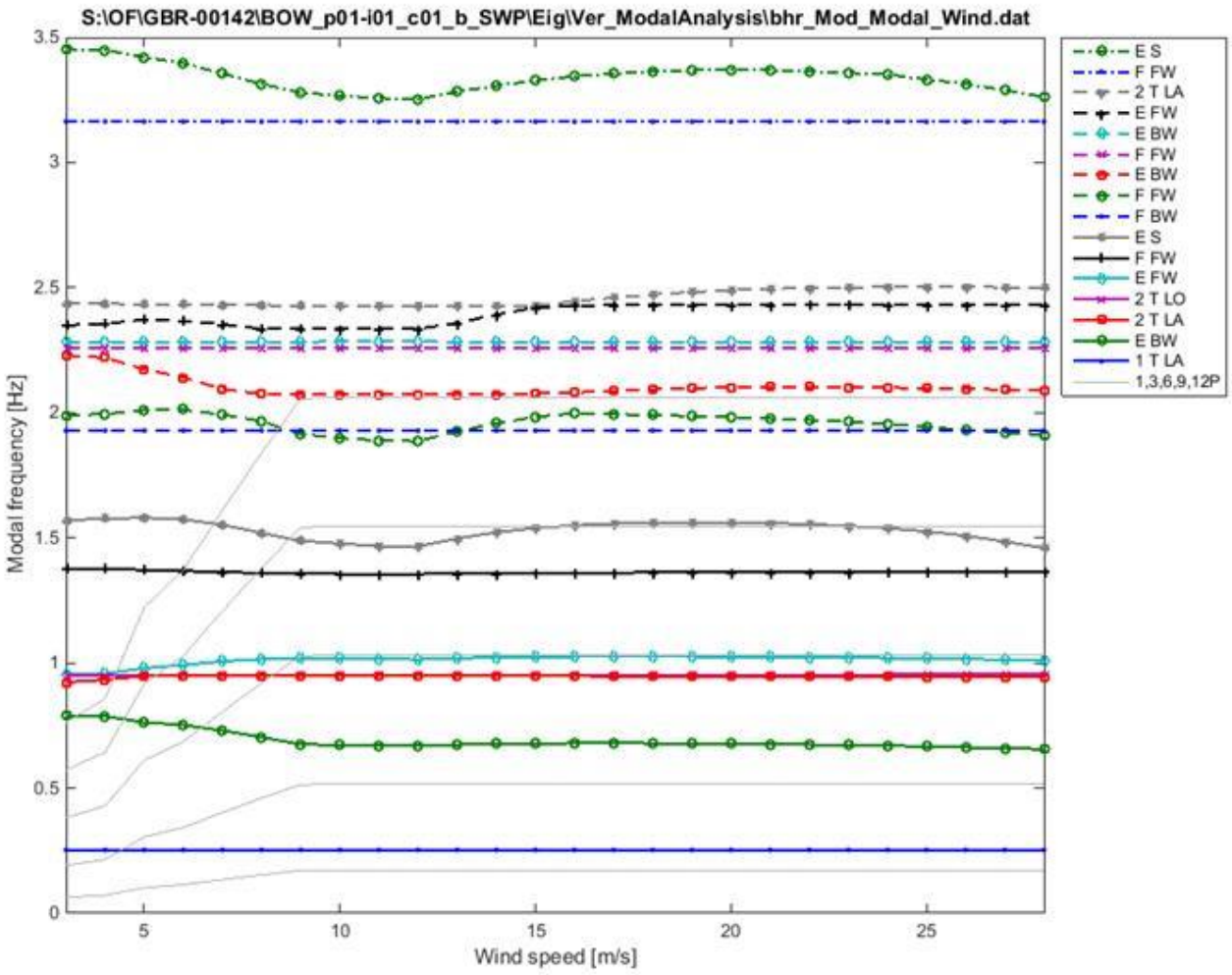

FIGURE J-0-1 WIND TURBINE STRUCTURE FORCING FREQUENCIES

Where

E	Edgewise
F	Flapwise
FW	Forward whirl
BW	Backward whirl
T	Tower
LO	Longitudinal
LA	Lateral

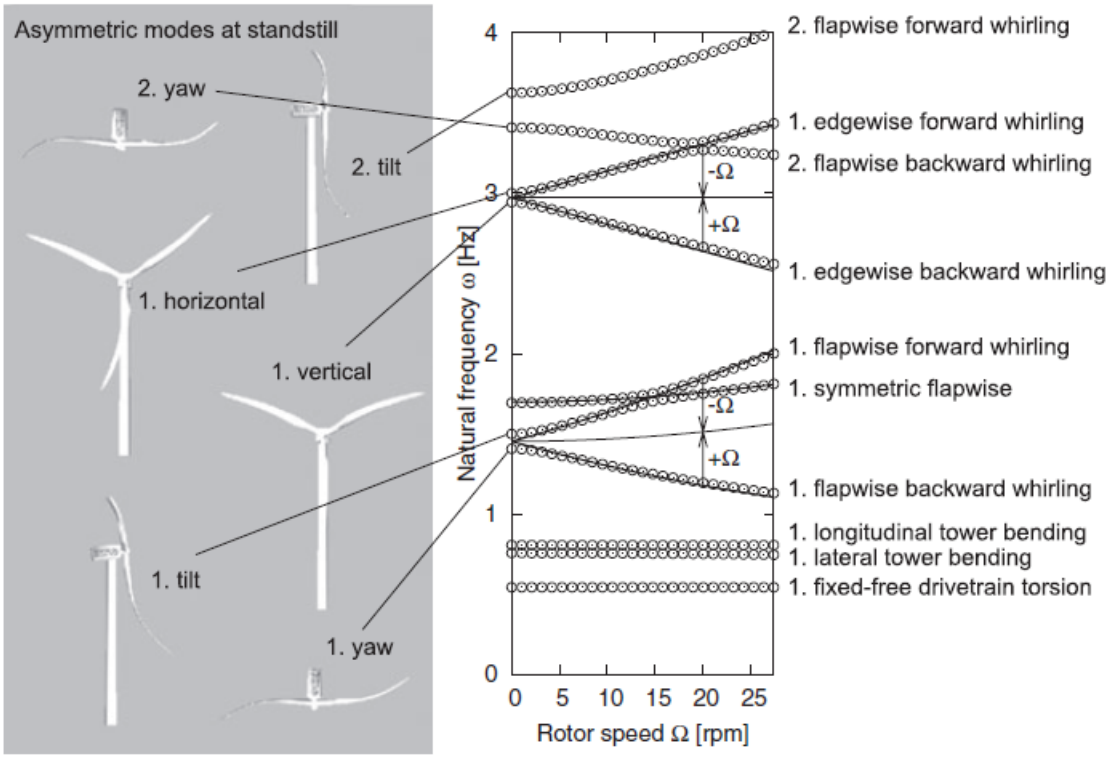

FIGURE J-0-2 WIND TURBINE NATURAL FREQUENCIES VS ROTOR SPEED [45]

APPENDIX K – GENERAL DESIGN PROCEDURE FLOWCHART

1

Wind turbine design

2

Substructure design

Check assumptions

Basis of design

Site Conditions
- Location
- Water depth
- Required air gap
- Site investigation – soil conditions

Environmental
- Wind
- Wave / current
- Ice

Required design life time

Concept design

Substructure selection (MCA)
- Tripod
- Monopile
- 3 or 4 legged jacket

Forcing frequencies

Preliminary design

FEED
- Layout
- Maximum size
- Maximum weight

Constraints
- Fabrication
- Transportation
- Installation
- Boat landing
- Maintenance
- Decommissioning

Detailed design

- Detailed member sizing
- Apply load combinations

Limit state design checks
- ULS
- SLS
- ALS
- FLS

Forcing Frequencies

$\omega n \neq \omega\_forcing$

$$\omega_n = \frac{c}{2\pi}\sqrt{\frac{k}{m}} = \frac{c}{2\pi}\sqrt{\frac{E\,I}{\rho\,A\,L^4}}$$

For single member

wind
wave/current
1P
3P
6P
9P
Tower
Flap FW
Blades

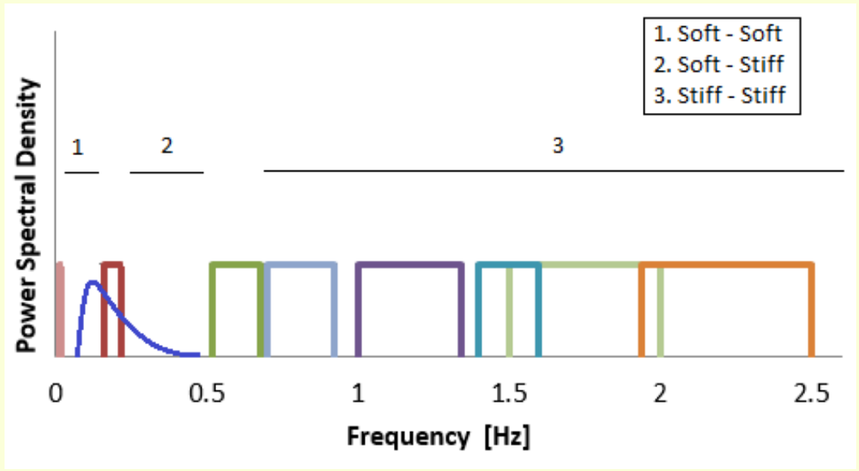

Detailed design with regard to avoiding resonance

Factors affecting ωn
- Mass
- Stiffness
- Hydrodynamic added mass
- Marine growth
- Diameter
- Shape
- Length
- Wall thickness

Factors affecting model
- Boundary conditions
- Mesh
- Element selection
- Damping

Mitigation Measures

	Increase ωn	Decrease ωn
Mass	M ↓ Remove anodes Remove MG	M ↑ ↑ wall thickness flooding braces Add concrete to members
stiffness	K ↑ ↑ member diameter Add extra cross braces ↓ brace length Diamond brace	K ↓ ↓ member diameter Remove cross braces ↑ brace length
Length	L ↓ ↓ jacket footprint ↓ jacket batter angle	L↑ ↑ jacket footprint ↑ jacket batter angle

optimatsation

Coupled analysis

Global stability

Modal analysis
- Global
- Local

Estimate fatigue life

Final Complete Design

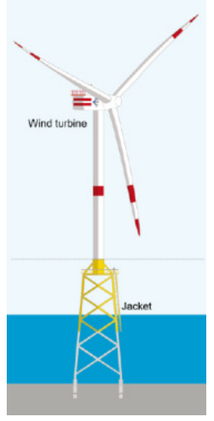

3

Pile Foundation design